A STUDY OF FILLER DISTRIBUTION IN BR/NBR BLENDS

NOOTJAREE PRAYOONCHATPHAN

A THESIS SUBMITTED IN PARTIAL FULFILLMENT
OF THE REQUIREMENTS FOR
THE DEGREE OF MASTER OF SCIENCE
(POLYMER SCIENCE)
FACULTY OF GRADUATE STUDIES
MAHIDOL UNIVERSITY
2000

ISBN 974-664-331-2

Thesis
entitled

A STUDY OF FILLER DISTRIBUTION IN BR/NBR BLENDS

Nootjaree Prayoonchatphan
Miss Nootjaree Prayoonchatphan
Candidate

Asst.Prof.Chakrit Sirisinha, Ph.D.
Major-advisor

Asst.Prof.Krisda Suchiva, Ph.D.
Co-advisor

K. Premphet
Asst.Prof.Kalyanee Premphet, Ph.D.
Co-advisor

Prof.Liangchai Limlomwongse,
Ph.D.
Dean
Faculty of Graduate Studies

Asst.Prof.Krisda Suchiva,
Ph.D.
Chairman
Master of Science Programme
in Polymer Science
Faculty of Science

Thesis
entitled

A STUDY OF FILLER DISTRIBUTION IN BR/NBR BLENDS

was submitted to the Faculty of Graduate Studies, Mahidol University
for the degree of Master of Science (Polymer Science)
on
June 2, 2000

Nootjaree Prayoonchatphan
Miss Nootjaree Prayoonchatphan
Candidate

Asst.Prof.Chakrit Sirisinha, Ph.D.
Chairman

Assoc.Prof.Pranee Phinyocheep,
Doctorat de l' Universite' du Maine
Member

Asst.Prof.Kalyanee Premphet, Ph.D.
Member

Mr.Pongdhorn Sae-Oui, Ph.D.
Member

Prof.Liangchai Limlomwongse,
Ph.D.
Dean
Faculty of Graduate Studies
Mahidol University

Prof.Amaret Bhumiratana,
Ph.D.
Dean
Faculty of Science
Mahidol University

ACKNOWLEDGEMENTS

I wish to express my sincere gratitude and appreciation to my advisor, Dr.Chakrit Sirisinha for his valuable guidance, helpful discussion and encouragement. Dr.Pranee Phinyocheep, Dr.Kalyanee Premphet and Dr.Pongdhorn Sae-Oui for their useful suggestion and completion of this thesis.

I would also like to extend my sincere thanks to all the lecturers of the polymer science groups, Mahidol University for valuable knowledge and suggestion. My appreciation is also extended to all my friends at Mahidol University and at Prince of Songkla University for their helpfulness throughout this thesis.

Furthermore, I would like to use this opportunity to express my grateful thanks to my lovely family for their support and understanding. In addition, I wish to thank my father for everything that he made my life complete.

Nootjaree Prayoonchatphan

4036453 SCPO/M: MAJOR: POLYMER SCIENCE; M.Sc. (POLYMER SCIENCE)
KEY WORDS : RUBBER BLENDS / CARBON BLACK DISTRIBUTION / DYNAMIC PROPERTIES

NOOTJAREE PRAYOONCHATPHAN: A STUDY OF FILLER DISTRIBUTION IN BR/NBR BLENDS. THESIS ADVISORS: CHAKRIT SIRISINHA, Ph.D., KRISDA SUCHIVA, Ph.D., KALYANEE PREMPHET, Ph.D., 124 p. ISBN 974-664-331-2

The distribution of carbon black in BR/NBR blends was studied by the use of Dynamic Mechanical Thermal Analysis (DMTA). The study consists of three parts. In the first part, the influences of blend ratio of BR/NBR, carbon black surface area and black loading on carbon black distribution in BR/NBR blends were investigated. It has been found that the black distribution was strongly affected by blend ratio and black loading. However, the black distribution was observed to be slightly affected by the black surface area. Variation in carbon black distribution in different rubber phases influences cure properties and mechanical properties of the blends. Scorch time and cure time decrease with increasing the ratio of amount of black in BR phase to the amount of BR. Upon increasing the ratio up to 0.6, cure rate was found to increase. Above the ratio of 0.6, cure rate decreases since BR was the dispersed phase. For the mechanical properties of unfilled compounds, the blend ratio strongly affects the % of elongation at break and slightly affects tensile strength, modulus and hardness. However, in the case of filled compounds, the effect of black distribution overrides the effect of blend ratio.

In the second part, factors affecting black distribution were investigated. It was found that the effects of blend ratio and mixing sequence on black distribution in blends were more significant than the effects of viscosity difference between BR and NBR and of rubber-filler interaction.

In the final part, the effects of some additives (Struktol 60NS, Struktol WB16, Ethylene octene rubber) on black distribution in blends were determined. From the results obtained, the cure properties and mechanical properties of unfilled compounds were strongly influenced by blend ratio and loading of additives studied. Nonetheless, in the case of filled compounds, the influence of black distribution overrides those effects of blend ratio and loading of additives. Further investigation of the black distribution on the other blend systems and/or additives are recommended.

4036453 SCPO/M: สาขาวิชา: วิทยาศาสตร์พอลิเมอร์; วท.ม. (วิทยาศาสตร์พอลิเมอร์)

นุจรีย์ ประยูรฉัตรพันธุ์: การศึกษาการกระจายตัวของฟิลเลอร์ในยางคู่ผสมระหว่างยางบิวทาไดอีนและยางไนไทรล์ (A STUDY OF FILLER DISTRIBUTION IN BR/NBR BLENDS) คณะกรรมการควบคุมวิทยานิพนธ์: ชาคริต สิริสิงห, Ph.D., กฤษฎา สุชีวะ, Ph.D., กัลยาณี เปรมเพ็ชร, Ph.D. 124 หน้า. ISBN 974-664-331-2

การศึกษาการกระจายตัวของเขม่าดำในยางคู่ผสมระหว่างยางบิวทาไดอีนและยางไนไทรล์ด้วยเครื่องมือวิเคราะห์สมบัติเชิงกลทางความร้อน โดยในการศึกษาประกอบด้วยสามส่วน ในส่วนแรกศึกษาอิทธิพลของสัดส่วนการผสมระหว่างยางบิวทาไดอีนและยางไนไทรล์ พื้นที่ผิวและปริมาณของเขม่าดำต่อการกระจายตัวของเขม่าดำในยางคู่ผสมระหว่างยางบิวทาไดอีนและยางไนไทรล์ พบว่าสัดส่วนการผสมของยางและปริมาณของเขม่าดำมีผลอย่างมากต่อการกระจายตัวของเขม่าดำในขณะที่ขนาดอนุภาคของเขม่าดำมีผลเพียงเล็กน้อย ความแตกต่างของการกระจายตัวของเขม่าดำในยางคู่ผสมจะส่งผลต่อการสุกของยางและสมบัติเชิงกล โดยช่วงเวลาที่ยางสามารถไหลได้และเวลาที่ใช้ในการทำให้ยางสุกตัวลดลงเมื่อสัดส่วนระหว่างปริมาณของเขม่าดำในยางบิวทาไดอีนและยางบิวทาไดอีนเพิ่มขึ้น ซึ่งการเพิ่มขึ้นของสัดส่วนนี้จะช่วยเพิ่มอัตราเร็วของการสุกตัวของยาง โดยอัตราเร็วจะมากสุดเมื่อสัดส่วนนี้มีค่าประมาณ 0.6 หลังจากค่านี้อัตราเร็วจะลดลงเนื่องจากยางบิวทาไดอีนจะเปลี่ยนไปเป็นเฟสกระจาย (dispersed phase) สำหรับสมบัติเชิงกลของคอมพาวด์ที่ไม่มีการเติมเขม่าดำจะพบว่าสัดส่วนของยางคู่ผสมมีผลอย่างมากต่อ % elongation at breakในขณะที่มีผลเพียงเล็กน้อยต่อ tensile strength, modulus และ hardness อย่างไรก็ตามในกรณีของยางคอมพาวด์ที่เติมเขม่าดำผลของการกระจายตัวของเขม่าดำจะมีมากกว่าและบดบังผลของสัดส่วนของยางคู่ผสม

ในการศึกษาในส่วนที่สองเป็นการศึกษาปัจจัยที่มีผลต่อการกระจายตัวของเขม่าดำ พบว่าผลของสัดส่วนของยางคู่ผสมและขั้นตอนที่ใช้ในการผสมยางมีผลต่อการกระจายตัวของเขม่าดำมากกว่าผลของความแตกต่างของความหนืดระหว่างยางบิวทาไดอีนและยางไนไทรล์ และผลของ rubber-filler interaction

ในส่วนสุดท้าย ศึกษาผลของสารตัวเติมบางชนิด (Struktol 60NS, Struktol WB16 และ ethylene octene rubber) ต่อการกระจายตัวของเขม่าดำในยางคู่ผสม จากผลการทดลองพบว่า สมบัติการสุกตัวของยางและสมบัติเชิงกลของคอมพาวด์ที่ไม่มีการเติมเขม่าดำจะได้รับผลอย่างมากต่อสัดส่วนของยางคู่ผสม ชนิดและปริมาณของสารตัวเติมที่ใช้ อย่างไรก็ตามผลเหล่านี้จะถูกบดบังโดยผลของการกระจายตัวของเขม่าดำเมื่อมีการเติมเขม่าดำลงในยางคอมพาวด์ สำหรับข้อแนะนำควรศึกษาในระบบของยางคู่ผสมคู่อื่นๆ หรือผลของสารตัวเติมชนิดอื่น

LIST OF CONTENTS

Page

Page

CHAPTER II EXPERIMENTAL

Page

CHAPTER III RESULTS AND DISCUSSION

Page

LIST OF TABLES

LIST OF FIGURES

Figure **Page**

Figure **Page**

Figure **Page**

Figure **Page**

LIST OF ABBREVIATIONS

BR	=	Butadiene rubber
NBR	=	Acrylonitrile butadiene rubber
CBS	=	N-Cyclohexylbenz-thiazylsulphenamide
DCP	=	Dicumyl peroxide
ODR	=	Oscilating Disc Rhometer
T_{max}	=	maximum torque
T_{min}	=	minimum torque
t_2	=	scorch time
t_{90}	=	curing time
phr	=	parts per hundred of rubber

CHAPTER I

INTRODUCTION

1.1 Elastomer Blends

Blending or mixing of elastomers is undertaken for three main reasons: (i) improvement of the technical properties of the original elastomer, (ii) achievement of improved processing behavior, and (iii) reduction in compound cost. All elastomers have deficiencies in one or more properties and blending is a way of obtaining optimum all-round performance. Compounds with good properties also need to be capable of factory processing without difficulty and of providing uniformity in behavior.0 The critical factors which influence the success of elastomers blending need to be understood and controlled to achieve optimum product performance with good levels of quality control.

1.1.1 Blending Techniques

The general mixing techniques for preparing elastomer blends include: latex, solution, solution and latex, mechanical and powdered blending.

1.1.1.1 Latex blending

Mixing of lattices is the simplest blending method available: no expensive equipment is required and high temperature is not needed. Moreover, as the coagulation of a mixture of lattices appears to be a random process entirely dependent on soap concentration, latex blending offers the possibility of finer-scale dispersions than solution and melt blending. Thus, much attention has been directed to its use in commercial manufacturing processes [1-2].

1.1.1.2 Solution blending

In solution blending, the high mobility of polymer solutions prior to a recovery by solvent evaporation permits relatively gross separation of the polymers into their constituent phase. Such blends may be macroheterogeneous rather than microheterogeneous [3].

1.1.1.3 Solution and Latex blending

A number of processes have been developed for a preparation of elastomer blends from combinations of polymer solutions and lattices. Advantages claimed for the processes are simplified polymer recovery procedures and the products with better filler dispersion than those obtained from the mechanical blending technique [2].

1.1.1.4 Mechanical blending

The most widely used method for preparing elastomer blends in industrial operations is the mechanical mixing. It has been recognized that although two high-molecular-weight polymers may be mutually insoluble, macroscopic homogeneity of the blends may be produced. Mechanical mixing must be sufficiently intense and the viscosities after mixing must also be sufficiently high to prevent gross phase separation [4-5].

1.1.1.5 Powdered Rubbers blending

As more elastomers become available in powdered and particulate forms, two types of blending are possible. A powdered elastomer may be blended with a solid elastomer using conventional mixing techniques, or two elastomers, both in powdered form, may be blended [2].

1.1.2 Compatibility

The most pertinent polymeric properties pertaining to elastomer blends are homogeneity of mixing (phase morphology) and cure compatibility. The complete miscibility of polymers requires that the free energy of mixing is negative, which can only be achieved by an exothermic mixing or a large entropy of mixing. Therefore, most blends of elastomers are practically immiscible because the mixing is generally endothermic and entropic contribution is small due to the high molecular weight of

elastomers. Fortunately, miscibility is not a main requirement for most rubber applications. Homogeneity at a fairly fine level is necessary for optimum performance but some degree of microheterogeneity is usually desirable to preserve the individual properties of the respective polymer components [6].

Callan et al. [7] used phase contrast optical and electron microscopic techniques to study morphology of elastomer blends and found that almost all bulk mixes of elastomer blends are microheterogeneous to various zone sizes. Generally, it is found that homogeneity characterised by microscopic techniques and thermal analysis is favored by [8]:

(a) Elastomers with similar values of solubility parameter.

(b) Rubber with similar viscosity.

(c) Mixing method capable of giving good disaggregation of compounding ingredients and satisfactory distribution between the constituent rubber.

(d) Rubber with similar curative requirement, cure rate and curative systems capable of giving interlocking networks.

(e) Suitable choices of plasticizer, which may offset slight deficiencies in (a) and (b).

1.1.2.1 Cure compatibility

Although true miscibility may not be required for good rubber properties, adhesion between the polymer phase is necessary and the respective interfacial energies are important in this respect.

The nature of the polymer (e.g. unsaturation, polarity) determines curative reactivity, which is also influenced by solubility of curatives in polymers. Vulcanizates with components having similar curative reactivity generally give better properties than those with components having a large difference in curative reactivity [9]. However, the means of achieving good covulcanization in blends of high and low unsaturation elastomer require curing agents, which can distribute uniformly and have similar activities for different elastomers (e.g. peroxides and reactive resins) [10].

1.1.3 Factors affecting filler distribution

It is generally recognized that blending of two elastomers does not lead to a molecular-scale homogeneous blend (true solution), but to a heterogeneous system. The zone-size of the dispersed phase in blends is dependent upon the relative compatibility of the elastomers and on the processing conditions.

The heterogeneity of polymer blends is magnified on an addition of compounding ingredients (curatives & filler) if the affinity of polymers to these ingredients is unequal. The distribution of ingredients in blends is important in controlling the physical properties of rubber products.

Considerable progress in the study of carbon black distribution was reported by Callan et al. [11] on blends of butyl and EPDM. They used both phase contrast light and electron microscopic techniques to classify polymer zone size and the relative location of carbon black between the two phases. They found that blends containing carbon black loading up to 50 phr can successfully be examined in the electron microscope via ultramicrotomy of frozen specimen blocks. However, good interzone

contrast becomes increasingly difficult as carbon black loading are above 20 phr. One of the most significant results obtained from this work is that butyl rubber shows considerably lower affinity to carbon black than does the EPDM. On this basis, it is possible to explain certain abnormalities in the physical properties of carbon black-filled blends of these elastomers. Similar observations were also made by Hess et al. [12]. They reported that, in NR/BR blend, carbon black preferentially migrates to BR phase. However, when fillers are added to a blend, particularly at high loading, the resolution of zone boundaries and interzone contrast are relatively poor. In another approach, Callan et al.[7] studied the distribution of carbon black in a blend of 50/50 of a wide range of commercially elastomers. In their study, 40 phr of a high structure HAF carbon black was added to elastomer preblends. Filler distribution was then assessed from the number of aggregates in the separate polymer zones. The result obtained showed that BR and SBR have the highest affinity to the standard-type carbon black. Polychlorobutadiene and Nitrile rubber show somewhat lower affinity, though appreciably higher than that of NR. EPDM and IIR show the lowest affinity to carbon black. In addition, the carbon black transfer was investigated in various polymer systems using electron microscopy and pyrolytic gas chromatography. The extent of carbon black transfer from IIR to BR, NR and SBR is significant. In summary, the carbon black transfer occurs when the adsorptive capacity of carbon black has not been fully utilized. This situation exists if the masterbatch has minimum heat or mechanical history, or involves with low molecular weight or low unsaturation elastomer. Maiti and coworkers [13] measured the distribution of carbon black in the blend of NR and ENR (immiscible binary rubber-rubber blends) by DMTA, based on a

change in mechanical damping properties of unfilled and filled vulcanizates. The main advantages of this method are that it gives quantitative and reproducible results within a short time and applicable to compounds with high filler loading.

The distribution of filler between the separate phase in elastomeric blends is affected by a number of factors; nature of rubber, viscosity of rubber, filler and mixing sequence [7, 12-14].

A) Nature of rubber (polarity, unsaturation, MW&MWD)

A large difference in unsaturation existing between two or more elastomeric components affects strongly the filler distribution. The bulk of the carbon black is always found in the component with relatively high unsaturation. The distribution of carbon black in blends of NR with different elastomers such as BR, SBR, CR and NBR is illustrated in Figure1.1 [7]. It is clear that the amount of black residing in NR phase is relatively small when blended with the high-unsaturated rubber like BR, CR and NBR.

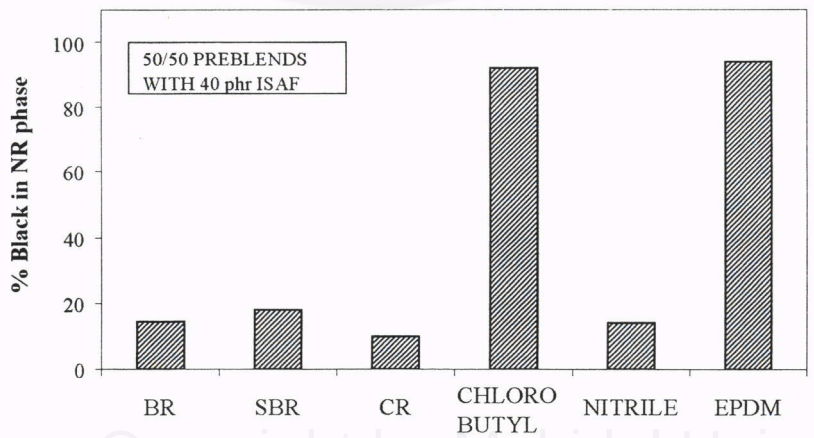

Figure 1.1 Carbon black distribution in blends of NR with different elastomers [7]

Regarding the molecular weight effect, it has been reported that the change in molecular weight plays only a slight role on black phase distribution, as illustrated in Table 1.1 [14].

Table 1.1 Effect of molecular weight of natural rubber on carbon black distribution in 50/50 NR/SBR filled with 45-phr N339 black [14]

Molecular weight of NR[a], 10^{-3}Mw	Bound rubber, %	% NR in bound rubber[b]	Carbon black loading (%) in	
			NR	SBR
1203	26.6	49.6	36.1	53.9
1011	25.6	42.3	33.5	56.5
568	24.8	39.5	33.0	57.0
345	28.7	35.6	31.2	58.8

[a] Molecular weight calculated from GPC analysis using calibration curve for polystyrene

[b] % NR in bound rubber measured from pyrolysis/gas chromatography analysis of bound rubber

B) Viscosity of rubber

The effect of rubber viscosity in the blend on carbon black distribution is shown in Figure 1.2 [12]. Clearly, as polybutadiene viscosity increases, ISAF black locates in NR increasingly. In other words, ISAF black preferentially resides in the phase with lower viscosity.

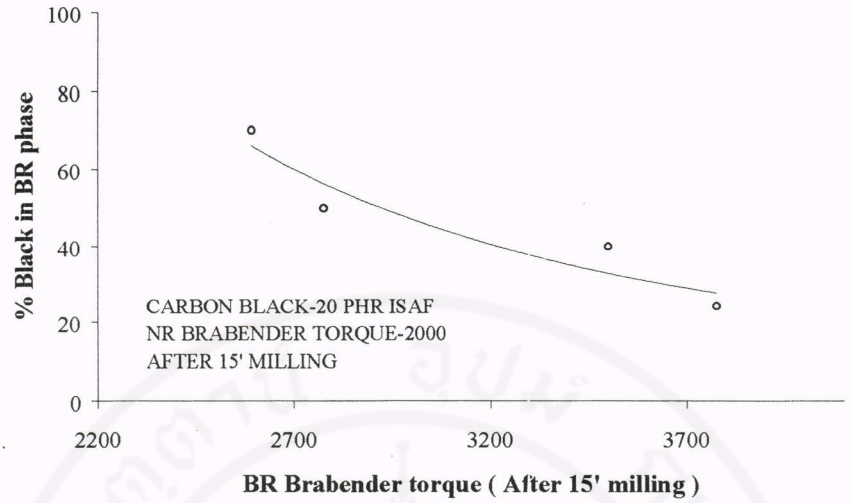

Figure 1.2 Effect of polybutadiene Brabender viscosity on black distribution in 50/50 NR/BR blends

C) Filler (types, particle size, polarity, loading)

The effect of loading on filler distribution in a 50/50 NR/ENR blend is shown in Table 1.2 [13]. It can be seen from Table 1.2 that with low level of silica loading, ENR is more preferential to silica than NR. As the filler loading increased, ENR becomes gradually saturated, and silica thereafter, migrates to NR. The reason for preferential migration of silica to ENR phase may be due to either the low viscosity of ENR, strong physical interaction between the epoxide groups of ENR and silanol groups of silica, or both. This result is in agreement with the work reported by Hess et al. [12], working on the NR/BR blend with a carbon black loading of up to 40 phr. Apart from the NR/ENR system, the carbon black distribution in 50/50 NR/BR blend has been reported as shown in Figure 1.3 [12]. It is obvious that at low filler loading, there is no significant preference of the carbon black for either elastomer in NR/BR blends. As the

carbon black loading is increased, the black preferentially locates in the BR phase. At the highest loading investigated, i.e. 40 phr, approximately 80 % of carbon black is in the BR phase.

Apart from the filler loading, the interaction between filler and rubber has been reported to be influential on the filler distribution in blends. Hess et al.[12] investigated the role of rubber-silica interaction in NR/BR blend and found that the silica appears mainly in the NR (light zone), as shown in Figure 1.4, which is tentatively attributed to the interaction of the protein component of NR with the hydroxylated surface of the precipitated silica.

Table 1.2 Distribution of silica in a one-to-one blend of NR and ENR-25 [13]

Precentage of silica migrated to	Filler loading, %				
	10	**20**	**30**	**40**	**53**
NR phase	12	18	24	35	53
ENR phase	88	82	76	65	47

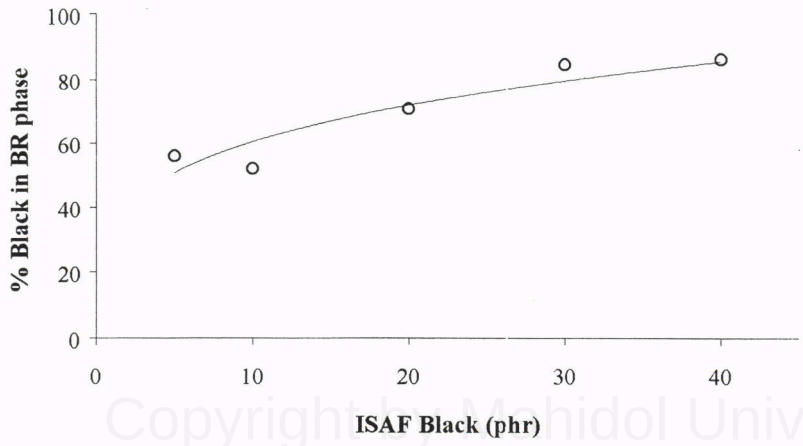

Figure 1.3 Effect of loading on carbon black distribution in 50/50 NR/BR blends [12]

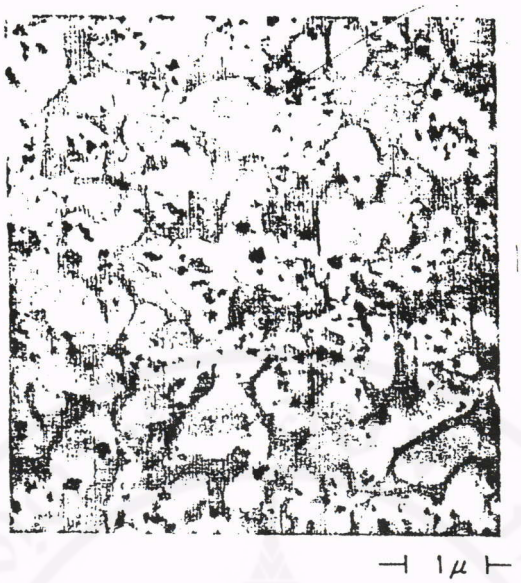

Figure 1.4 Distribution of silica in a 50/50 preblend of NR/BR [12]

In addition, from Table 1.3, it can be seen that the interaction between rubber and fillers can be either chemical or physical interaction. In the case of chlorobutyl blended with NR, about 90% of each filler resides in NR phase. As for the NR/BR blends , both silica and chemically oxidized black show similar affinity to elastomers. Likewise, the effect of surface groups on the distribution of carbon black between NR and SBR phase has been examined using three sets of N220 black. The first set is treated at 1500°C in inert atmosphere to remove all the surface groups and deactivate the surface (as shown by a great reduction in bound-rubber concentration). The second set is oxidised with nitric acid in order to increase the concentration of oxygenated groups at carbon black surface. The last set is the controlled black. Results show that the effect of oxygenated groups or surface activity of carbon black on distribution of black in NR/SBR blends is relatively small as illustrated in Table 1.4 [14].

Table 1.3 Distribution of fillers in 50/50 blends of natural rubber with other elastomers [12]

Blend	Percent of fillers[a] in NR		
	Standard ISAF	Chemically oxidized ISAF	Precipitated silica
NR/Chlorobutyl	88	91	90
NR/BR	28	60	70

[a] 20 phr filler added to preblend

Table 1.4 Effect of surface activity of carbon black in 50/50 NR/SBR blend filled with 45-phr N220 black [14]

Carbon black treatment	Bound rubber	%NR in bound rubber	Carbon black loading (%) in	
			NR	SBR
Original NR Mw = 1,203,000				
Heat treated (1500°C)	12.5	63.1	33.1	56.9
None	27.5	47.9	33.0	57.0
Oxidized	38.6	52.5	39.7	50.3

D) Mixing sequence

The changes in filler distribution in blends caused by different mixing sequences are shown in Table 1.5 [13]. The distribution result shows that when all of silica is added to ENR or to preblend, only 5% of the total silica migrates to the NR phase. By

contrast, when all of silica is added to NR before blending with ENR, 81% silica migrates to the ENR phase. Similar result is obtained when silica is added in equal proportion to the two polymers before blending. Also, similar trend of the result has been observed by Hess and co-workers, as illustrated in Table 1.6 [12]. If NR and BR masterbatches with similar filler loading is blended together, it is found that carbon black transfers from NR to BR phases. The black transfer also occurs when NR masterbatch is cutback by BR. Heat and chemical promotions of NR black masterbatch before cutting back with BR reduce greatly the black transfer.

Table 1.5 Distribution of silica in 50/50 NR/ENR-20 blend prepared from different mixing sequences with filler loading of 20 phr [13]

Percentage of silica in	Sequences of mixing			
	All of silica in NR	**All of silica in ENR**	**Silica is added in equal proportion in NR and ENR before blending**	**All of silica is added to preblend**
NR	19	5	18	5
ENR	81	95	82	95

Table 1.6 Effect of mixing technique on carbon black distribution in 50/50 NR/BR blends [12]

Sequences of mixing	% Black in polybutadiene
Black added to preblend	75
Separate masterbatches	59
NR-black masterbatch	40
NR-black masterbatch "promoted"	18

Two blend systems containing conventional NR (i.e. high molecular weight) prepared from the standard and solution masterbatching processes show no significant difference in black distribution (i.e., 36.1 versus 35.5 phr in NR) as illustrated in Table 1.7. However, a larger amount of carbon black in NR is observed in the blends containing degraded NR (i.e., lower molecular weight) prepared by the solution masterbatching technique than that prepared from the standard masterbatching process (38.3 versus 31.2 phr in NR) [14]. Additionally, during the blending of SBR and NR masterbatches, carbon black tends to migrate from NR to SBR, as shown in Table 1.8. Such behavior suggests the relatively weak interaction between NR and carbon black surface, and therefore the polymer becomes detached by the shear forces developed during the mixing operation that can be supported by the consistent drop in carbon black loading in NR as the mixing time increased (see Table1.9).

Table 1.7 Comparison of standard mixing to solution masterbatch (50/50 NR/SBR blend containing 45 phr N339 black) [14]

Molecular Weight of NR[a] 10^{-3} Mw	Method of incorporation	Bound rubber, %	% NR in bound rubber	Carbon black loading (%) in	
				NR	SBR
1203	std. mixing	26.6	49.6	36.1	53.9
1203	soln. mb	28.2	48.9	35.5	54.5
345	std. mixing	28.7	35.6	31.2	58.8
345	soln. mb	22.0	44.9	38.3	51.7

[a]Molecular weight calculated from GPC analysis using calibration curve for polystyrene

Table 1.8 Transfer of carbon black during blending of masterbatches in 50/50 NR/SBR blend containing 45 phr N339 black [14]

Carbon black loading in NR			
in masterbatches, phr	80	45	30
found in blend, phr	54	35	16
Carbon black loading in SBR			
in masterbatches, phr	10	45	60
found in blend, phr	36	55	74

Table 1.9 Effect of mixing time on N330 distribution in 50/50 NR/SBR blend [14]

Mixing time, min	**Bound rubber, %**	**% NR in bound rubber**	**Carbon black loading, % , in:**	
			NR	**SBR**
3	25.9	51.1	34.0	56.0
5	27.6	47.6	33.1	56.9
10	30.2	44.7	31.1	58.9
20	30.8	42.7	30.0	60.0
60	30.3	39.0	28.1	61.9

1.2 Characterisation Techniques

In this section, the useful characterisation techniques generally used with elastomer blends will be reviewed. The areas of characterisation have been divided into two categories: (i) homogeneity and morphology, and (ii) filler inter-phase distribution.

1.2.1 Homogeneity and Morphology

Methods which have widely been utilized to assess the homogeneity and morphology of polymer blends are as follows:

- Optical microscopy (OM)
- Transmission electron microscopy (TEM)
- Scanning electron microscopy (SEM)
- Glass transition behavior determination

All of these methods are applicable to bulk rubber compounds but some are subject to the limitations with the filled polymers. When applicable, the microscopic techniques are the most suitable since they provide information on overall homogeneity and phase morphology, simultaneously.

1.2.1.1 Optical microscopy (OM)

Phase contrast light microscopy is mainly applicable to the study of unfilled polymer blends and has been applied extensively to the analyses of binary elastomer combinations [7, 12, 15-16]. This technique is based on differences in the refractive indices of the polymers. The microscope produces a phase shift between the diffracted and transmitted light, which provides interference contrast with only small differences in refractive indices. Phase contrast optical microscopy requires very thin specimens ($\approx$ 1-4 μm), which can be prepared by cryo-sectioning technique. Callan and co-worker [7, 12] used this technique to study compatibility and morphology of binary

blends containing NR, SBR, BR, CR, NBR, EPDM, IIR and CIIR. They also employed the automated image analysis to measure the zone size of domains.

The phase contrast light micrographs of the different pure gum blends were analyzed for the zone size by means of a Quantimet Image Analyzing Computer. The Quantimet (QTM) is a television scanning device which can analyze the microscope image directly or a micrograph by means of epidiascope. The results of these studies are illustrated in Table 1.10 which are the measured areas of the dispersed phases in more than 50 combinations of Banbury-mixed 75/25 binary blends containing eight different elastomers. Excluded are blends of IIR/CI-IIR (no contrast) and SBR/BR (too low in contrast for the image analysis measurements). Only the 75/25 blend proportion was measured to assure that there would be a dispersed-phase rather than a co-continuous morphology. The smaller the average dispersed phase area, the more the compatibility of the blends. This generalization obviously correlates to the similarities in solubility parameter, viscosity and polarity. It can be seen that NBR produces the greatest heterogeneity in all blends except those with CR. Many of the CR blends are also quite heterogeneous with BR, SBR and NBR.

Gardiner [16] also utilized this technique to study the compatibility and morphology of binary blends, which are prepared from the solution blending process to eliminate some factors affecting compatibility, e.g. difference in viscosity. The film product obtained is examined microscopically. A miscibility chart shown in Table 1.11 gives the overall results of microscopic results of these blends. The limitations of the phase contrast technique could be drawn as follows:

(1) low resolution and poor contrast with certain polymer combinations

(2) distortion of the polymer phases due to swelling

(3) non-applicability to carbon-black filled systems.

Table 1.10 Average areas (μ^2) of dispersed phases in 75/25 pure gum blends [7]

Disperse phase 25%	Matrix (75%)							
	NR	CR	BR	SBR	NBR	EPDM	IIR	CI-IIR
NR	-	45	1.5	1.2	300	1.5	2.0	3.2
CR	35	-	4.0	2.5	1.5	25	20	15
BR	0.7	4.5	-	-	15	2.2	2.1	2.5
SBR	0.5	2.7	-	-	20	2.1	12	10
NBR	400	1.3	17	30	-	250	100	225
EPDM	3.5	75	2.8	2.6	225	-	2.0	1.5
IIR	3.0	15	3.0	4.2	75	1.0	-	-
CI-IIR	2.2	25	2.3	2.5	85	1.2	-	-

Table 1.11 Miscibility chart [16]

Rubber	Butyl	Chloro-butyl	EPDM	SBR	NR	Cis-1,4-Polybuta-diene
Chlorobutyl	M	-	-	-	-	-
EPDM	B	B	-	-	-	-
SBR	I	I	I	-	-	-
NR	I	I	I	B	-	-
Cis-1,4-Polybutadiene	I	I	I	B	B	-
Neoprene	I	I	I	I	I	I

M = Miscible (no visible phase separation)
B = Unusual network type phase separation
I = Complete phase separation

It has been reported that the swelling problems can be eliminated by the use of a rotary microtome for TEM sectioning [17]. The presence of carbon black generally raises the refractive indices of the polymer mixtures and eliminates the phase contrast mechanism.

1.2.1.2 Transmission electron microscopy (TEM)

This technique gives high resolution and applicability to both filled and unfilled systems. The preparation of thin section ($\approx$ 0.1 μm or less) is considerably more difficult than the optical microscopy. The major problem of TEM in rubber blends is an image contrast. For most elastomer combinations, there is no contrast between rubber phase in TEM. If the elastomers in a blend differ significantly in a degree of unsaturation, osmium tetroxide (OsO_4) staining is the best way to develop the contrast. The stain is picked up selectively by the phase with high unsaturation, which then becomes darker in TEM [19].

Achieving contrast for TEM analysis of a blend with high unsaturation elastomers is very difficult. Smith and Andries [20] used the technique, applicable to SBR/BR blends, which is based on the sulphur hardening called "ebonite method". The contrast is achieved by selective adsorption of the zinc salt in the SBR phase, giving the darker in SBR than the BR. The electron micrographs show that SBR/BR blends are heterogeneous, although the two polymers form very good blends, i.e. they give small zone size. In addition, it has been reported that the phase contrast in TEM can be improved by the addition of carbon black [18].

1.2.1.3 Scanning electron microscopy (SEM)

SEM generally requires much simpler specimen preparation than TEM. The OsO_4 and RuO_4 staining techniques still work efficiently in SEM and can be applied to bulk specimens, i.e. cut or fractured surfaces. A smooth cut surface prepared by microtome is, however, preferred. Contrast is achieved by imaging with backscatter electrons where emission increases in a direction of the greater atomic number elements. Therefore, the OsO_4 stained phase in a blend appears brighter in SEM than the unstained phase, which is opposite to that observed in TEM.

1.2.1.4 Glass transition behavior

Glass transition temperature (T_g) measurement is one of the most commonly used technique to define the overall homogeneity of elastomer blends [7-8]. However, there is no specific information on a blend morphology provided. Heterogeneous blends clearly exhibit the separate Tg for the individual polymer components. A single Tg peak is indicative of homogeneity, but does not necessarily mean miscibility.

Callan and co-workers [7] studied BR/SBR blends using DTA and found that the vulcanised blends of several types of BR with SBR ordinarily exhibit only one glass transition temperature. However, the similar blends in uncured state show separate T_g values of each pure polymer. As a consequence, the blends of BR/SBR, though more compatible than most polymer systems (e.g., NR/BR), are not homogeneous at the molecular level.

A number of other test methods have also been utilized for determining Tg values in elastomer blends. Corish [8] employed both dilatometry and a rolling ball loss spectrometer to investigate BR/NR and BR/NBR blends. The rolling ball loss spectrometer shows sharp peak at rubber transition temperatures and is more sensitive instrument than the dilatometer for monitoring the effect of cure. At a low state-of-cure, the cis-BR and NR components show several resolved peaks which progressively merge as a state-of-cure increases. Cis-BR and NBR are completely incompatible, showing two separate loss peaks independent of the state-of-cure. Unlike the cis-BR/NBR blend, the compatibilisation of BR/CIIR blend by the vulcanisation has been reported [21].

1.2.2 Filler inter-phase distribution

1.2.2.1 Microscopy

Electron microscopic techniques have been employed more widely than any other techniques for determining the relative amounts of filler in the different components of elastomer blends whilst phase contrast light microscopy is limited to the low resolution and relatively ineffective in compounds with high filler loading, particularly of carbon black [11-12]. However, inter-phase contrast is still a major problem in both TEM and SEM analyses. Thus, a development of phase contrast is required.

Development of phase contrast

A) Differential swelling technique

This technique needs to embed the blend in a glassy component, which can be carried out by swelling the vulcanisate in a large excess of polymerisable monomer which is subsequently polymerised to a glassy state. The embedded vulcanisate can then be sectioned readily using the ultramicrotome. The embedding resin undergoes substantial decomposition and evaporation when exposed to the electron bombardment in the electron microscope. Hess and co-workers [12] studied NR/BR blends using the embedding mixture of 50 parts of methyl metacrylate, 40 parts of butyl methacrylate, and 10 part of styrene. Benzoyl peroxide (1 part) is used as a catalyst. The methacrylate is partially polymerized and readily degraded before removed from the sections during the electron bombardment. Certainly, this technique is an electron beam etching which produces much sharper phase boundaries than the swelling of cryosections.

The limitations of the methacrylate embedding technique are, however, associated with the difficulty in controlling the amount of specimen swelling and the inability to analyze the blends with high carbon black and oil loadings [7].

B) Staining technique

A molten sulphur has been employed in order to transform the uncured rubber to an ebonite that could then be polished for characterising under microscopy [20]. It has

been found that the ebonite can easily be ultrathin-sectioned for the electron microscopical examination. By this means, the main disadvantage is the difficulty in maintaining accurate geometrical relationships within the specimen.

Figure 1.5 shows a comparison of micrographs obtained from methacrylate and ebonite methods. It can be seen that the drawback of the methacrylate method is that the distances between carbon black aggregates in the methacrylate-swollen section are glossly exaggerated and do not present a true image of spatial relationships, compared to the ebonite technique. Another advantage of the ebonite method lies in the fact that the uncured and uncompounded polymers can be used as starting materials. Thus, samples can be examined without the need of curative incorporation.

The development of contrast between phases of polymer blends under TEM is dependent upon the hardness of the blends, i.e. the extent of cure and the curing systems used. The harder phase with higher sulphur and zinc content shows the darker colour than the adjacent softer phase due to the greater electron scattering by sulphur and zinc atoms. In addition, the harder phase is more stable in electron beam and has a lesser tendency to "thin-out" and, therefore, an even greater contrast between the phases is achieved without attendant distortion.

The ebonite method has been applied to a variety of polymer systems. However, the main limitation of this technique is that the polymers must have sufficient degree of unsaturation for sulphur-vulcanisation.

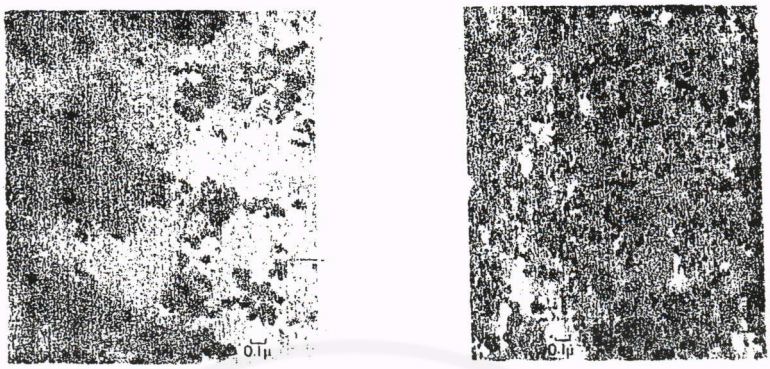

Methacrylate Method **Sulphur Method**

Figure 1.5 Comparison of methacrylate and ebonite hardening method × 40,000 [20]

C) Differential pyrolysis technique

This method has specifically been developed to produce a contrast under the electron microscopy between the separated polymer phases in thin section (50-100 nm) of carbon black filled blends. The method is applicable only to a certain polymer combinations which have a distinct difference in their temperature-time decomposition pattern.

Hess and Chirico [22] utilized the technique to investigate the phase morphology and carbon black distribution in NR/SBR and NR/BR blends. By selectively removing NR from the sectioned specimens of the blends, the zones of this polymer then appear as a light image under the electron microscope. A distinct advantage of this technique over the differential swelling method is the fact that the thin unswollen frozen section can be employed, and therefore, no appreciable distortions of zone size and shape are obtained.

1.2.2.2 Pyrolysis / gas chromatography analysis of bound rubber

Bound rubber represents the amount of rubber insolubilized by the solvent and is measured by swelling small pieces of unvulcanized rubber for an extended period of time (at least overnight) in good solvent. All of the carbon black remains in the carbon-rubber gel and the soluble rubber is removed. The relative percentages of rubber in the bound rubber can be used to determine the distribution of carbon black in elastomer blend by the use of pyrolysis technique [14]. The pyrolysis/gas chromatography analysis is utilised for an estimation of carbon black distribution in blends, based on the measurement of the area ratios for major degradation peaks in the chromatograms. Composition can then be determined by comparing the ratio to the known blends.

However, this technique is not applicable to the determination of carbon black distribution in vulcanized compounds and does not provide any information on phase morphology.

1.2.2.3 Mechanical damping studies

Generally, the peak value of tan δ_{max} decreases with increasing filler loading due to the dilution effect. Therefore, the extent of a reduction in tan δ_{max} can be used to estimate the filler distribution in an immiscible rubber blend. The magnitude of this effect is governed by filler type and polymer type. The decrease in tan δ_{max} is influenced by differences in: (i) filler/polymer ratio, (ii) filler/polymer interaction, (iii) crosslink density between gum and filled vulcanizate, and (iv) immobility of the dispersed phase [13,23].

There is a proposed relationships between $\tan\delta_{max}$ and filler distribution in blends as shown in equation (1.1) [13].

$$R = \frac{(\tan\delta_g)_{max} - (\tan\delta_f)_{max}}{(\tan\delta_g)_{max}} \quad (1.1)$$

Subscripts g and f represent gum and filled systems, respectively. The term R is related to the filler-to-polymer weight fraction, W, according to equation (1.2)

$$R = \alpha W \quad (1.2)$$

α represents the polymer-to-filler interaction parameter. The application of equation (1.2) to single and blend systems, separately, gives the following equations:

$$R_1 = \alpha_1 W_1 \quad (1.3)$$

$$R_2 = \alpha_2 W_2 \quad (1.4)$$

$$R_1' = \alpha_1' W_1' \quad (1.5)$$

$$R_2' = \alpha_2' W_2' \quad (1.6)$$

W'_1 and W'_2 denote the weight fraction of filler in polymer 1 and 2 in the blend, respectively.

$$W = W_1' + W_2' \quad (1.7)$$

Assuming $\alpha_1/\alpha_2 = \alpha_{1'}/\alpha_{2'}$, equations (1.3) to (1.6) can be rearranged to equation (1.8)

$$\frac{W_1'}{W_2'} = \frac{R_1' R_2}{R_2' R_1} \quad (1.8)$$

From equations (1.7) and (1.8), equation (1.9) can be obtained.

$$W_1' = \frac{R_1' R_2 W}{R_1' R_2 + R_2' R_1} \quad (1.9)$$

The multiplication of W'_1 and W'_2 by 100 gives the percentage of filler residing in polymer 1 and 2, respectively.

1.3 Physical properties in rubber blends

Blends of elastomers are employed in rubber products for a variety of reasons which include: an improvement in physical properties, an increase in service life, an improvement in processibility, and a reduction in product cost. The performance characteristics of elastomer blends are frequently predictable from the ratios of the respective polymer components. In some instances, however, blends can be compounded to perform at a higher level for particular properties than would be anticipated from the relative proportions of the individual elastomers. The main factors contributing to the enhanced performance are the size and continuity of the separate polymer phases and the manner in which filler is distributed between those phases. It has been reported that the properties of blends are affected more strongly by filler distribution than by phase morphology [10, 17].

1.3.1 Rheological properties

The changes in the rheological behavior of NR/BR blends, caused by a sequence of blending, with the presence of HAF black has been investigated [25]. Rheological characteristics of four sets of blends are determined at different temperatures and shear rates as shown in Table 1.12. It is obvious that for blends A and B, zero shear viscosity

(K) decreases with increasing processing temperature; however, for blends C and D, values of K increases as temperature increases from 80 to 100°C, and then decreases. Over the temperature range of 80-120°C, blend B shows the highest K whereas blend C shows the lowest. The explanation is proposed in terms of carbon black dispersion in each phase, depending on the blending sequence and processing temperature. Black added in NR phase (blend B) gives higher viscosity whereas black added in BR phase (blend C) shows lower viscosity.

Table 1.12 Rheological parameters of the blends at different temperatures [25]

Blend	Black added in	Temp.(°C)	n	K (Pa.S)
A	Pre-blend	80	0.17	1.65×10^5
B	NR	80	0.16	2.21×10^5
C	BR	80	0.24	8.8×10^4
D	NR and BR	80	0.25	1.1×10^5
A	Pre-blend	100	0.180	1.35×10^5
B	NR	100	0.154	1.88×10^5
C	BR	100	0.130	1.2×10^5
D	NR and BR	100	0.140	1.48×10^5
A	Pre-blend	120	0.210	1.08×10^5
B	NR	120	0.200	1.43×10^5
C	BR	120	0.176	8.5×10^4
D	NR and BR	120	0.180	1.08×10^5

1.3.2 Mechanical properties

Carbon black distribution in blends has a particularly significant effect on dynamic modulus at low strain amplitudes [26, 27]. The elastic dynamic modulus increases with increasing carbon-carbon networking. It has been reported that the degree of networking in descending order is as follows: NBR, CR, CIIR, EPDM, SBR, NR, BR, OE-SBR and OE-BR [26]. In the blend systems where black is added to preblend rubber, the networking is more complicated due to the compatibility of rubbers, the nature of the continuous phase and black distribution in blends [27]. At low amplitude, storage modulus (G') and loss modulus (G") values increase with reducing compatibility of rubber due to uneven black migration and redistribution of black toward the interface. Therefore, blends of SBR with CIIR, NBR and EPDM show the highest modulus due to highest networking followed by NR/EPDM, BR/NBR, BR/CIIR, respectively. The blends with the smallest degree of networking are NR/BR and SBR/BR showing low dynamic modulus.

In addition, a study of tensile properties in 50/50 NR/BR, NR/SBR and SBR/BR blends as a function of carbon black distribution in blend has been reported [22]. Modulus at 300% strain and tensile strength were strongly affected by type of rubber in blend but slightly affected by black distribution. However, there is a report showing that tensile strength increases with increasing carbon black in BR phase in 50/50 NR/BR blend [12].

It has been reported the criteria for maximizing tear resistance in rubber blends: (1) small black unit size with low structure; (2) higher loading of carbon black in the

continuous polymer phase than the dispersed phase; and (3) polymer with higher strength as a continuous phase [22]. It has been investigated the carbon black distribution in NR/SBR and NR/BR using electron microscopy and found that black added to NR/SBR or NR/BR preblends shows significant preferential migration to SBR or BR phase. The uneven distribution of carbon black in each phase of blends plays significant role in tear resistance. From Table 1.13, it can be seen that the tear resistance of NR/SBR preblend is in agreement with that of the blend where black-SBR masterbatch is used. It can therefore be concluded that the carbon black preferentially resides in SBR phase in NR/SBR preblend. Likewise, in NR/BR blends, the tear resistance of the preblend is close to that of the blend where black-BR masterbatch is used, indicating that carbon black preferentially reside in BR phase in NR/BR preblend. There is also a report of tear strength as a function of black reside in BR phase of 50/50 NR/BR blend showing the highest when 60% of carbon black reside in BR phase, as shown in Figure 1.6 [12].

Table 1.13 Tear strength of 50/50 polymer blends with N-220 type carbon black [22]

Polymer system	Black addition	Tearing energy[a], %
NR-SBR	To preblend	49.6
NR-SBR	75% in SBR	51.6
NR-SBR	75% in NR	33.4
NR-BR	To preblend	47.6
NR-BR	75% in BR	51.0
NR-BR	75% in NR	66.8

[a] Modified trouser tear test at 100°C.

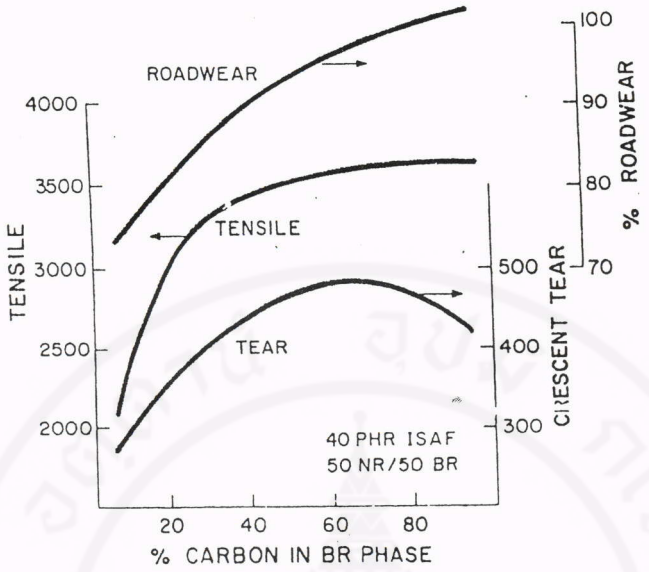

Figure 1.6 Effects of carbon black distribution on vulcanizate properties in 50/50 NR/BR blend [12]

1.4 Scope of the present thesis

The present study consists of three main parts, as follows:

Part I Effects of blend ratio of BR/NBR, carbon black surface area and black loading on carbon black distribution in BR/NBR blends

The main objective in this part aims to measure the carbon black distribution in BR/NBR blend by the use of damping properties. Some factors affecting the black distribution which are BR/NBR blend ratio, carbon black surface area and black loading will be investigated. Afterward, the relationships between carbon black distribution, cure and mechanical properties will be studied.

Part II Factors affecting carbon black distribution in BR/NBR blends

In this part, some additional factors affecting carbon black distribution, which are viscosity difference between BR and NBR, rubber-filler interaction and mixing sequence, are to be investigated.

Part III Effects of some additives on carbon black distribution in blends

The main objectives of this part are to investigate the effects of some commercial additives including Struktol 60NS, Struktol WB16 and Ethylene octene rubber on the carbon black distribution in BR/NBR blends.

CHAPTER II

EXPERIMENTAL

2.1 Compound Preparation

2.1.1 Materials

The materials used in the study are summarised in Table 2.1.

Table 2.1 Materials used in the study

Chemical name	Grade	Supplier
cis-1,4 polybutadiene or Butadiene Rubber (BR)	BR 01 (97% cis-1,4 configuration)	Japan Synthetic Rubber (JSR) Co. Ltd.
Acrylonitrile Butadiene Rubber or Nitrile Rubber (NBR)	N230S (35% Bound Acrylonitrile content), N220S* (41% Bound Acrylonitrile content)	Japan Synthetic Rubber (JSR) Co. Ltd.
Zinc oxide (ZnO)	White seal	Chemmin Co., Ltd.
Stearic acid	ST-DDK	Polychem Co., Ltd.
Carbon black	N330, N220**, N660**	Thai carbon product Co. Ltd.
Sulphur	Local-made	Chemmin Co., Ltd.

Table 2.1 Materials used in the study (continued)

Chemical name	Grade	Supplier
N-Cyclohexylbenz-thiazylsulphenamide (CBS)	Santocure CZ	Monsanto Co. Ltd.
Struktol	WB 16, 60NS Flakes	Schill&S Co. Ltd.
Ethylene Octene Rubber (EOR)	Engage 8200	DuPont Dow Elastomers Co. Ltd.
Precipitated silica	HiSil ®	PPG-Siam Silica Co.,Ltd.
Dicumyl peroxide (DCP)	Percumyl D	Chemmin Co., Ltd.

* *Used in a study of high nitrile group effect.*

** *Used in a study of black surface area effect.*

2.1.2 Apparatus

The apparatus used in the present study are summarised in Table 2.2.

Table 2.2 List of apparatus used in the present study

Apparatus	Supplier/Trade Mark
Internal Mixers	Local-made banbury internal mixer, Haake Rheocord 90
Two-Roll Mill	Labtech model LRM 150, Nishimura NS76
Oscillating Disc Rheometer	Monsanto Rheometer model 100S
Mooney Viscometer	Monsanto Rheometer model 1500
Hydraulic hot press	Wabash Genesis Series Hydraulic Press Model G30H
Dynamic Mechanical Thermal Analyser	Polymer Laboratories, MkII
Tensile Tester	Instron Universal Tester model 4301
Hardness Tester	Zwick D-7900 Hardness Tester (Shore A)

2.1.3 Compound Formulation

Raw rubber was compounded according to the formulation given in Table 2.3.

Table 2.3 Compound formulation of sulphur-cured system

Ingredients	Part per hundred of rubber (phr)
Rubber [a]	100.0
ZnO	5.0
Stearic acid	2.0
Carbon black	0.0, 30.0, 50.0[b]
Sulphur	2.5
CBS	1.5

a = Blends ratio of BR/NBR used for this study were 100/0, 80/20, 50/50, 20/80, 0/100

b = Used in a study of filler loading effect

The effect of carbon black surface area was also studied using carbon black with greater and smaller surface areas than N330, which are N220 and N660, respectively.

For an investigation of filler polarity effect, 30 phr of either carbon black or silica was used as a filler.

As for the investigation of influences of some additives, the additives studied were Struktol 60NS, Struktol WB16 and EOR 8200. The amounts used were varied between 5 and 15 phr for 60NS, between 1 and 3 phr for WB16, between 3 and 10 phr

for EOR. The additive studied was used in the compound formulation shown in Table 2.3 with the blend ratios of 100/0, 50/50, 20/80 and 0/100.

For a study of curing system effect, compounds with both sulphur and peroxide curing systems were investigated. The compound formulation used in sulphur cured-system is shown in Table 2.3 and that of peroxide-cured system is shown in Table 2.4.

Table 2.4 Compound formulation of peroxide-cured system

Ingredients	Part per hundred of rubber (phr)
Rubber [a]	100
DCP	1

a = Blends ratio used for this study were 100/0 , 80/20 , 50/50 , 20/80 and 0/100

2.1.4 Mixing Procedure

NBR was first masticated for 6 mins. in a 1.2-liter local-made banbury internal mixer before being used in blending process in order to reduce a viscosity difference between BR and NBR. All rubber compounds were prepared using the internal mixer. A rotor speed of 50 rpm and a set temperature of 40°C were used with a fill factor of 0.6. Detail of mixing procedure is shown in Table 2.5.

Table 2.5 Mixing procedure used in preblended compound preparation

Action	Time (min)
Add BR and masticated NBR	0
Add stearic acid and ZnO and additive	1
Add filler	4
Add sulphur and CBS or DCP	10
Dump the mix	13

To compare the black-NBR interaction, NBR and carbon black were mixed for 6 mins using the internal mixer at mixing temperatures of 30°C and 100°C. NBR masterbatches were then kept at room temperature overnight before being used in blending process at 30°C. Detail of mixing procedure is shown in Table 2.6.

Table 2.6 Mixing procedure used in cutback of NBR black-masterbatches

Action	Time (min)
Add BR and NBR black-masterbatches	0
Add stearic acid and ZnO	1
Add sulphur and CBS	10
Dump the mix	13

For a study of viscosity effect, NBR and BR were prepared as preblended masterbatches in Haake Rheomix at a set temperature of 140°C, rotor speed of 40 rpm and filled factor of 0.6 in order to equalise the viscosity between BR and NBR.

Mixing procedure is shown in Table 2.7. Thereafter, the preblended masterbatches were kept at room temperature overnight before adding curing agent at 30°C using Haake Rheomix according to the mixing procedure as described earlier in Table 2.6.

Table 2.7 Mixing procedure for preblended masterbatches preparation at high temperature of 140°C

Action	Time (min)
Add BR and NBR	0
Add carbon black	9
Dump the mix	14

In all cases, after dumping from the mixing chamber, the rubber mix was sheeted using cold two-roll mill.

2.2 Determination of Mooney viscosity

Mooney viscometer (Monsanto Model 1500) with a large rotor was used to measure the Mooney viscosity. The test temperature was set at 100 °C. The Mooney viscosity was determined according to ASTM D1646-87 and reported as (ML 1+4) in Mooney Unit. At least 5 samples for each formula were used for a measurement.

2.3 Determination of bound rubber content

The bound rubber content was determined in the following way. At first, 0.2 g of rubber compound (W) was soaked in 25 ml of tetrahydrofuran (THF) and kept in the dark at room temperature for 14 hours. Thereafter, the rubber sample was filtered using filter paper (#1) and dried at 50 °C until a constant weight (W_{fg}) was obtained. For each measurement, 3 rubber samples were determined for the bound rubber content. The %bound rubber content was calculated from equation (2.1).

$$R_b = \frac{W_{fg} - W[M_f/(M_f + M_p)]}{W[M_p/(M_f + M_p)]} \times 100 \quad \textbf{(2.1)}$$

where R_b = Bound rubber content (%)

W = Weight of compound used for extraction (g)

W_{fg} = Weight of dried rubber after being extracted by THF (g)

M_f = Weight of filler (g)

M_p = Weight of polymer (g)

2.4 Determination of cure characteristics

Cure characterisatics of rubber compounds were determined using the Oscillating Disk Rheometer (Monsanto 100 S) at the test temperature of 155 °C. The main cure characteristics obtained were scorch time (t_2) and cure time (t_{90}). At least 4 samples were determined for a measurement.

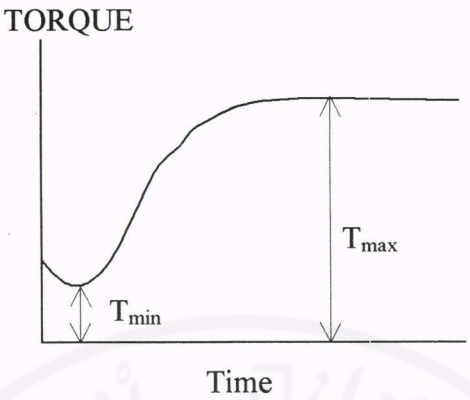

Scorch time (t_2) = Time to reach 2% of (T_{max}-T_{min})

Cure time (t_{90}) = Time to reach 90% of (T_{max}-T_{min})

Figure 2.1 Typical cure curve determined from ODR

2.5 Preparation of rubber vulcanisate for mechanical property measurement

Vulcanisates to be used for measuring mechanical properties were prepared by compression moulding in the hot press at 155 °C, under a pressure of 150 kg/cm^2. Cure time used was determined from ODR with an additional time of 3 minutes for thermal equilibrium. The mould dimensions used are given in Table 2.8.

Table 2.8 Mould dimensions

Properties	Mould dimension (mm) length×width×thickness
Tensile	160×160×2
Hardness	25×25×6

2.6 A measurement of carbon black distributed in each phase of blends

Filler distribution in blends was determined using a Dynamic Mechanical Thermal Analyser (DMTA, Polymer Laboratories , MkII), based on the reduction in tan δ_{max} as filler loaded. The rectangular specimens were cut from the compression-moulded sheets with known dimensions. The specimen length (l) is the distance between the specimen supports; in this work the small frame was used, i.e. 5.00 mm. The test was carried out under bending mode of deformation with a single cantilever. Frequency selected was 3 Hz and the strain selected was 45 μ (nominal peak-to-peak displacement). The experiments were carried out from -130 °C to 50 °C at a heating rate of 5 °C/min. A low-temperature sample reclamping technique was used to tackle the possibility of sample shrinkage at low temperatures, particularly at the temperature below glass-transition temperature. At least 2 samples were used for a measurement. Carbon black distribution in each phase of blend was calculated using equation (2.2) and (2.3) [13].

$$R = \frac{(\tan \delta_g)_{max} - (\tan \delta_f)_{max}}{(\tan \delta_g)_{max}} \qquad \textbf{(2.2)}$$

where tan δ_{max} = damping peak height values determined from DMTA

g and f = gum (unfilled) and filled systems, respectively

$$W'_1 = \frac{R'_1 R_2 W}{R'_1 R_2 + R'_2 R_1} \qquad \textbf{(2.3)}$$

where 1 and 2 = two different single rubber system

W = filler-to-polymer weight fraction

Details regarding equations (2.2) and (2.3) were mentioned in section 1.2.2.3.

2.7 Mechanical property measurement

2.7.1 Tensile properties

Tensile strength, modulus and elongation at break were measured per ASTM D412-92 using the Instron tensile tester (Model 4301) at a cross head speed of 500 mm/min with the load cell of 1 kN. Vulcanised sheets were cut into the dumb-bell shape with the dimensions as shown in Figure 2.2. The thickness of the dumb-bell test pieces was measured by a micrometer and 15 pieces of test samples were used for each measurement.

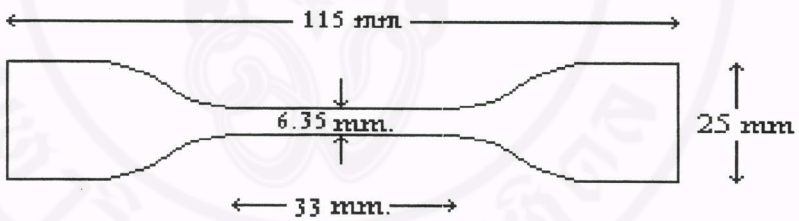

Figure 2.2 Dimensions of the tensile specimen

2.7.2 Hardness

The hardness of rubber vulcanisate was determined at room temperature using Zwick D-7900 Durometer with Shore A hardness scale. The cylindrical shape samples (16 ± 0.3 mm in diameter and 6 mm in thickness) were used for the test. The method of measurement was based on ASTM D2240-9. At least 4 samples were used for a measurement.

2.7.3 Oil Resistance

The test method provides a procedure for exposing test specimens to the test oil. The resulting deterioration was determined by changes in sample weight and hardness after immersion in the test oil at 100 °C for 70 hours.

The cylindrical shape samples (16±0.3 mm in diameter and 6 mm in thickness) were used for the test. Hardness (H_1) and weight of the test specimen in air (M_1) were measured initially. Four specimens of a single composition were used for each measurement, and were immersed in the bottle containing 70 cm^2 of the test oil (GRENA DX, see Appendix D).

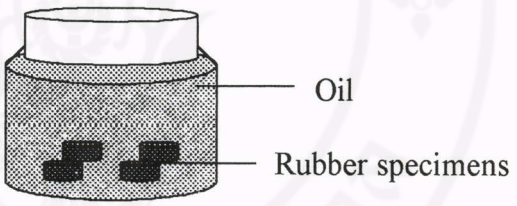

Figure 2.3 Oil resistance apparatus for weight and hardness change determinations

After oil immersion at 100 °C, the test specimens were removed from the oil. The specimens must be cooled down to room temperature by transferring the specimens to cool oil for 60 mins. Any excess oil at the surface of the specimen must be eliminated by diping the specimens quickly in acetone, and bloting lightly with filter paper before determining the hardness (H_2) and mass (M_2). The percentage of changes in hardness and mass were calculated using equations (2.4) and (2.5), respectively.

$$\text{Change in hardness (\%)} = \frac{(H_2 - H_1)}{H_1} \times 100 \quad \textbf{(2.4)}$$

$$\text{Change in mass (\%)} = \frac{(M_2 - M_1)}{M_1} \times 100 \quad \textbf{(2.5)}$$

where H_1 = Hardness of specimen before immersion (Shore A)

H_2 = Hardness of specimen after immersion (Shore A)

M_1 = Mass of specimen before immersion (g)

M_2 = Mass of specimen after immersion (g)

CHAPTER III

RESULTS AND DISCUSSION

3.1 Effects of blend ratio of BR/NBR, carbon black surface area and black loading on carbon black distribution in BR/NBR blends

3.1.1 Rheological properties

The results obtained reveal that the viscosity of blends is affected by factors such as viscosity of individual rubber, blend ratio, filler dispersion and interaction between rubber and filler. Each factor will be discussed separately as follows.

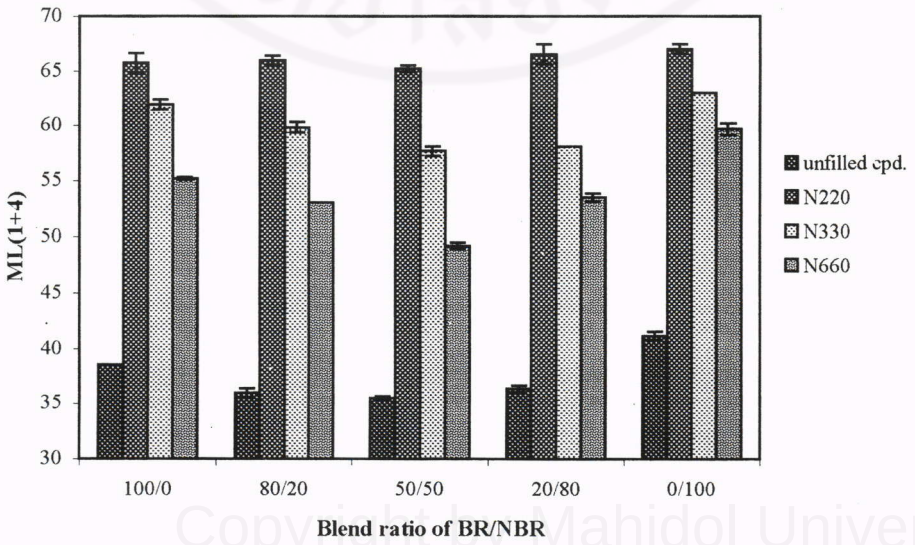

Figure 3.1 Relationship between blend ratio and Mooney viscosity

Figure 3.1 shows viscosities of blend compounds with varied blend ratios and grades of carbon black. It has been found that the Mooney viscosities of the blends are lower than the theoretical values (which are obtained from the mixture rule), and also lower than the pure components, which are probably attributed to : (1) curing system effect [6] and (2) poor interaction between BR and NBR [28-29]. The former hypothesis has been investigated on the compounds with different curing systems as well as without curing agent. The Mooney results obtained, as shown in Figure 3.2, reveal that the viscosities of compounds without curing agent are higher than that of peroxide and sulphur curing systems respectively. The lowest compound viscosity observed in sulphur curing system is due to the stearic acid added performing as a softener. However, it is obvious that the viscosities of blends are still lower than the additive line, indicating that the curing system is not mainly responsible for the blend viscosities lower than the theoretical values, and can therefore be disregarded.

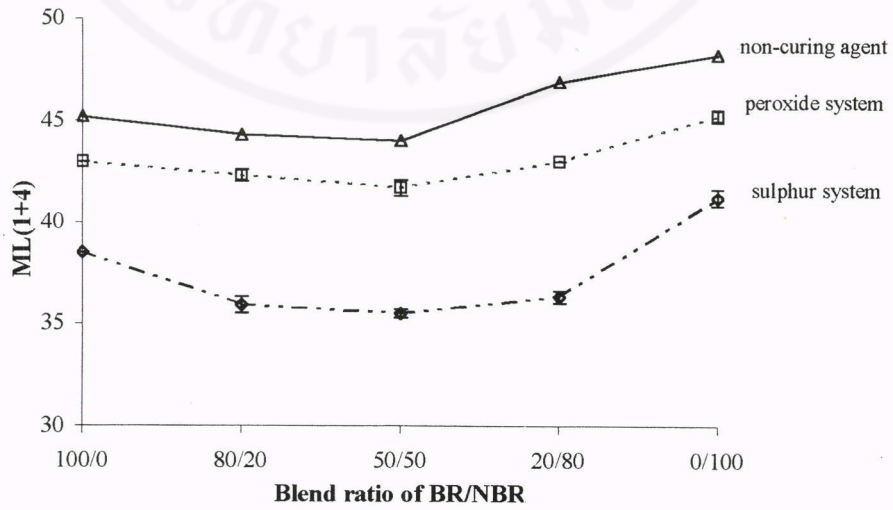

Figure 3.2 Relationship between curing systems and Mooney viscosity

The poor interaction between BR and NBR has been investigated by indirect method based on calorimetry as suggested by Schuster [30]. In immiscible blends, an increase in temperature generally leads to a reduction in the deficiencies of blend mixing, i.e. better solubility and a reduction in the interfacial tension, or to an improved interpenetrating of polymer chains at the phase boundary resulting in the broad phase boundary layer formation. The development of the phase boundary layer becomes evident in rubber with a tendency of thermal crystallisation. The interaction of the different types of chains in the phase boundary layer results in a cessation of the arrangement in crystalline superstructures of rubber in blends [30]. In the present study, 100/0, 80/20 and 50/50 BR/NBR (without curing agent) samples were characterised by DSC and the normalised exothermal energy at T_c of BR was then calculated, as illustrated in Table 3.1.

Table 3.1 Normalised exothermal energy at T_c of BR in single system and blends

Unfilled compounds	Energy (J/g)
100/0	-38.0
80/20	-37.6
50/50	-35.8

It can be seen from Table 3.1 that % crystallization of blends is not significantly different from the pure BR which is a clear evidence of poor interaction between BR and NBR supporting the Mooney result as shown previously in Figures 3.1 and 3.2.

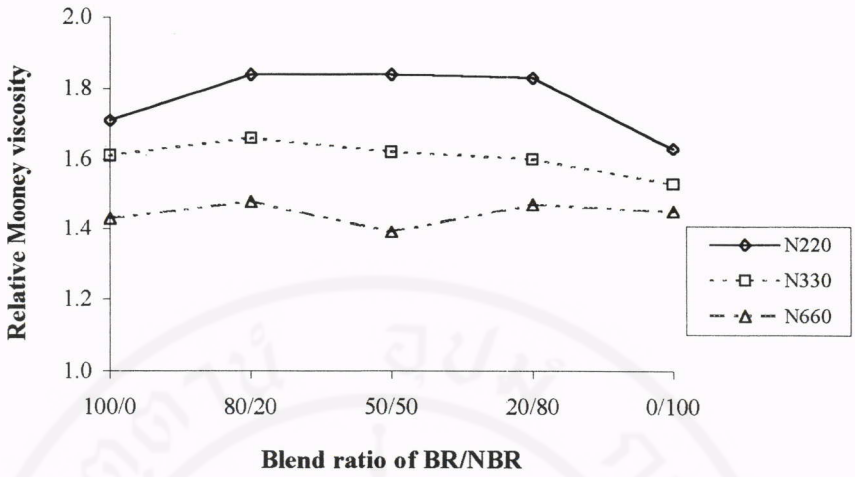

Figure 3.3 Relative Mooney viscosity of compounds with different blend ratios and surface areas of carbon black

From Figure 3.3, it is clear that the relative viscosity of BR is higher than that of NBR, due to the stronger interaction between carbon black and BR. The stronger interaction is confirmed by a larger amount of bound rubber content of BR than NBR for all grades of carbon black studied, as illustrated in Table 3.2.

Table 3.2 % Bound rubber content of BR and NBR

BR/NBR blend ratio	Bound Rubber Content (%)		
	N220	N330	N660
100/0	26.94 ± 0.13	23.91 ± 0.21	21.45 ± 0.33
0/100	24.60 ± 0.28	22.52 ± 0.58	20.73 ± 0.13

In addition, Figure 3.3 shows that N220 carbon black gives highest relative viscosity followed by N330 and N660, respectively which is due to the highest surface area of N220 [31].

3.1.2 Cure properties

Cure properties are illustrated in Figures 3.4-3.6. Figure 3.4 shows that, for the unfilled systems, the scorch time of a BR single system is somewhat shorter than that of NBR, and the scorch time of unfilled blends increases almost linearly with NBR content up to a BR/NBR ratio of 20/80. By contrast, the blend ratio of 0/100 exhibits slightly shorter scorch time than 20/80. Figure 3.5 shows that the cure time (t_{90}) of NBR is shorter than that of BR and that of the blends decreases with increasing of NBR. Figure 3.6 shows that the cure rate of NBR is higher than that of BR. Therefore, the cure time of blends decreases and the cure rate increases with increasing NBR content, which could be caused by solubility and diffusion differences of curatives in the blends (i.e. the curative imbalance between the component phases) [6, 32]. Sulphur and CBS are soluble curatives and tend to migrate readily from one rubber to the other. When added to the blends, curatives are distributed initially in the matrix and then migrate to the dispersed phase [6]. However, the matrix still contains a larger amount of curatives than the dispersed phase. In this study, BR and NBR are significantly different in polarity, which results in an imbalance of curatives between rubber phases, leading to a denser network in the BR phase as a matrix than in NBR dispersed phase for 80/20 and 50/50 BR/NBR blends. For 20/80 blend, NBR matrix is overcured while BR dispersed phase is undercured, which is in agreement with the experimental results of dynamic mechanical properties to be discussed below.

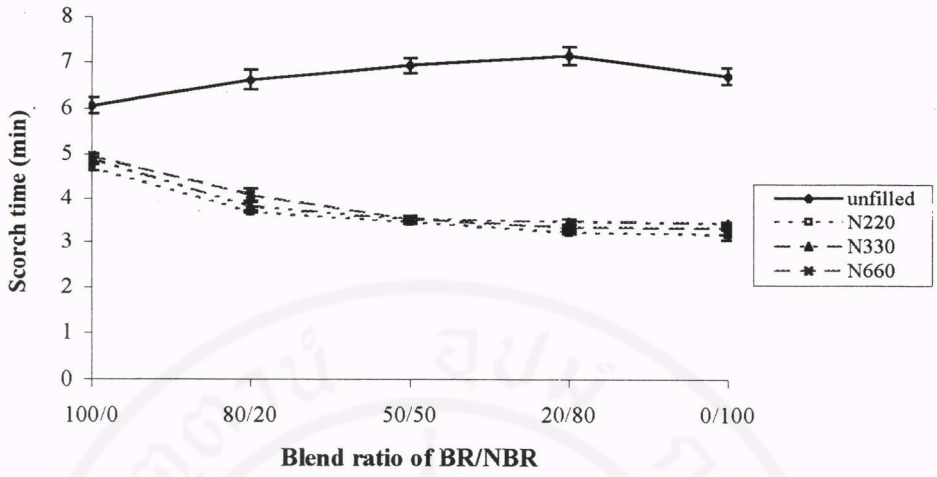

Figure 3.4 Relationship between scorch time and blend ratios

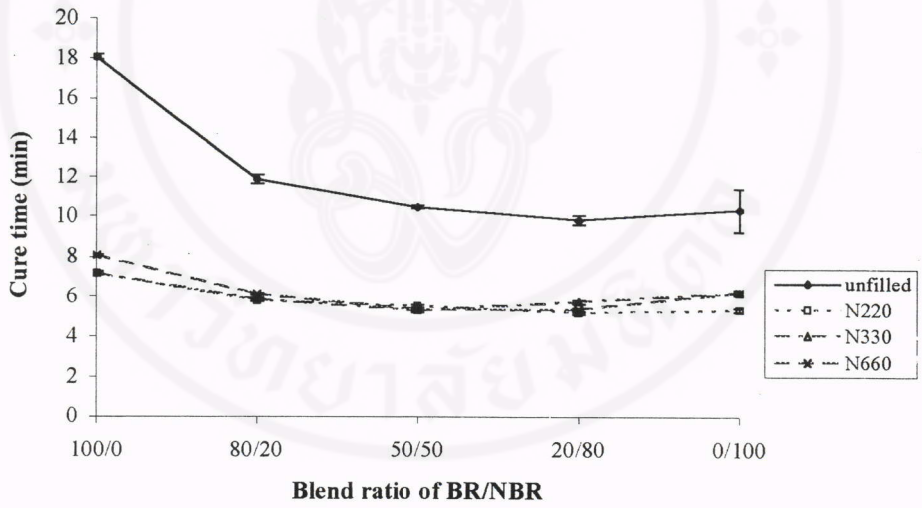

Figure 3.5 Relationship between cure time and blend ratios

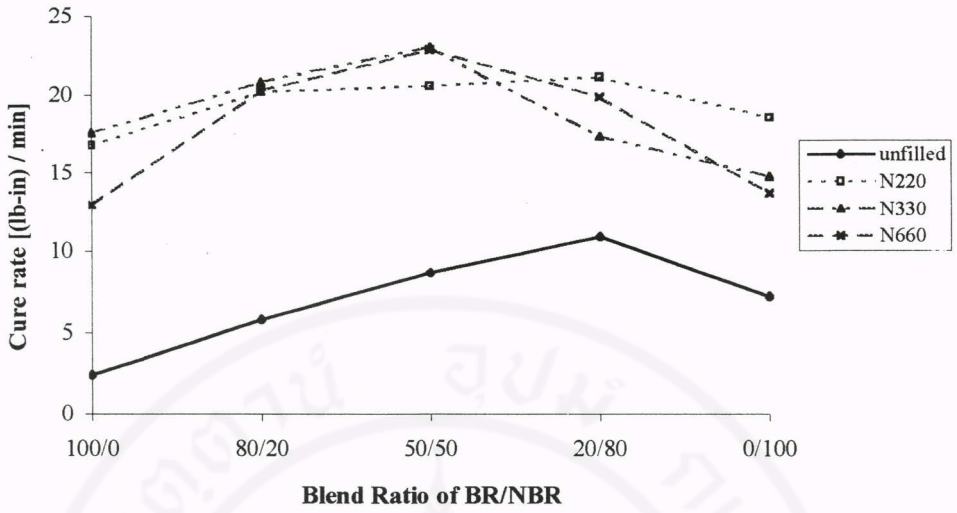

Figure 3.6 Relationship between cure rate and blend ratios

The degree of vulcanisation in the different phases of BR/NBR blend is measured by the dynamic mechanical thermal analyser (DMTA). The samples of the blend ratio of 50/50 BR/NBR are vulcanised to various degrees of cure (i.e. by varying vulcanisation time). The results obtained are shown in Figures 3.7 and 3.8.

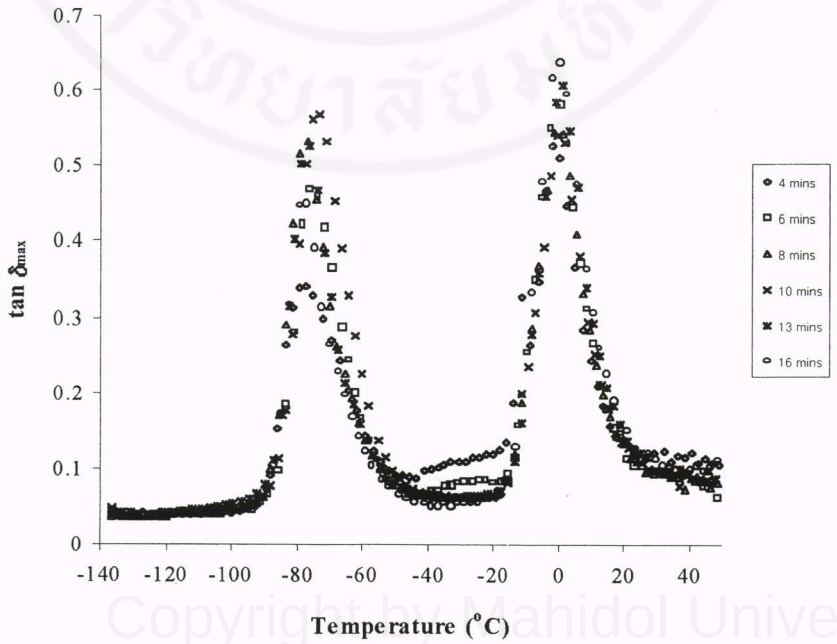

Figure 3.7 The extents of vulcanisation in different phases of 50/50 BR/NBR blends

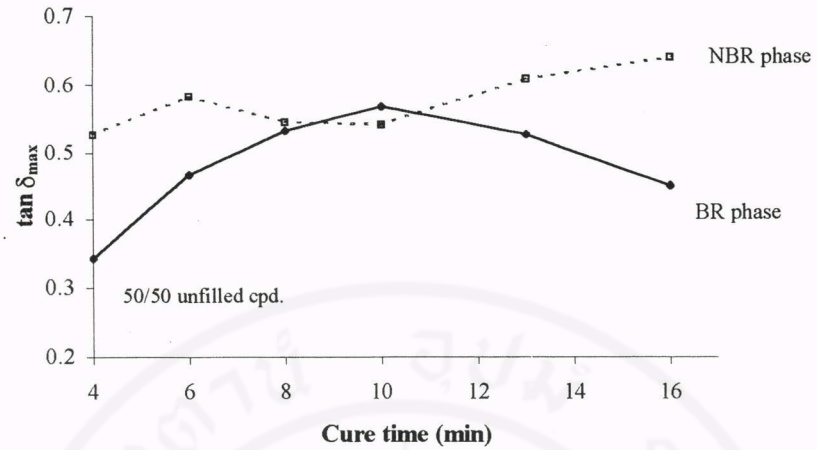

Figure 3.8 Relationship between cure time and tan δ_{max}

From Figure 3.8, it is obvious that the BR phase shows an increase in tan δ peak height whereas NBR phase shows a decrease in tan δ peak height with increasing cure time from 6 to 10 mins. After 10 mins, the tan δ peak height of BR phase decreases and that of NBR increases. The possible explanation is as follows. At curing time shorter than 6 mins, BR and NBR phases are still under-cured since the scorch times of BR and NBR are 6.06 and 6.72, respectively and scorch time of 50/50 is 6.94 (see Table 3.3).

Table 3.3 Scorch time (t_2) and cure time (t_{90}) of BR, NBR and 50/50 blend

BR/NBR blend ratio	Scorch time (min)	Cure time (min)
100/0	6.06 ± 0.18	18.04 ± 0.13
50/50	6.94 ± 0.16	10.48 ± 0.07
0/100	6.72 ± 0.18	10.34 ± 1.08

As cure time changed from 6 to 10 mins (i.e. nearly the optimum cure times for 50/50 and 0/100 blends), the tanδ peak height of NBR decreases due to an increase in degree of crosslinking. The observed increase in tan δ peak height of BR is due to the slow cure rate of BR as shown in cure curve of Figure 3.9.

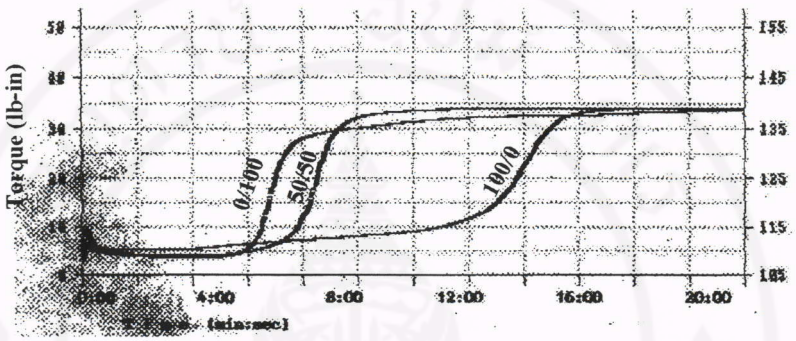

Figure 3.9 Cure curves of BR, NBR and 50/50 blend obtained from ODR

After 10 mins, cure rate of BR increases significantly, leading to a decrease in tan δ peak height of BR phase with increasing cure time. It must be noted that at the time shorter than the scorch time and that longer than cure time, the value of tan δ_{max} increases with increasing cure time, due mainly to the thermal degradation of rubber. In other words, the value of tan δ_{max} reduces when the increase in degree of crosslink overides the thermal degradation. By contrast, the value of tan δ_{max} increases when the effect of thermal degradation is dominated. The thermal degradation curves of BR and NBR are illustrated in Figure 3.10.

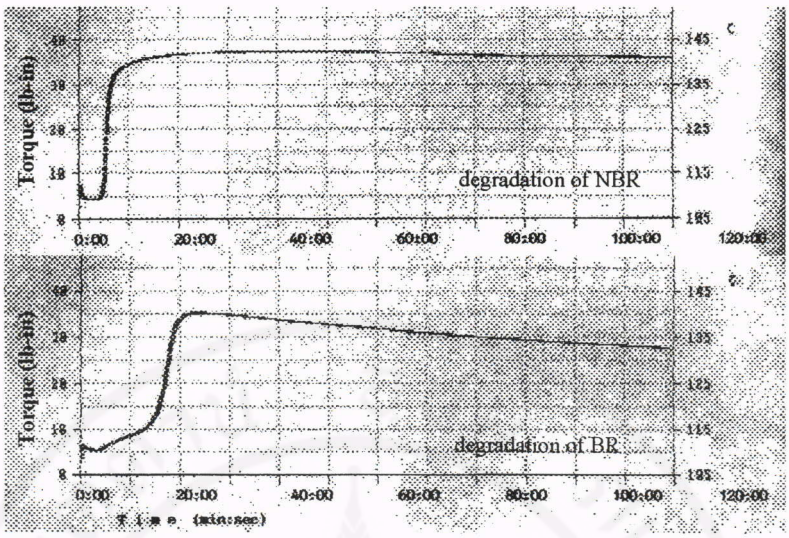

Figure 3.10 Thermal degradation curves of BR and NBR obtained from ODR

Relationship between maximum torque (T_{max}) and blend ratio measured from ODR illustrated in Figure 3.11 shows equal T_{max} of 100/0, 80/20 and 50/50, indicating similar phase morphology in these blends, i.e., the dispersed NBR in BR matrix. The proposed morphology is confirmed by transmission electron micrographs and by the oil resistance results (to be discussed in the next section). Torque of the blend ratio of 20/80 is in between that of 100/0 and 0/100 due to the dilution effect.

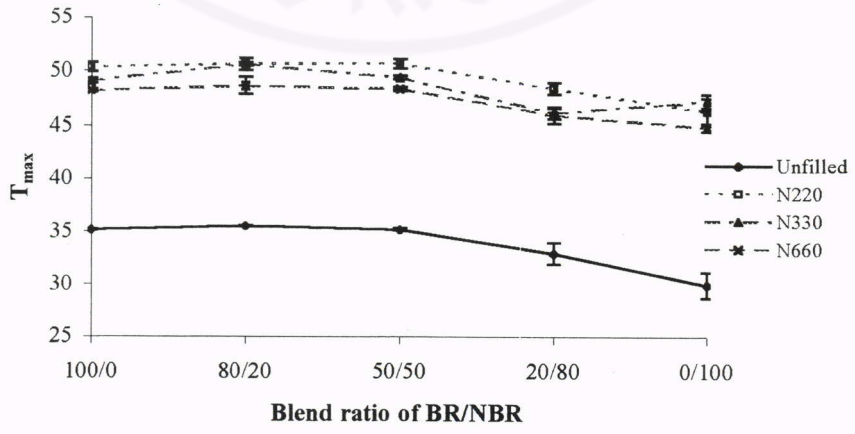

Figure 3.11 Relationship between T_{max} and blend ratio obtained from ODR

From Figures 3.5 and 3.6, it has also been found that cure times of filled compounds are shorter and cure rates are higher than those of the unfilled ones. This is simply due to the active chemical groups on carbon black surface [33] and of relatively good heat transfer of carbon black. Relationships between relative T_{max} as well as relative minimum torque (T_{min}) -ratio of torques of filled to unfilled compounds-, and blend ratio are illustrated in Figures 3.12 and 3.13.

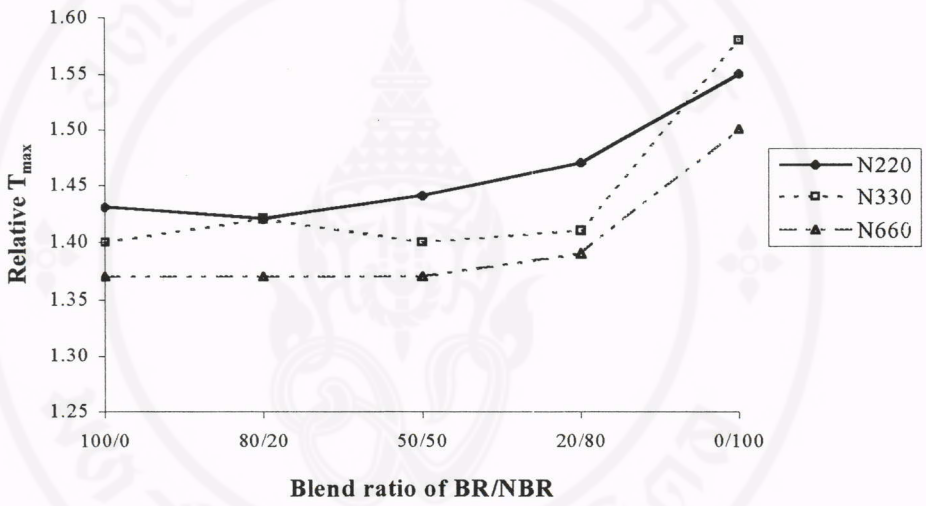

Figure 3.12 Relationship between relative T_{max} and blend ratios

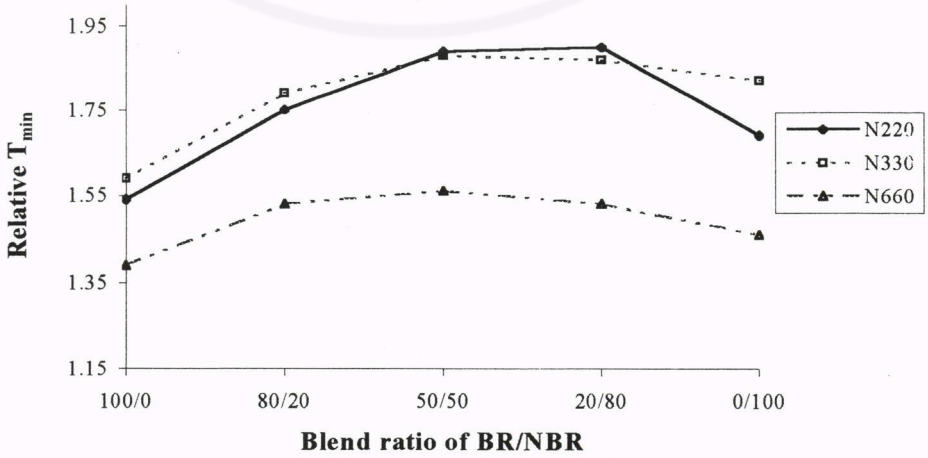

Figure 3.13 Relationship between relative T_{min} and blend ratios

It can be seen that the relative T_{max} and T_{min} of N220 are higher than those of N330 and N660 respectively, because of the reinforcing effect. Effects of carbon black distribution in blends, of blend ratio and of black loading on scorch time, cure time and cure rate are illustrated in Figures 3.14 to 3.16. It can be seen that the cure properties of the unfilled compounds are relatively affected by the blend ratio. However, in the case of filled compound, the effect of carbon black distribution in blends overrides the effects of blend ratio and black loading on cure properties. Scorch time and cure time decrease with increasing the ratio of amount of carbon black in BR phase to the amount of BR. When this ratio is larger than 0.6, the scorch time and cure time slightly change. Cure rate also sharply increases with increasing this ratio up to 0.6. With the ratio larger than 0.6, cure rate is slightly change since NBR is the matrix and BR is the dispersed phase in 20/80 blend.

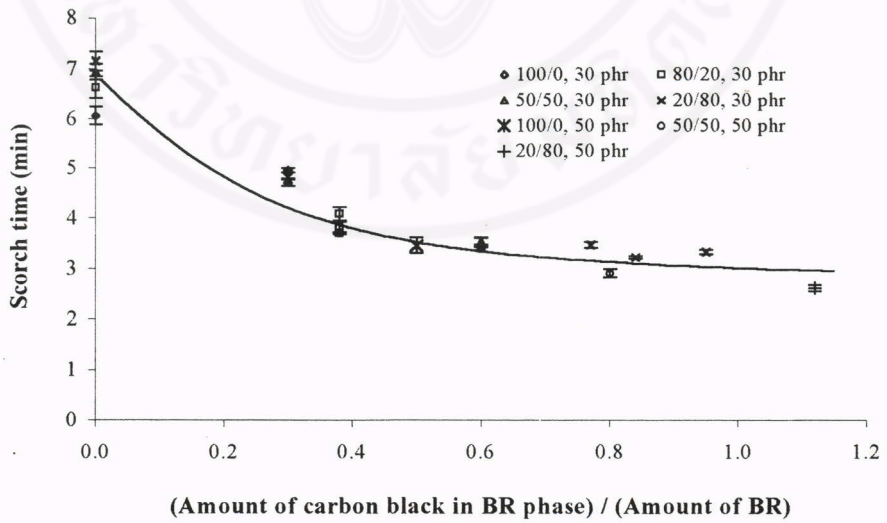

Figure 3.14 Effect of carbon black distribution on scorch time in compounds with different blend ratios and black loadings (marks on y axis are unfilled compound)

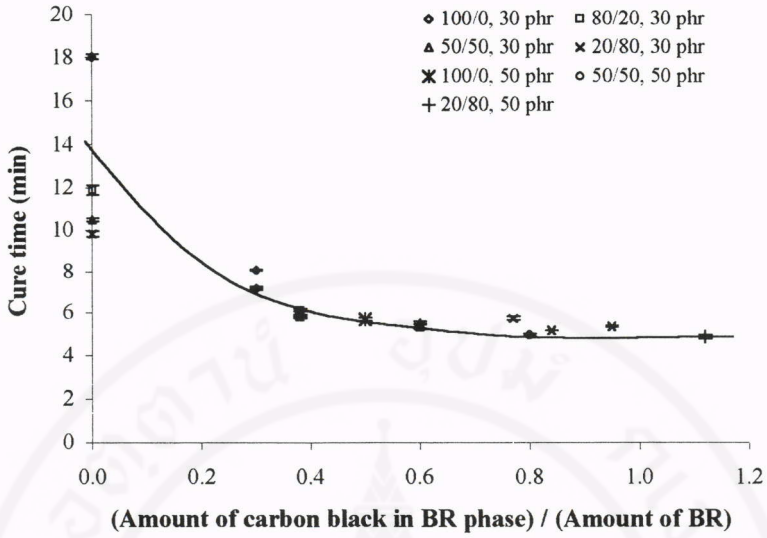

Figure 3.15 Effect of carbon black distribution on cure time in compounds with different blend ratios and black loadings (marks on y axis are unfilled compound)

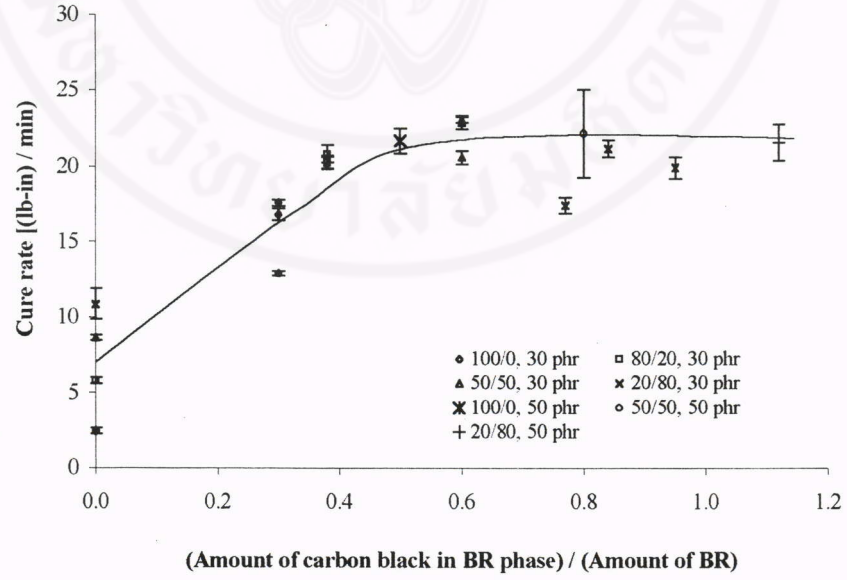

Figure 3.16 Effect of carbon black distribution on cure rate in compounds with different blend ratios and black loadings (marks on y axis are unfilled compound)

3.1.3 Dynamical properties

The DMTA results show that morphology of BR/NBR blend is the two-phase structures. There are two relaxation peaks at about –72 and 0°C, corresponding to the BR and NBR phases, respectively.

3.1.3.1 Effects of carbon black surface area on mechanical damping properties of BR, NBR and their blends

The DMTA results obtained reveal that the tan δ_{max} of BR and NBR decreases with increasing carbon black surface area or with reducing black size. From Figures 3.17 to 3.19, it is clear that the magnitude of decrease in tan δ_{max} is more significant in BR than in NBR, due to the stronger interaction between carbon black and BR. The strong interaction between carbon black and BR can be supported by the result of bound rubber content, as illustrated previously in Table 3.2.

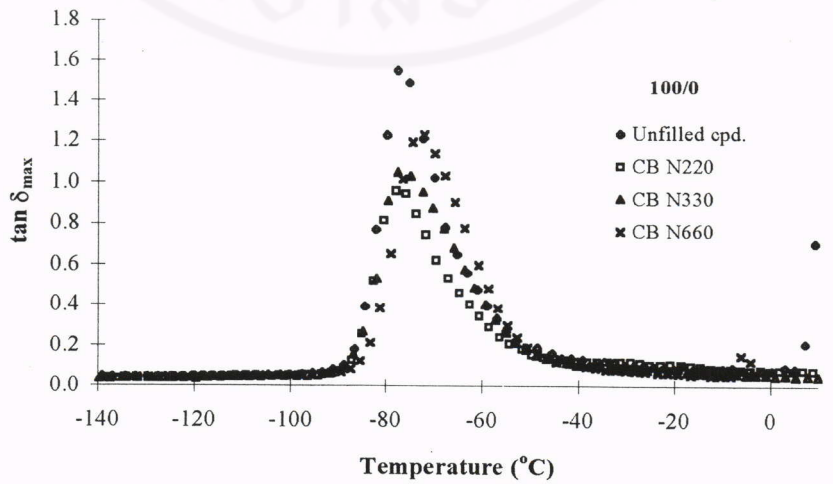

Figure 3.17 Relationship between carbon black surface area and damping properties in BR

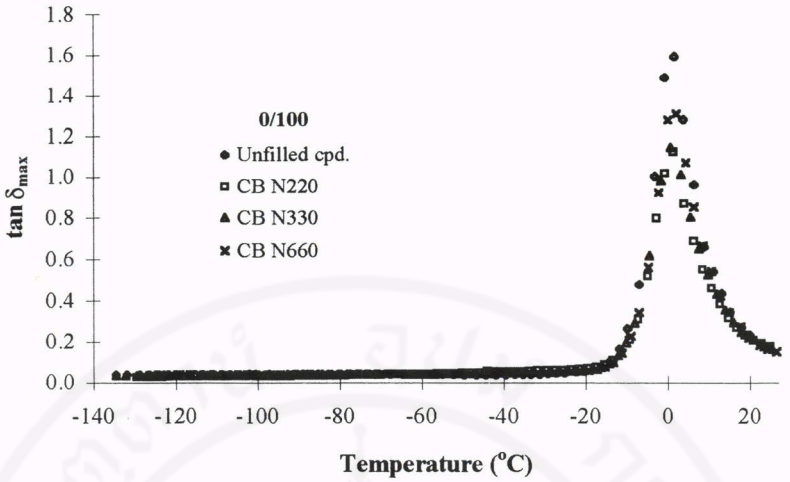

Figure 3.18 Relationship between carbon black surface area and damping properties in NBR

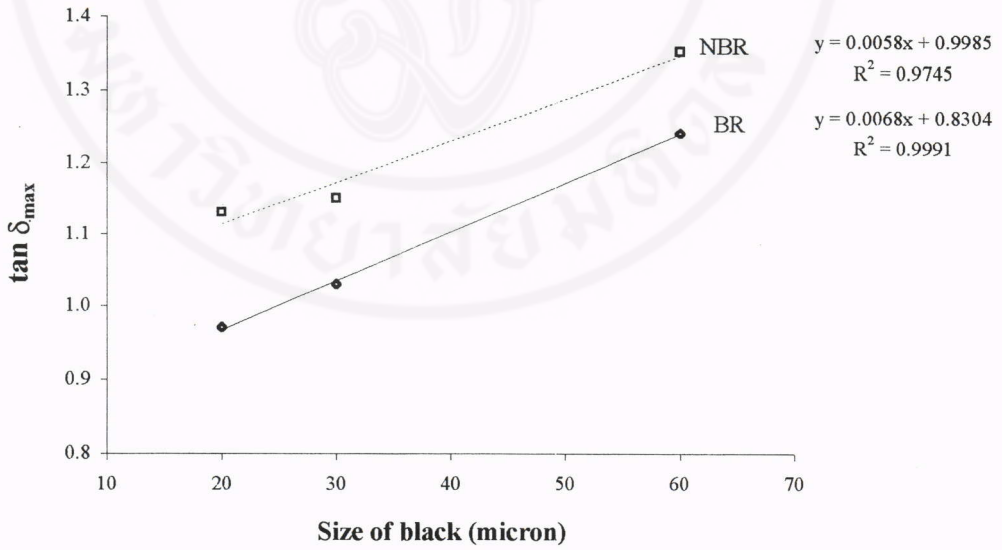

Figure 3.19 Relationship between damping properties and size of carbon black in BR and NBR

The use of damping peak (tan δ_{max}), which decreases with filler loading, will enable one to calculate the distribution of carbon black in each phase of blends [13, 23]. Results of carbon black distribution in BR/NBR blends are shown in Tables 3.4-3.6. It can be seen that BR is more preferential for all 3 particle sizes of carbon black to reside than NBR. As the BR/NBR ratio decreased, BR phase becomes gradually saturated with carbon black and the black will then migrate to NBR phase. Generally, the main reasons for the imbalance in carbon black migration to BR phase are due to the relatively low viscosity of BR phase [12, 7] and relatively strong interaction between carbon black and BR phase.

Table 3.4 Distribution of N220 carbon black in BR/NBR blends

BR/NBR blend ratio	Amount of carbon black distribution in each phase of blend (phr)	
	BR phase	NBR phase
80/20	30.0	0.0
50/50	30.0	0.0
20/80	16.3	13.7

Table 3.5 Distribution of N330 carbon black in BR/NBR blends

BR/NBR blend ratio	Amount of carbon black distribution in each phase of blend (phr)	
	BR phase	NBR phase
80/20	30.0	0.0
50/50	30.0	0.0
20/80	15.5	14.5

Table 3.6 Distribution of N660 carbon black in BR/NBR blends

BR/NBR blend ratio	Amount of carbon black distribution in each phase of blend (phr)	
	BR phase	NBR phase
80/20	30.0	0.0
50/50	30.0	0.0
20/80	20.5	9.5

3.1.3.2 Effects of carbon black loading on mechanical damping properties of BR, NBR and their blends

The effect of carbon black loading on tan δ_{max} of the single rubber, 50/50 and 20/80 BR/NBR blends is shown in Figures 3.20 to 3.23.

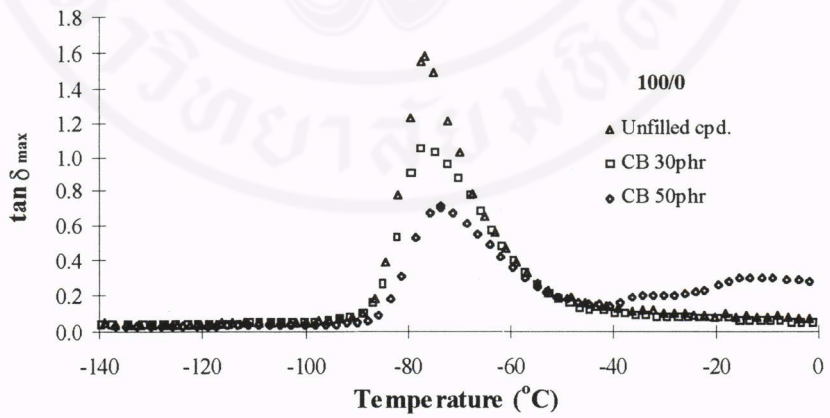

Figure 3.20 Relationship between damping properties and black loading in BR

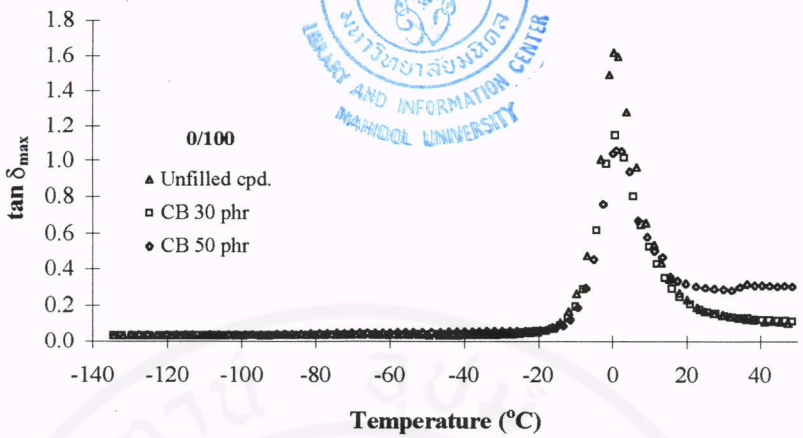

Figure 3.21 Relationship between damping properties and black loading in NBR

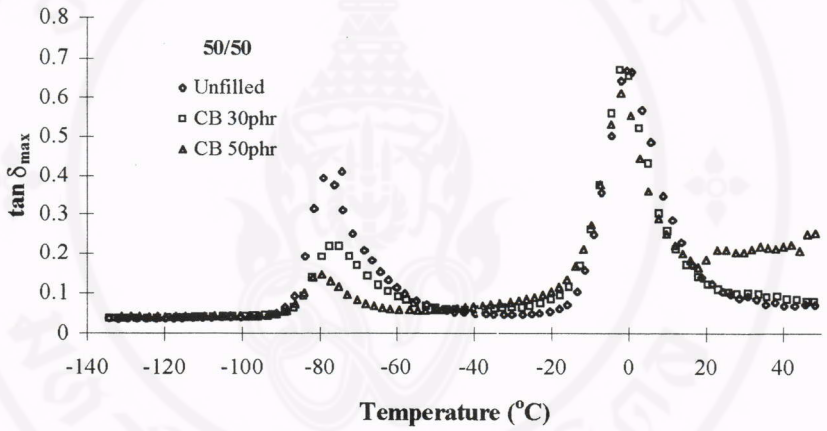

Figure 3.22 Relationship between damping properties and black loading in 50/50 BR/NBR blends

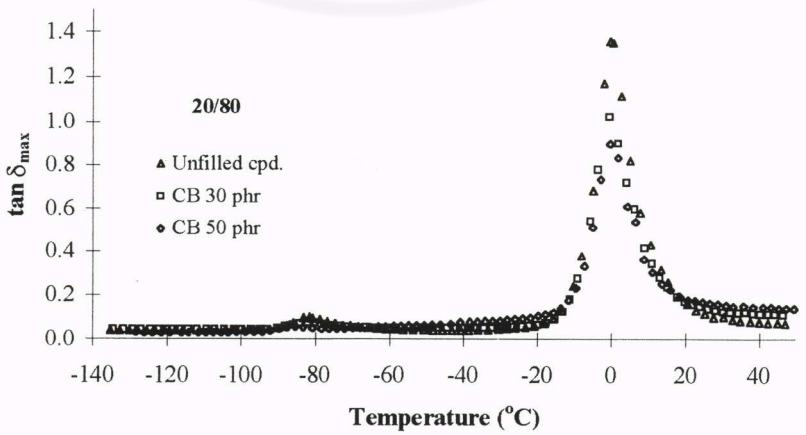

Figure 3.23 Relationship between damping properties and black loading in 20/80 BR/NBR blends

It is clear that tan δ_{max} decreases with black loading for both BR and NBR. NBR phase in 50/50 blend shows on unchange in tan δ_{max} when 30 phr of black is added, which is probably attributed whole 30 phr of carbon black residing in BR phase shown earlier in Tables 3.4-3.6.

Effect of black loading on carbon black distribution in 50/50 and 20/80 BR/NBR blends is shown in Tables 3.7 and 3.8. It can be seen that BR is more preferential for carbon black to reside than NBR, which is in agreement with results reported previously elsewhere [23]. As the BR/NBR ratio decreased and/or carbon black loading increased, BR phase becomes gradually saturated with black which will then migrate to NBR phase.

Table 3.7 Effect of carbon black loading on black distribution in 50/50 BR/NBR blend

Rubber phase	Amount of carbon black residing in each rubber phase (phr)	
	30-phr loaded compound	50-phr loaded compound
BR	30.00	40.38
NBR	0.00	9.62

Table 3.8 Effect of carbon black loading on black distribution in 20/80 BR/NBR blend

Rubber phase	Amount of carbon black residing in each rubber phase (phr)	
	30-phr loaded compound	50-phr loaded compound
BR	15.48	22.35
NBR	14.52	27.65

3.1.4 Mechanical Properties

3.1.4.1 Tensile Properties

The tensile properties of compounds are shown in Figures 3.24-3.28. It has been found that modulus and tensile strength of blends are higher than the theoretical additive line indicating the synergistic effect. Relative tensile strength illustrated in Figure 3.27 increases with increasing surface area or reducing size of carbon black due to the increased reinforcing effect in rubber compounds (i.e., N220>N330> N660).

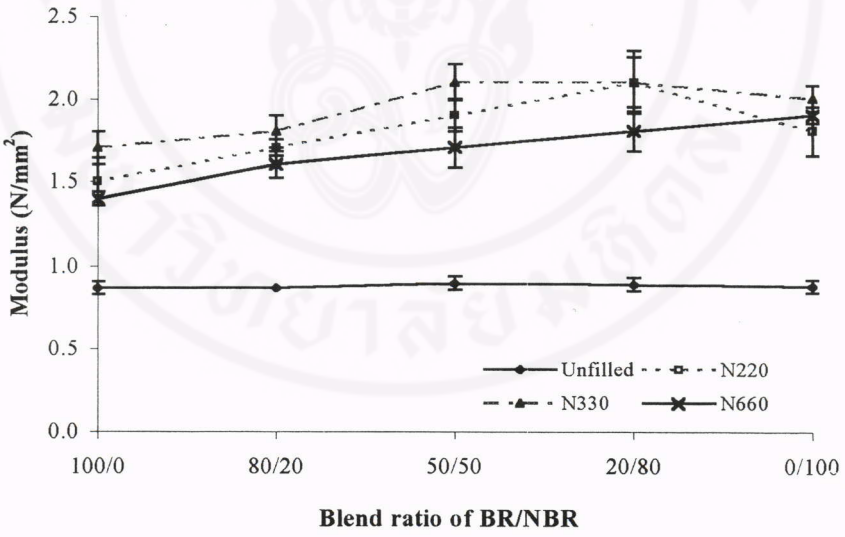

Figure 3.24 Relationship between modulus at 50 % strain and blend ratios

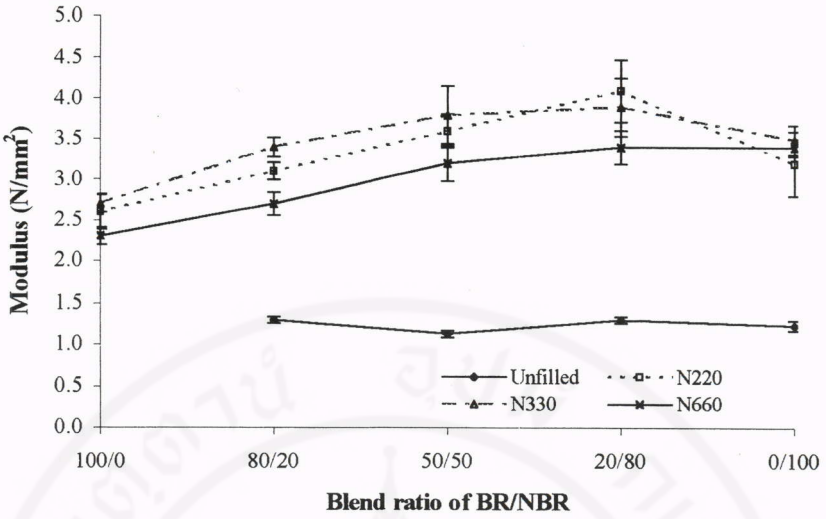

Figure 3.25 Relationship between modulus at 100% strain and blend ratios

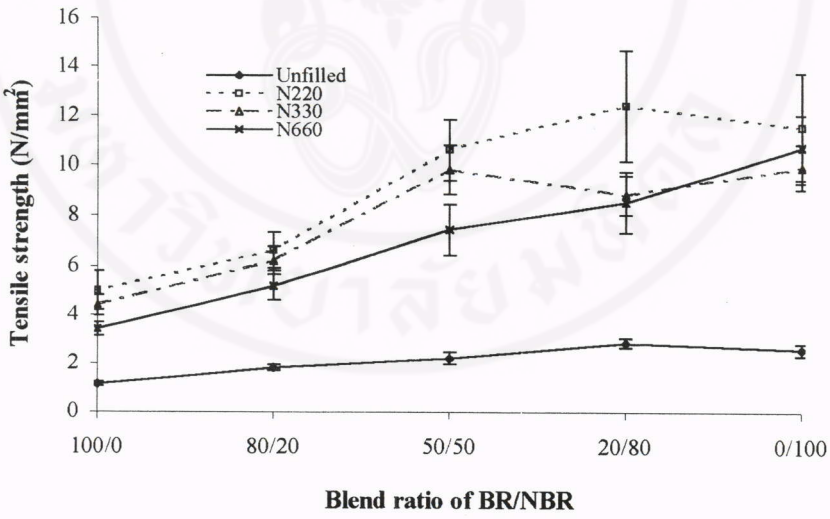

Figure 3.26 Relationship between tensile strength and blend ratios

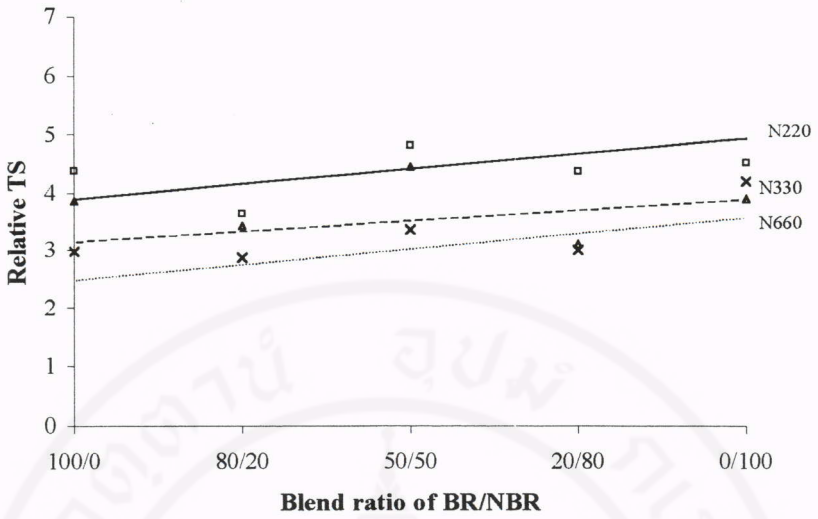

Figure 3.27 Relationship between relative tensile strength and blend ratios

The blend ratio of 100/0 of the filled compound shows higher elongation at break than the unfilled one as shown in Figure 3.28, which is possibly affected by the decrease in crosslink density of BR that can be supported by the swelling test of BR with and without carbon black. The crosslink density of BR phase is calculated from equation (3.1).

$$(\%)\ \text{Oil swelling} = \frac{W_2 - W_1}{W_R} \times 100 \qquad (3.1)$$

where

W_1 and W_2 = weights of sample before and after immersed in oil, respectively

W_R = weight of BR in sample

The swelling results obtained are illustrated in Table 3.9 showing that the crosslink density of the unfilled compound is higher than that of filled compound. Therefore, it

is clear that the high elongation at break of 100/0 filled compound is due to the decrease in crosslink density, as carbon black is added.

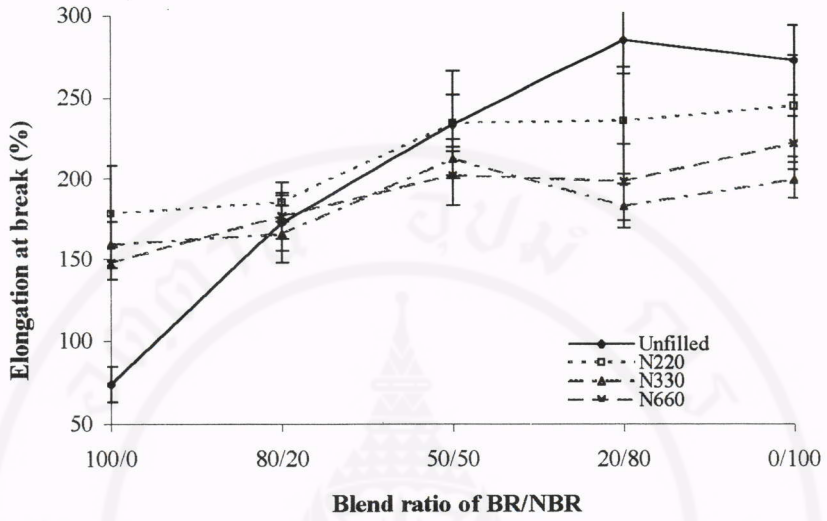

Figure 3.28 Relationship between % elongation at break and blend ratios

Table 3.9 Effect of carbon black[a] on crosslink density in BR

Compound	Oil swelling in BR phase (%)
100/0 unfilled compound	18.74 ± 0.75
100/0 filled compound	20.86 ± 0.18

[a] *carbon black 30 phr added*

Effects of carbon black distribution in blends, of black loading and of blend ratio on tensile properties are illustrated in Figures 3.29 to 3.31. It is clear that in the case of unfilled compounds, the blend ratio strongly affects the elongation at break but slightly influences tensile strength and does not affect the modulus. However, in the case of filled compound, the effects of carbon black distribution and black loading override the effect of blend ratio. The tensile strength and % elongation at break

increase with increasing the ratio of amount of black in BR phase to the amount of BR up to 0.8. Above this ratio where NBR becomes the matrix in 20/80 blends, the tensile strength and % elongation at break decrease. When higher black levels are added (i.e. 50 phr), the tensile strength is not affected which is opposite to % elongation at break.

It can be seen from Figure 3.29 that modulus at 50% strain increases with this ratio up to 0.7. When the ratio is greater than 0.7, modulus is approximately independent of the ratio and is strongly affected by black loading instead. The hardness results shown in Figure 3.32 reveal obviously similar trend to the modulus results.

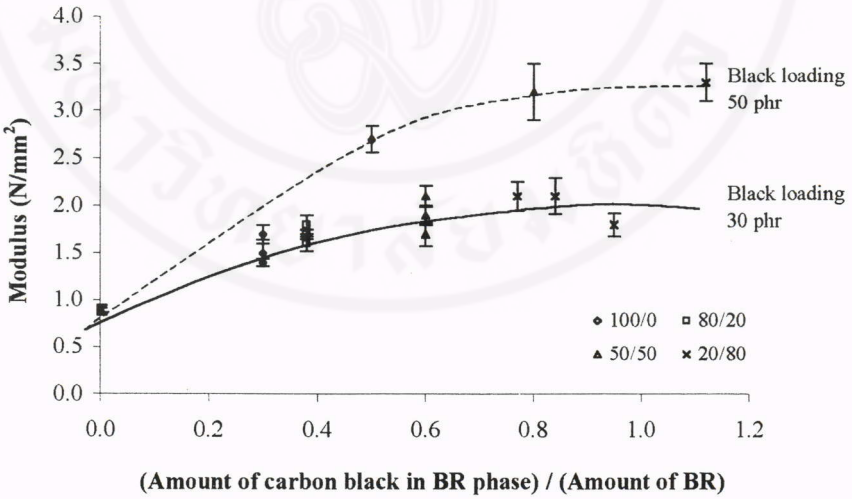

Figure 3.29 Effect of carbon black distribution on modulus at 50% strain in compounds with different black loadings and blend ratios of BR/NBR (marks on y axis are unfilled compound)

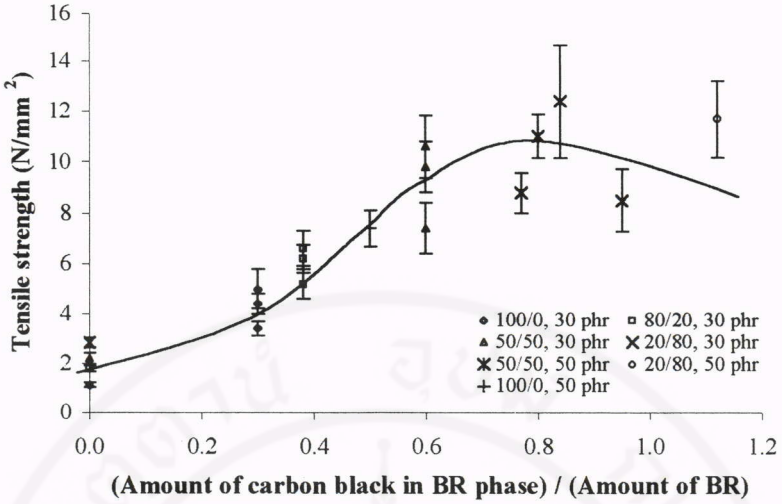

Figure 3.30 Effect of carbon black distribution on tensile strength in compounds with different black loadings and blend ratios of BR/NBR (marks on y axis are unfilled compound)

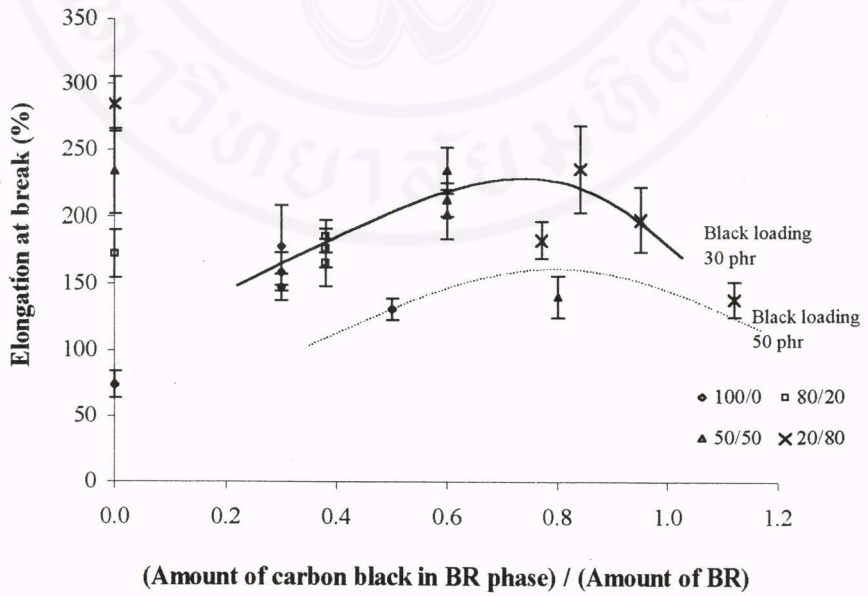

Figure 3.31 Effect of carbon black distribution on % elongation at break in compounds with different black loadings and blend ratios of BR/NBR (marks on y axis are unfilled compound)

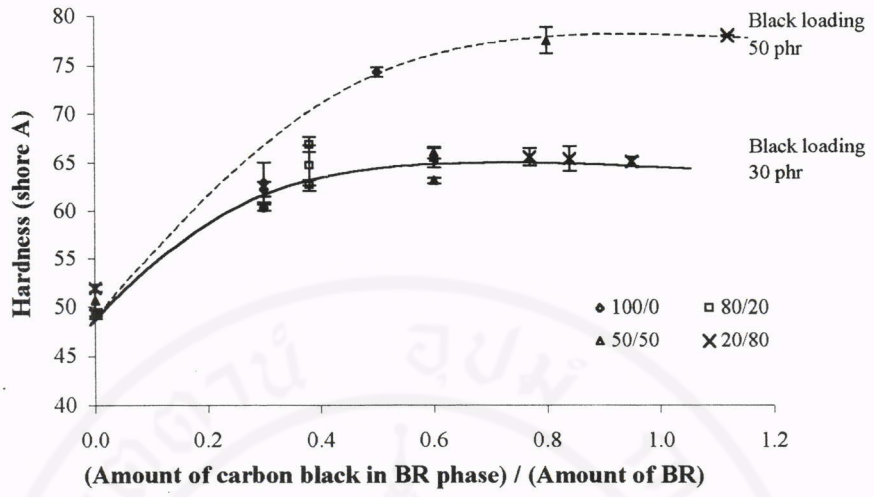

Figure 3.32 Effect of carbon black distribution on hardness in compounds with different black loadings and blend ratios of BR/NBR (marks on y axis are unfilled compound)

3.1.4.2 Oil resistance properties

Nitrile rubber has been widely used as oil resistant rubber because of its polar nitrile groups on polymer chains. Therefore, the blends with NBR as a matrix shows higher oil resistance than those with BR as a matrix. The oil resistance results obtained are shown in Figures 3.33 and 3.34. It can be seen that weight and hardness of compounds with blend ratios of 100/0, 80/20 and 50/50 change more significantly after immersed in oil than those of 0/100 and 20/80 blends. The key factor responsible for the results is the phase morphology of the blends. In other words, oil resistance of the blends increases with increasing NBR content. As mentioned earlier, NBR is the matrix in 20/80 blend whereas BR is the matrix in 80/20 and 50/50 blends.

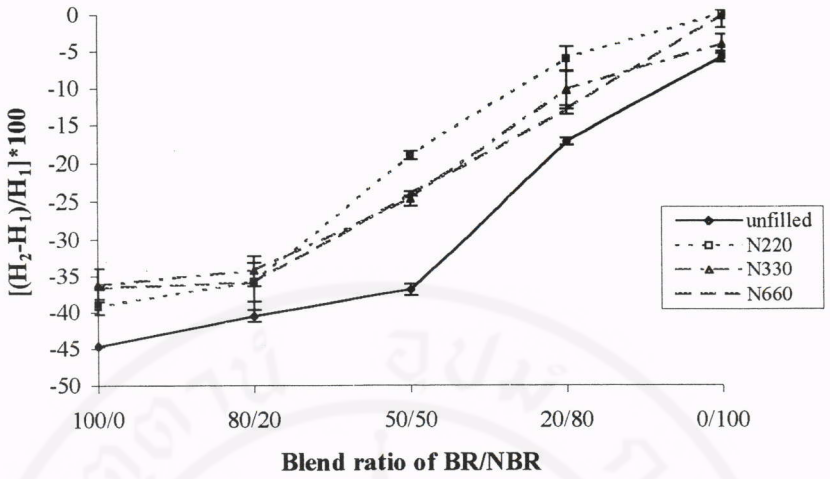

Figure 3.33 Relationship between blend ratios and oil resistance based on the hardness change

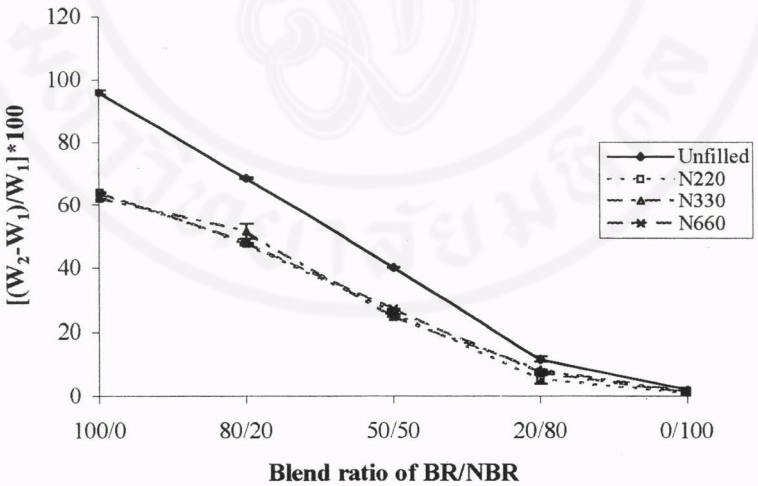

Figure 3.34 Relationship between blend ratios and oil resistance based on the weight change

3.2 Factors affecting carbon black distribution in BR/NBR blends

From results in the first part (section 3.1), it is believed that origins of the uneven black distribution in blends (i.e., carbon black resides preferentially in BR phase) are : (1) relatively low viscosity of BR, (2) relatively high unsaturation of BR and (3) relatively strong interaction between filler and BR. In this part, factors affecting carbon black distribution were studied in detail.

3.2.1 Viscosity difference between BR and NBR

The viscosity difference between BR and NBR was varied using temperature for preparing the preblended masterbatches. The main adventage of the use of temperature to control viscosity difference between BR and NBR is that it gives resproducible results within a short time when compared with a conventional mastication method, due to the high mastication-resistance of BR and NBR. The effect of temperature on rubber viscosity is illustrated in Figure 3.35.

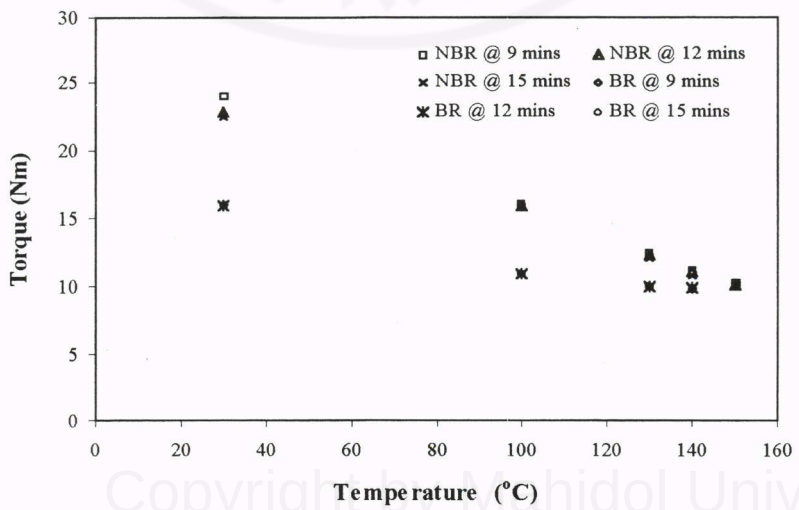

Figure 3.36 Relationship between mixing temperature and torque obtained from torque rheometer with different mastication times

Figure 3.35 shows that the viscosity differences between BR and NBR reduce with increasing temperature. Since BR starts to degrade at a temperature of 150°C, temperatures of 30 and 140°C were chosen for controlling the viscosity ratio in this study. The detail of mixing procedure was described earlier in section 2.1.4. The results of black distribution in blends are illustrated in Table 3.10.

Table 3.10 Distribution of N330 carbon black in blends with different temperatures of preblends

BR/NBR Blend Ratio	Amount of carbon black[a] in BR phase (phr)	
	30°C	140°C
80/20	30.00	30.00
50/50	30.00	30.00
20/80	16.67	9.95

[a] *30 phr carbon black added to preblend*

Table 3.10 shows that the effect of compound morphology is more significant than the effect of viscosity difference. In other words, as long as the BR is the matrix (i.e. the blend ratio of 80/20 and 50/50), the black distribution in blends is not affected by the change in viscosity difference. By contrast, when BR is the dispersed phase (i.e. the blend ratio of 20/80), the viscosity difference plays significant role in black distribution and the amount of carbon black residing in NBR phase increases when the viscosity difference reduced.

3.2.2 Rubber-filler interaction

The interaction between filler and rubber is influenced by a number of factors such as polarity of filler, polarity of rubber and temperature in compound preparation. In the present study, the effect of rubber-filler interaction on the filler distribution was examined using filler with different polarity; silica and N330 carbon black. The result obtained is shown in Table 3.11.

Table 3.11 Filler distribution in BR/NBR blends

BR/NBR Blend Ratio	Amount of filler[a] in BR phase (phr)	
	Carbon black	Silica
50/50	30.00	30.00
20/80	15.48	9.18

[a] *30 phr filler added to preblend*

For the blend ratio of 20/80, the amount of filler residing in NBR phase increases with increasing polarity on filler surface, indicating the strong interaction between silanol groups on silica surfaces and acrylonitrile groups of NBR. However, for the blend ratio of 50/50, the effect of phase morphology with BR as a matrix overrides the effect of filler polarity or filler-rubber interaction.

Apart from the filler polarity, the effect of rubber polarity was studied by varying acrylonitile content of NBR from 35-41%. The result obtained is illustrated in Table 3.12.

Table 3.12 Distribution of N330 carbon black in 20/80 blend with different % acrylonitrile contents of NBR

% Acrylonitrile of NBR	Amount of carbon black[a] distribution in each phase of blend (phr)	
	BR phase	NBR phase
35	15.48	14.52
41	25.37	4.63

[a] *30 phr carbon black added to preblend*

From Table 3.12, it can be seen that the carbon black distribution is affected significantly by the difference in polarity between the BR and NBR. It appears that the amount of carbon black residing in BR phase increases with increasing acrylonitrile content of NBR, i.e., with increasing polarity of NBR.

The further experiment was carried out in order to vary the rubber-filler interaction using temperature. It has been reported earlier elsewhere that the interaction between filler and rubber increases with increasing temperature of masterbatch [34]. Therefore, when the black masterbatch is cutback with the other rubber, the filler migration from the NBR black-masterbatch to BR should, in theory, reduce with increasing temperature for preparing the black masterbatch due to the strong interaction (see Figure 3.36a). Unexpectedly, it can be seen from Table 3.13 that the amount of carbon black migrating from NBR black-masterbatch prepared at 100°C is greater than that prepared at 30°C. The proposed explanation deals with the change in magnitude of black-NBR interaction caused by the degree of black dispersion. The low mixing temperature of 30°C provides greater shear stress available for black dispersion in black NBR masterbatch, due to the higher viscosity,

as shown in Table 3.14. The improved dispersion will then increase the black-NBR interaction, leading to a decrease in black migration to BR phase [11, 35-36] (see also Figure 3.36 b). The evidence of black dispersion in NBR masterbatch was confirmed by optical micrographs, as illustrated in Figure 3.37. The micrographs reveal the large black agglomerates in the compound prepared from masterbatching at high temperature of 100°C. In other words, the carbon black dispersion reduces with increasing temperature for preparing NBR masterbatches.

Table 3.13 Distribution of filler in blends with different temperatures for preparing NBR black-masterbatches

BR/NBR Blend Ratio	Amount of carbon black[a] in BR phase (phr)	
	30°C	100°C
50/50	21.35	25.61
20/80	11.90	15.32

[a] *30 phr carbon black added to NBR for preparing NBR black-masterbatches*

Table 3.14 Mixing torque obtained from Haake Rheomix at the mixing time of 6 mins for preparing NBR masterbatch prepared for cutting back with BR

NBR masterbatch to be used for the blend ratio of	Mixing torque from Haake (Nm)	
	30°C	100°C
50/50	46	35
20/80	34	26
0/100	34	24

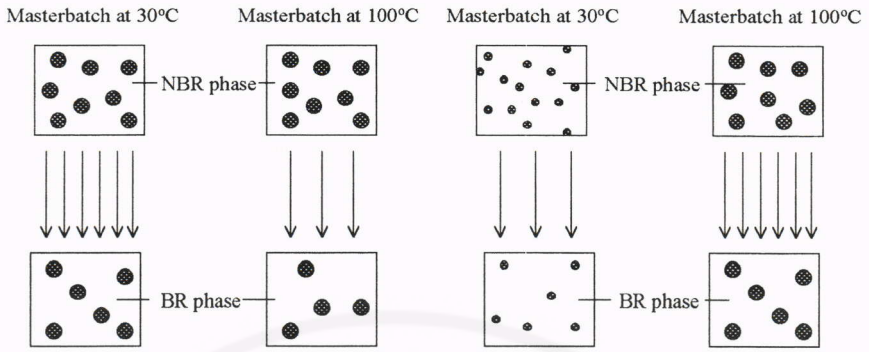

(a) In theory **(b) In experimental**

Figure 3.36 Migration of carbon black from NBR black-masterbatch to BR phase

(● : carbon black agglomerate , • : carbon black aggregate , → : degree of black migration)

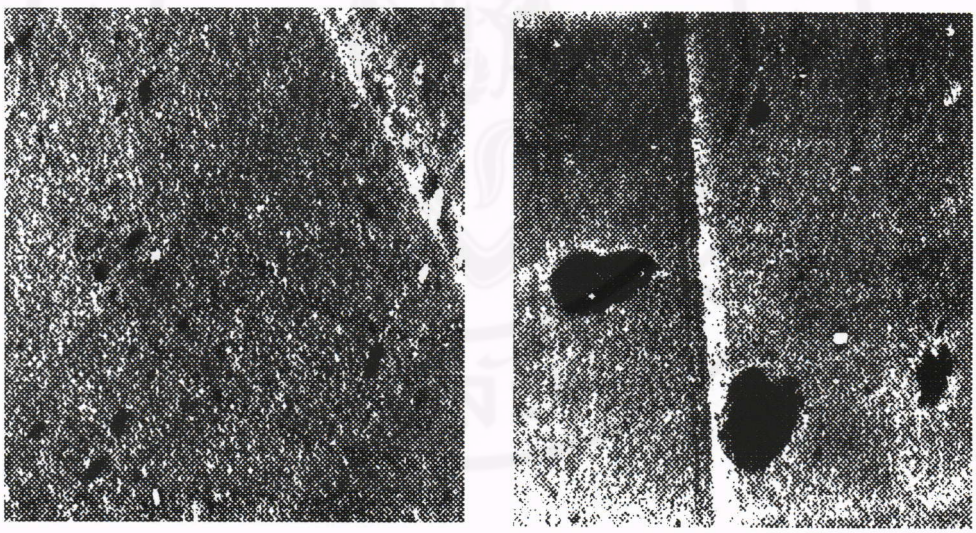

(a) Masterbatch at 30°C **(b) Masterbatch at 100°C**

Figure 3.37 Micrographs of NBR black-masterbatches prepared from different mixing temperatures (× 400)

3.2.3 Mixing sequence

From Table 3.15, it is clear that for both BR/NBR blend ratios of 50/50 and 20/80, the mixing procedure affects strongly the carbon black distribution. When carbon black is initially added to NBR, the migration of carbon black from black-masterbatch NBR to BR phase reduces drastically. The effect is more evident in the blend with BR as a matrix, i.e. in 50/50 blend.

Table 3.15 Effect of mixing sequence on carbon black distribution in blends

BR/NBR Blend Ratio	Carbon black added	Amount of carbon black[a] in BR phase (phr)
50/50	Preblend	30.00
50/50	NBR masterbatch	21.35
20/80	Preblend	16.67
20/80	NBR masterbatch	11.90

[a] *30 phr carbon black added*

3.3 Effects of some additives on carbon black distribution in blends

Struktol 60NS (a mixture of light-colored aliphatic hydrocarbon resin), Struktol WB16 (a mixture of fatty acid soap), and Ethylene octene rubber were used. The objective of this part is to investigate the effect of these additives on carbon black distribution in BR/NBR blends.

3.3.1 Struktol 60NS Flakes

In theory, Struktol 60NS which is a mixture of light-colored aliphatic hydrocarbon resin is designed and made to improve blending characteristics of elastomers with dissimilar polarity and/or viscosity, and to improve phase compatibility.

From Figures 3.38 and 3.39, it can be seen that the Mooney viscosity decreases with an addition of 60NS, which is caused by the plasticizing effect. At low loading of 60NS (i.e., 5 phr), the relative Mooney viscosity (i.e., the ratio of Mooney viscosity of compounds with to without 60NS) of 100/0 is slightly lower than 0/100 due to the greater efficiency in plasticizing effect of 60NS on BR than on NBR. However, at high loading (15 phr), 0/100 shows lower relative viscosity than 100/0, possibly due to the wall slip occurring in the Mooney viscometer. In other words, the relatively low solubility of 60NS in NBR causes a migration of 60NS to the NBR surface, leading to a wall slip between NBR and metal surfaces of Mooney rotor and chamber.

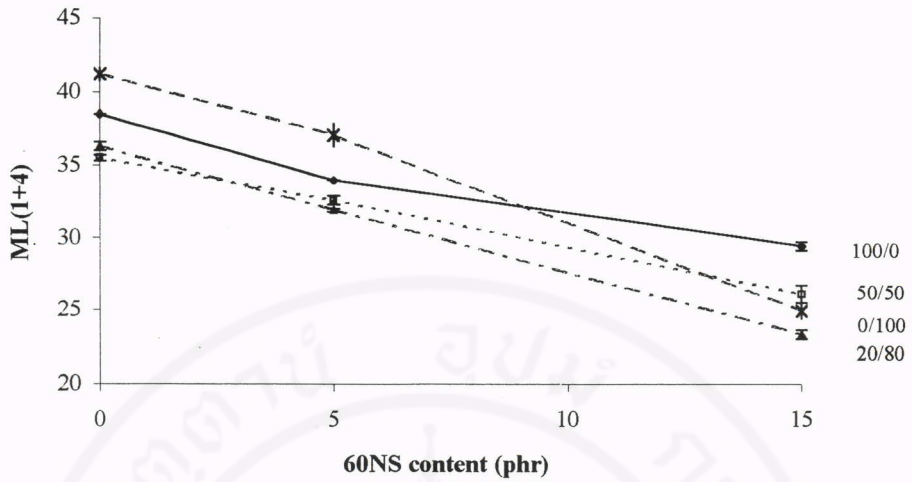

Figure 3.38 Relationship between Mooney viscosity and 60NS content with different blend ratios of BR/NBR

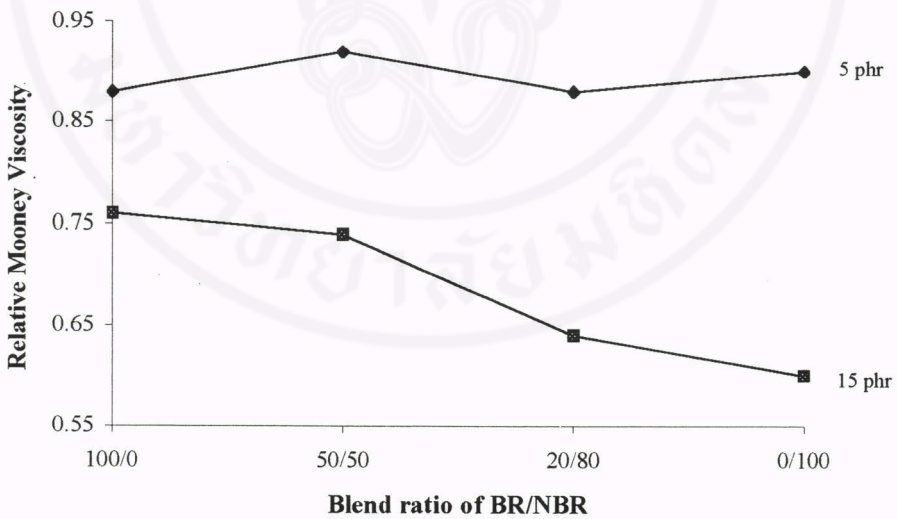

Figure 3.39 Relationship between relative Mooney viscosity and blend ratio with different 60NS loadings

From Figure 3.40, it is found that the T_{max} decreases with increasing 60NS loading due to the plasticizing effect. Wall slip effect can approximately be neglected for the ODR test because of the small amplitude of shear oscillation. Figure 3.41 shows that scorch time increases with increasing 60NS, except for the blend ratio of 20/80 and 0/100 where the effect is inversely observed at low loading of 60NS. However, cure time is insignificantly affected by 60NS as shown in Figure 3.42. From Figure 3.43, it appears that pure NBR shows a decrease in cure rate whereas pure BR shows a slightly increase in cure rate with increasing 60NS. At low loading of 60NS, cure rate of the blend increases with increasing 60NS, but decreases at high loading of 60NS. The possible explanation is that BR is more preferential for 60NS to reside than NBR. As loading of 60NS increased, BR phase becomes gradually saturated with 60NS, and 60NS then migrates to NBR phase.

The effect of 60NS on carbon black distribution in blends is illustrated in Table 3.16. Carbon black resides preferentially in BR phase, due to the viscosity of BR phase reduced by the addition of 60NS. Notably, the amount of 60NS added does not influence the black distribution in 50/50 blends since the amount of BR phase is probably sufficient for the whole 30 phr of carbon black to reside in BR phase.

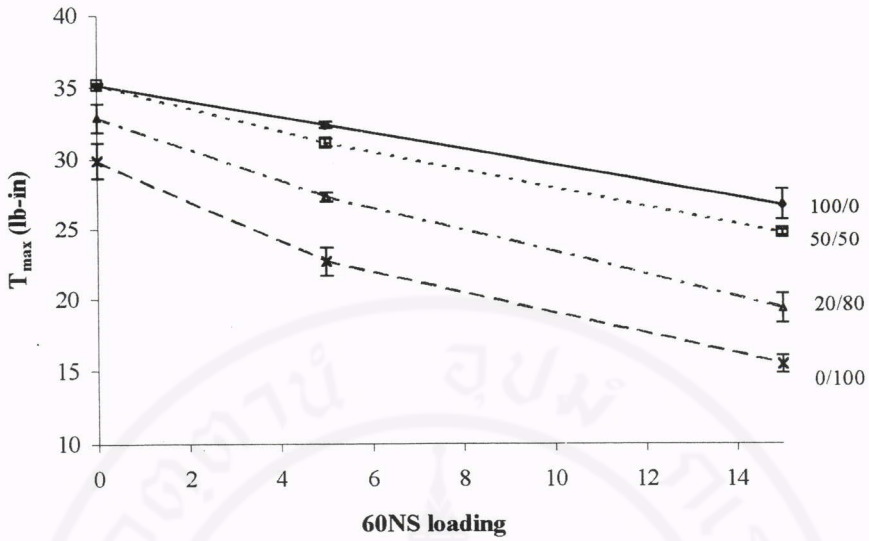

Figure 3.40 Relationship between T_{max} and loading of 60NS with different blend ratios of BR/NBR

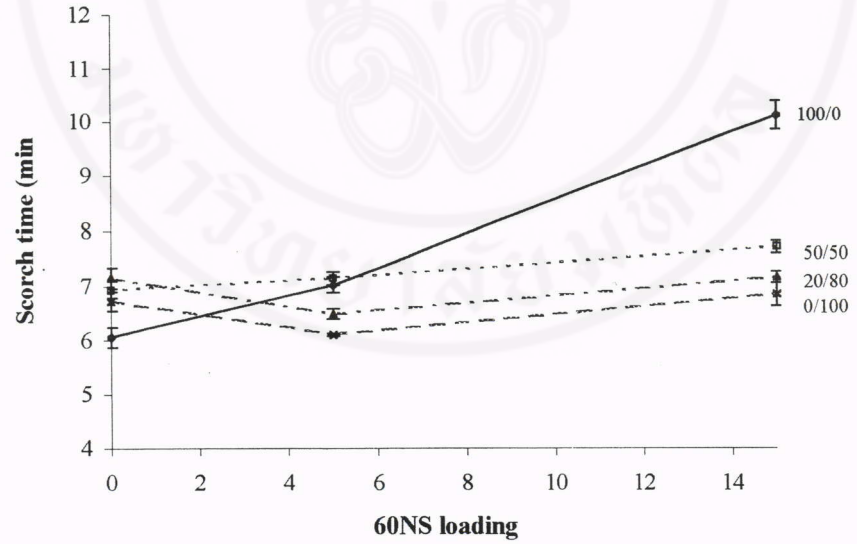

Figure 3.41 Relationship between scorch time and loading of 60NS with different blends ratios of BR/NBR

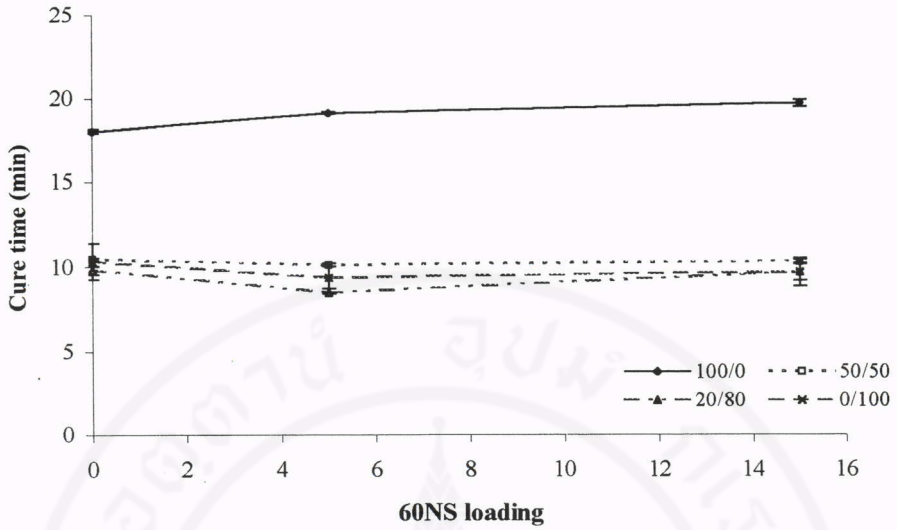

Figure 3.42 Relationship between cure time and 60NS loading with different blend ratios of BR/NBR

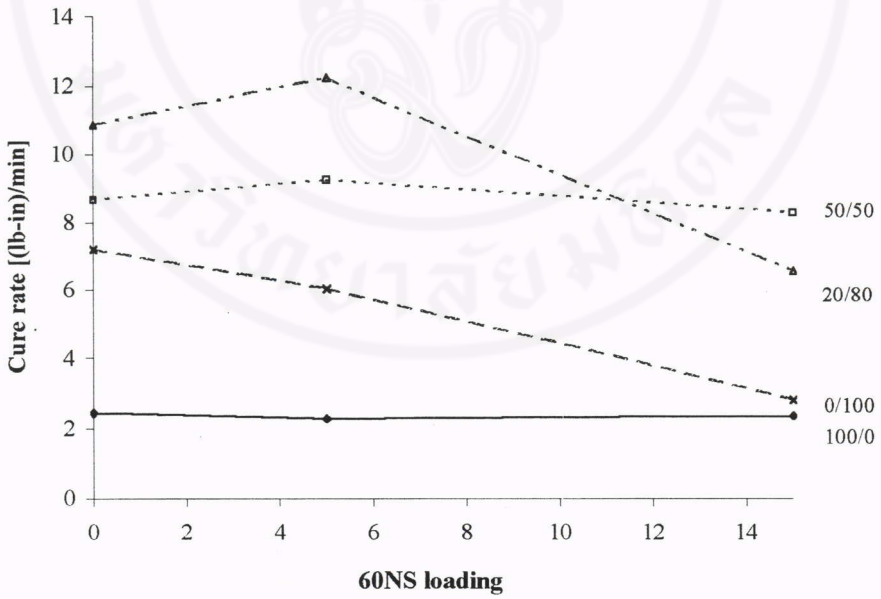

Figure 3.43 Relationship between cure rate and 60NS loading with different blend ratios of BR/NBR

Table 3.16 Distribution of black in blends with different 60NS loadings and blend ratios

BR/NBR Blend Ratio	Amount of carbon black[a] in BR phase (phr)		
	0 phr	5 phr	15 phr
50/50	30.0	30.0	30.0
20/80	15.5	21.6	20.9

[a] *N330 carbon black loading of 30 phr*

The interaction between 60NS and BR or NBR, and the migration of 60NS in the blends are confirmed by DMTA results, as illustrated in Figures 3.44 to 3.46. Since the 60NS is the mixture of non-polar aliphatic hydrocarbons, it interacts strongly with BR particularly at 15 phr 60NS resulting in an increase in T_g of BR. The opposite trend is observed in the case of NBR, i.e. approximately no shift of T_g with an addition of 60NS, indicating relatively weak interaction between 60NS and NBR (see Figure 3.44).

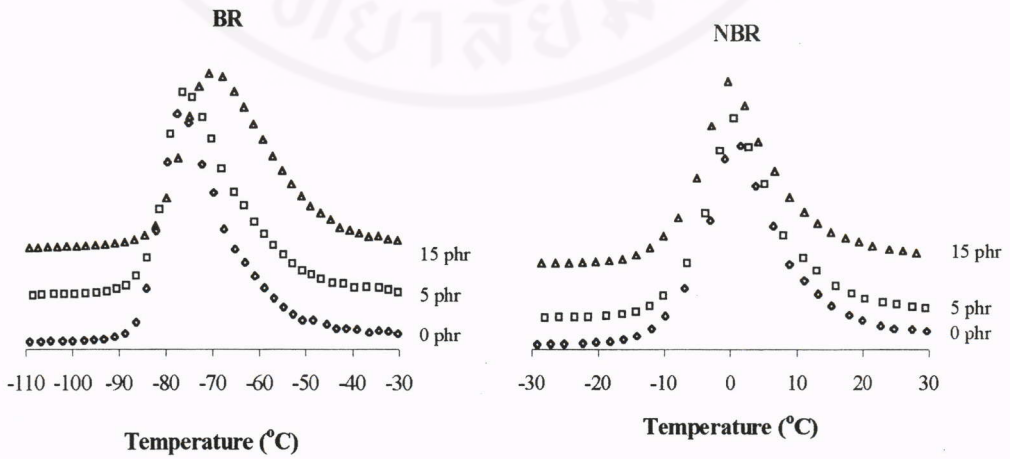

Figure 3.44 Glass transition temperature of single rubber systems determined from damping properties

For the blend systems, the distribution of aliphatic resin in each phase of the blend is controlled by the rubber-resin interaction in each phase, which can be seen from a shift in the position of the T_g of each phase, as illustrated in Figures 3.45 and 3.46. It is obvious that the position of T_g of BR phase increases as 60NS added, compared to NBR phase. Therefore, it is evident that the 60NS preferentially migrates to BR phase.

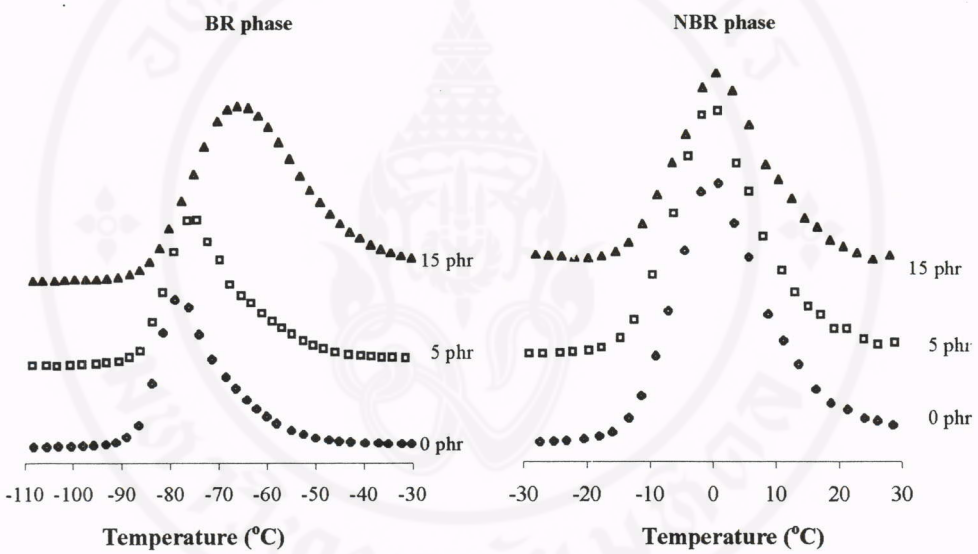

Figure 3.45 Glass transition temperature of 50/50 BR/NBR blends determined from damping properties

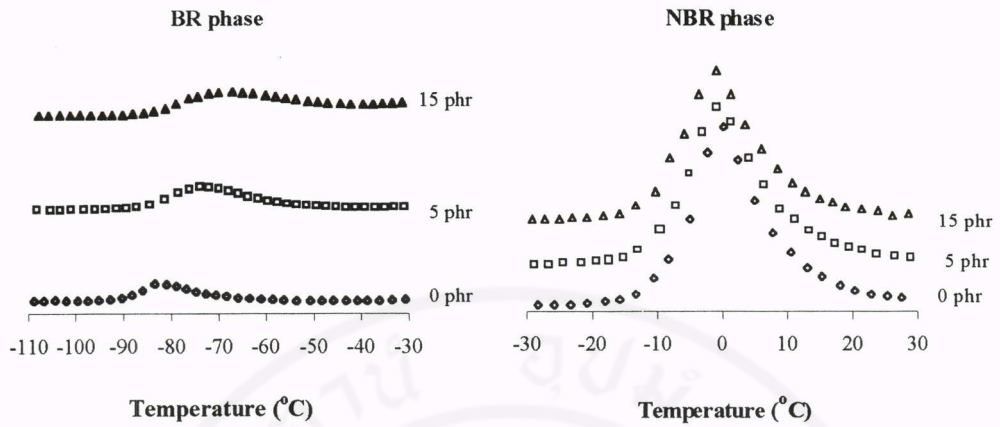

Figure 3.46 Glass transition temperature of 20/80 BR/NBR blends determined from damping properties

From Figures 3.47-3.49, it can be seen that the cure properties of unfilled compounds are affected significantly by the blend ratio and loading of the 60NS. However, in the case of filled compounds, the influence of carbon black distribution appears to override the effects of blend ratio and 60NS loading. Scorch time and cure time decrease with increasing the ratio of the amount of carbon black in BR phase to the amount of BR in blends. When the ratio is greater than 0.6, the scorch time and cure time are approximately independent of the ratio. Cure rate appears to increase with increasing the ratio up to 0.6. Then, the cure rate decreases as NBR becomes the matrix in 20/80 blend.

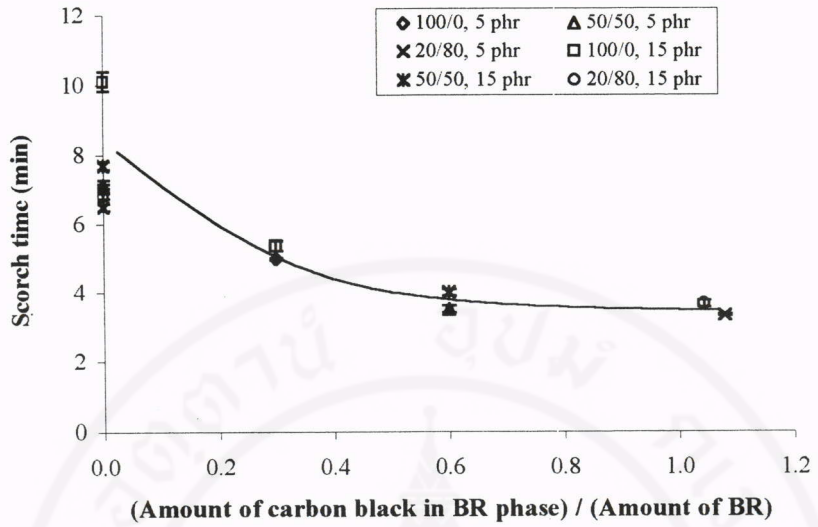

Figure 3.47 Effect of carbon black distribution on scorch time in compounds with different blend ratios and 60NS loadings (marks on y axis are unfilled compound)

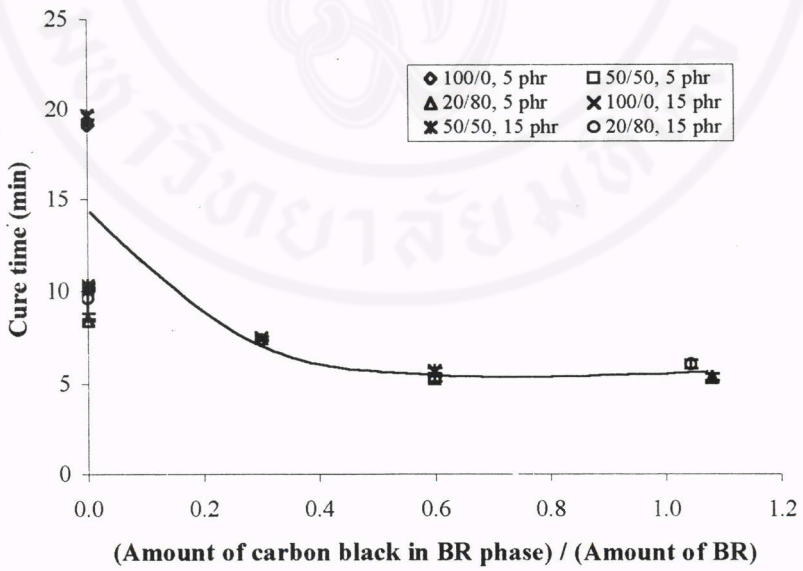

Figure 3.48 Effect of carbon black distribution on cure time in compounds with different blend ratios and 60NS loadings (marks on y axis are unfilled compound)

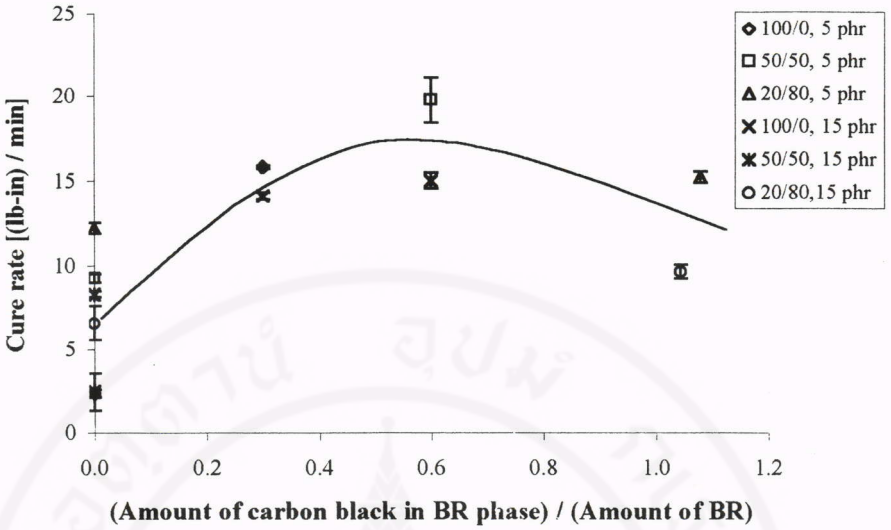

Figure 3.49 Effect of carbon black distribution on cure rate in compounds with different blend ratios and 60NS loadings (marks on y axis are unfilled compound)

The effects of blend ratio, carbon black distribution and loading of 60NS on tensile properties and hardness are illustrated in Figures 3.50 to 3.53. Figure 3.52 reveals that the % elongation at break of unfilled compounds is affected by blend ratio and loading of 60NS. However, these factors slightly affect tensile strength, modulus at 50% strain and hardness of the unfilled compounds (see Figures 3.50, 3.51 and 3.53). In the case of filled compounds, the effect of carbon black distribution overrides the effect of blend ratio and 60NS loading. Modulus increases with increasing the ratio of the amount of carbon black in BR phase to the amount of BR. When the ratio is greater 0.4, the modulus is slightly changed. The tensile strength and % elongation at break increase with the ratio up to 0.6, and then decrease as NBR becomes the matrix in 20/80 blend. The hardness results show similar trend to the modulus results.

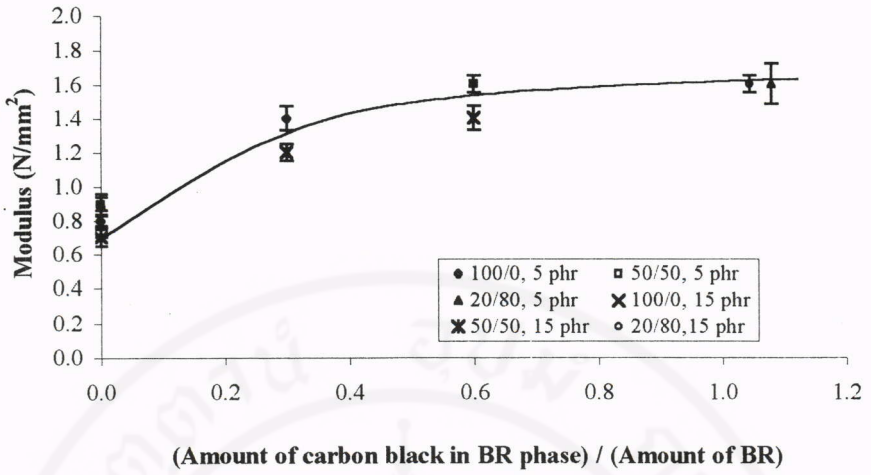

Figure 3.50 Effect of carbon black distribution on modulus at 50% strain with different blend ratios and 60NS loadings (marks on y axis are unfilled compound)

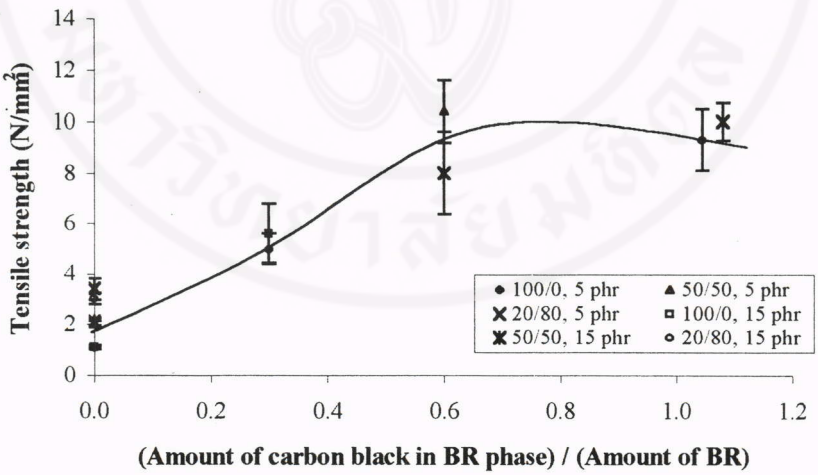

Figure 3.51 Effect of carbon black distribution on tensile strength with different blend ratios and 60NS loadings (marks on y axis are unfilled compound)

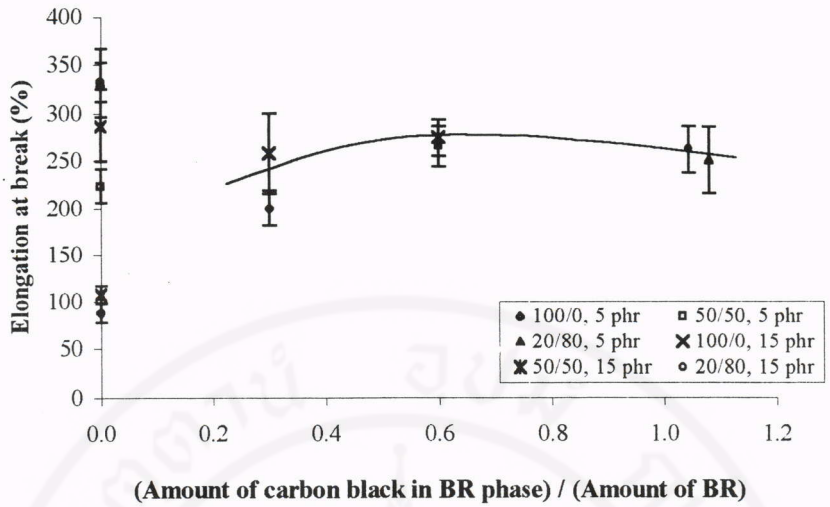

Figure 3.52 Effect of carbon black distribution on % elongation at break with different blend ratios and 60NS loadings (marks on y axis are unfilled compound)

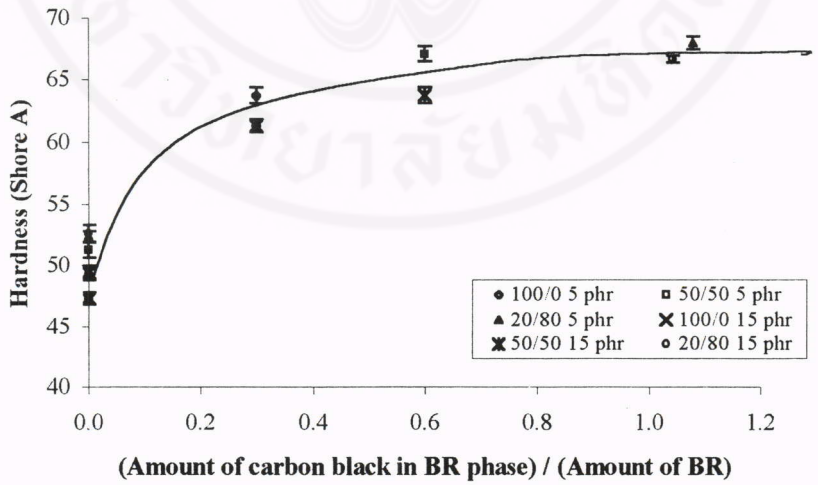

Figure 3.53 Effect of carbon black distribution on hardness with different blend ratios and 60NS loadings (marks on y axis are unfilled compound)

3.3.2 Struktol WB16

According to the data sheet supplied by manufacturer, Struktol WB16 is a mixture of metal salt and a fatty acid amide. The influence of WB16 on Mooney viscosity is shown in Figures 3.54 and 3.55. It can be seen that the addition of WB16 decreases the compound viscosity and the viscosity of blends is shifted closer to the theoretical mixture rule. However, the viscosity of 0/100 and 20/80 blends slightly increases when 1 phr of WB16 is added. The possible explanation is proposed as follows. At high loading of WB16, the Mooney viscosity measured appears to decrease which might be due to the plasticizing and/or wall slippage effects. Figure 3.56 shows the relative Mooney viscosity; the ratio of Mooney viscosity of compound with to that without WB16. It is clear that, the plasticizing and/or wall slip effects is dominated in compounds with BR as a matrix (i.e. 100/0 and 50/50 blends). However, the slight increase in Mooney viscosity of compounds with NBR as a matrix (i.e., 20/80 and 0/100 blends) when 1 phr of WB16 added, is not understood.

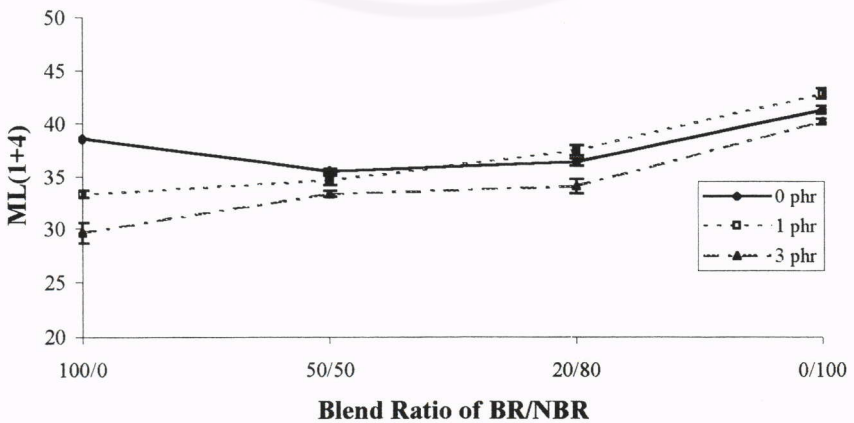

Figure 3.54 Relationship between Mooney viscosity and blend ratio in compounds with different WB16 loadings

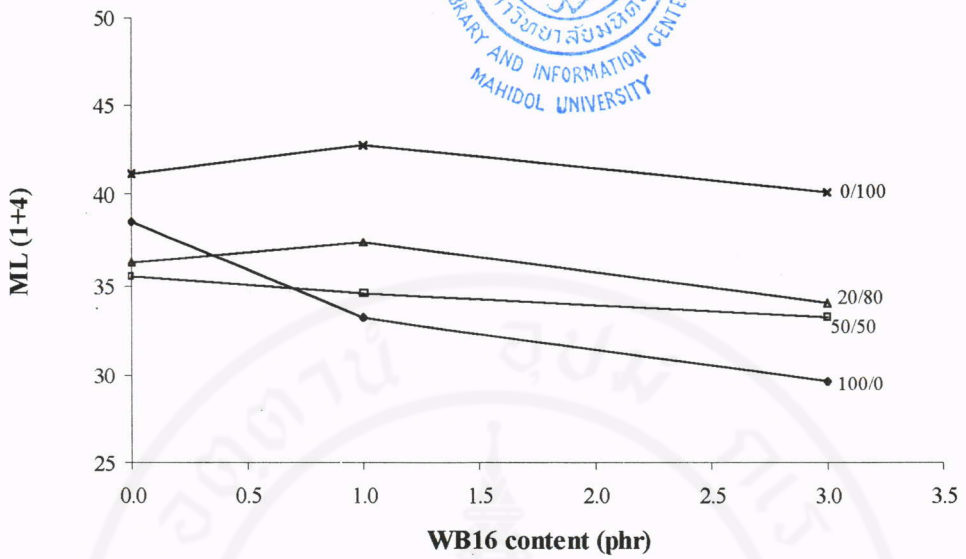

Figure 3.55 Relationship between Mooney viscosity and WB16 loading with different blend ratios of BR/NBR

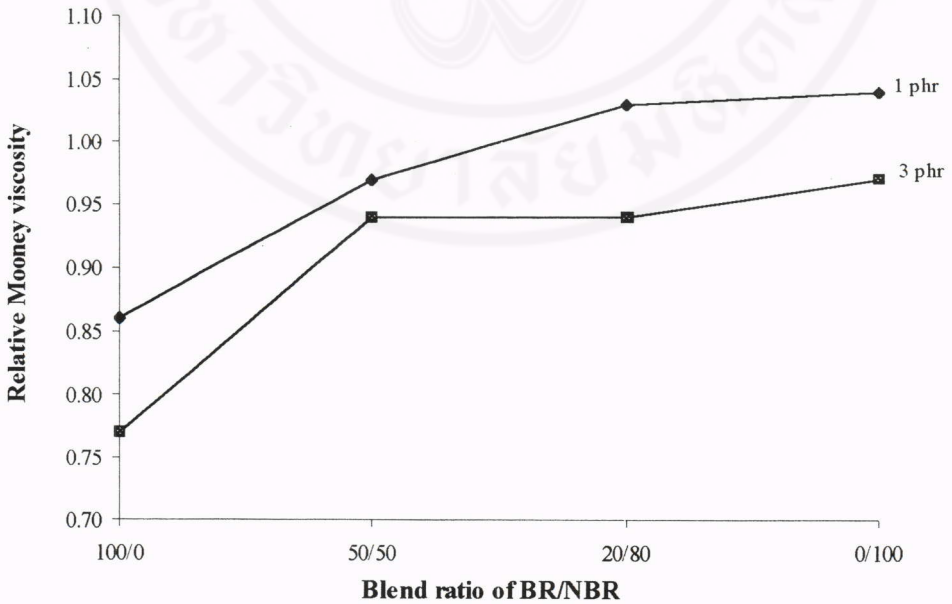

Figure 3.56 Relationship between relative Mooney viscosity and blend ratio in compounds with different WB16 loadings

The effect of WB16 loading on carbon black distribution in blends is illustrated in Table 3.17. It can be seen that as 1 phr of WB16 is added, the black residing in BR phase increases and unchanges for the blend ratios of 20/80 and 50/50, respectively. The increase in black residing in BR phase of 20/80 is believed to be due to the preferential migration of WB16 to BR phase, leading to a reduction in viscosity of BR phase. As mentioned in the first part of the study, black in blends tends to migrate to the phase with lower viscosity. By contrast, the unchange in black distribution of the 50/50 blend is the result of the sufficient amount of BR phase for carbon black to reside. Additionally, when 3 phr of WB16 is added to the blends, the amount of carbon black in BR phase decreases, which is probably caused by a reduction in NBR viscosity after a saturation of WB16 in BR phase.

WB16 in blends preferentially migrates to BR phase due to the strong interaction between WB16 and BR phase and/or good solubility of WB16 in BR phase. The strong WB16-BR interaction, and good solubility of WB16 in BR are confirmed by DMTA and by the dissolution of rubber in acetone, respectively. DMTA results of pure rubber are illustrated in Figure 3.57. It can be seen that the T_g of BR shifts toward the higher temperature, but no significance in T_g shift of NBR is observed with an addition of WB16. Therefore, it is evident that WB16 interacts strongly with BR, but weakly interaction with NBR. In the case of blends, the DMTA results are illustrated in Figures 3.58 and 3.59. It is found that the T_g of BR phase still shifts to the higher temperature, indicating a migration of WB16 to BR phase. From the solubility test in acetone, NBR could dissolve in acetone whereas WB16 and BR are not soluble. Consequently, WB16 should be more soluble in BR than NBR. It can be

seen that the DMTA and solubility results are the clear evidences of the preferential migration of WB16 to BR phase.

Table 3.17 Distribution of black in blends with different WB16 loadings

BR/NBR blend ratio	Amount of carbon black[a] in BR phase (phr)		
	0 phr	1 phr	3 phr
50/50	30.0	30.0	20.5
20/80	15.5	17.0	12.4

[a] *N330 carbon black loading of 30 phr*

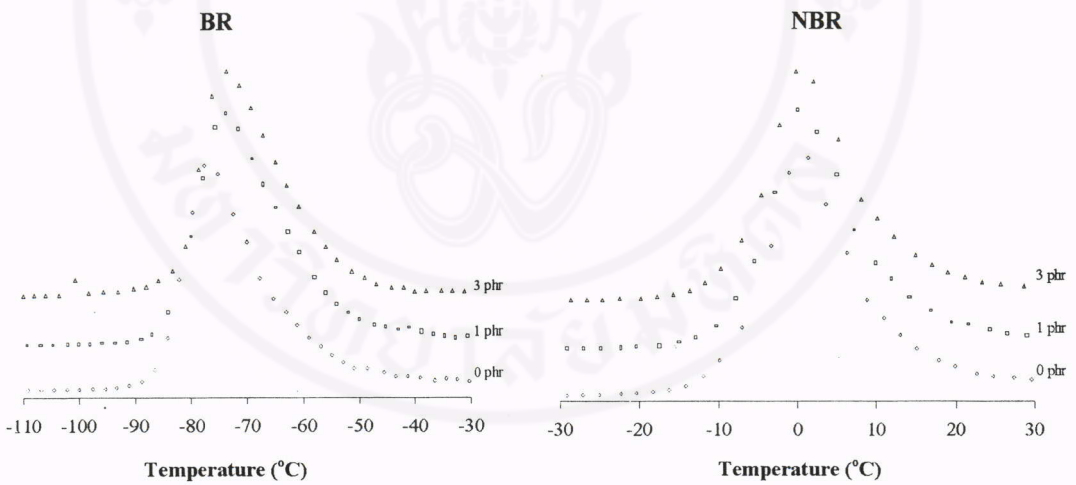

Figure 3.57 Glass transition temperature of single rubber systems with different WB16 loadings

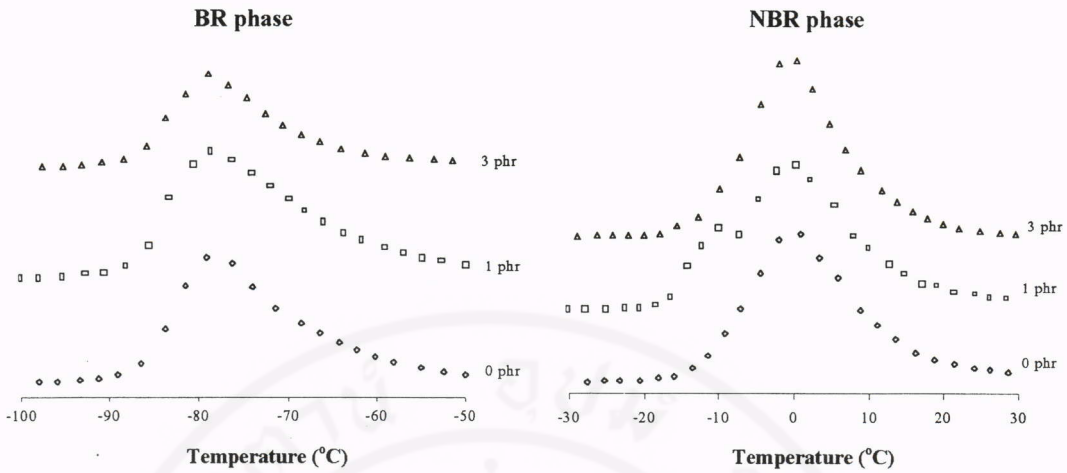

Figure 3.58 Glass transition temperature of 50/50 BR/NBR blend with different WB16 loadings

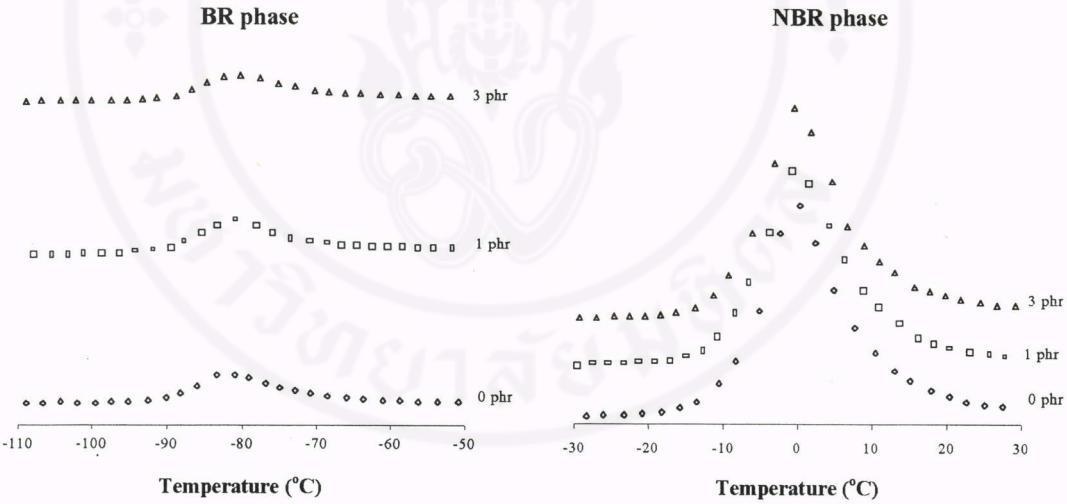

Figure 3.59 Glass transition temperature of 20/80 BR/NBR blends with different WB16 loadings

The effects of blend ratio, distribution of carbon black in each phase of blends and WB16 loading on cure properties are illustrated in Figures 3.60 to 3.62 and those on tensile properties as well as hardness are illustrated in Figures 3.63 to 3.66. It is obvious that the trends of the results are similar to those in the case of 60NS mentioned earlier. Therefore, similar discussion can be applied to the results.

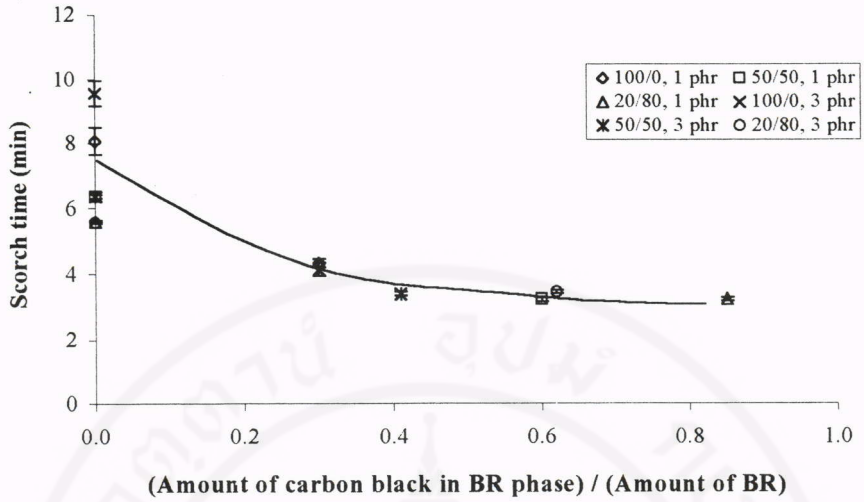

Figure 3.60 Effect of carbon black distribution on scorch time in compounds with different blend ratios and WB16 loadings (marks on y axis are unfilled compound)

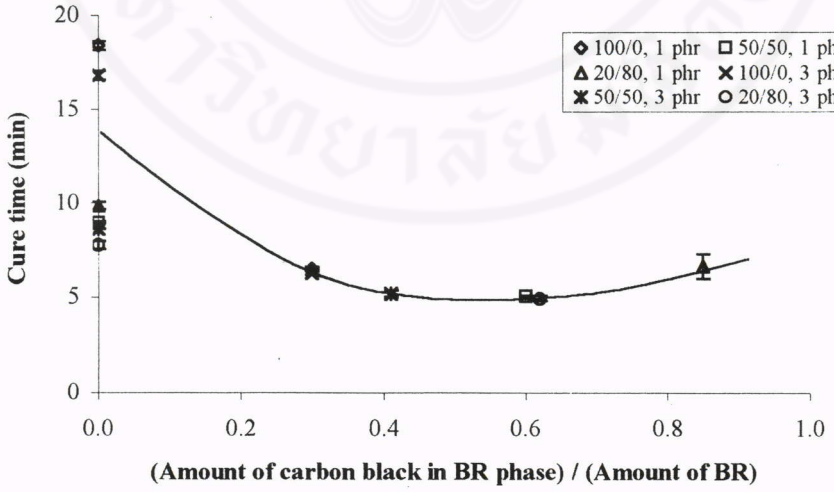

Figure 3.61 Effect of carbon black distribution on cure time in compounds with different blend ratios and WB16 loadings (marks on y axis are unfilled compound)

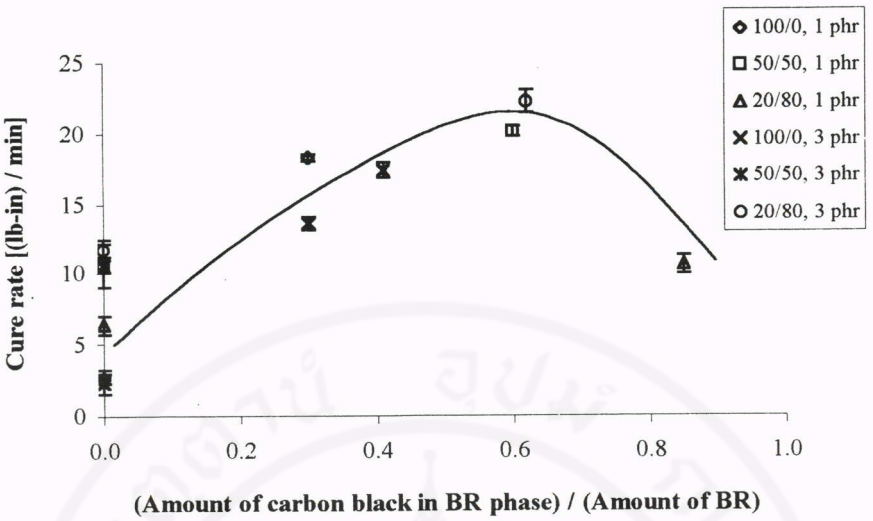

Figure 3.62 Effect of carbon black distribution on cure rate in compounds with different blend ratios and WB16 loadings (marks on y axis are unfilled compound)

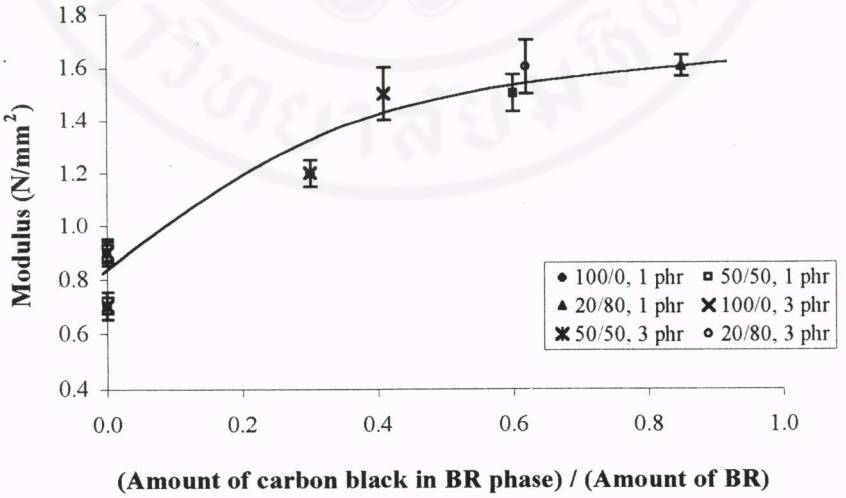

Figure 3.63 Effect of carbon black distribution on modulus at 50% strain with different blend ratios and WB16 loadings (marks on y axis are unfilled compound)

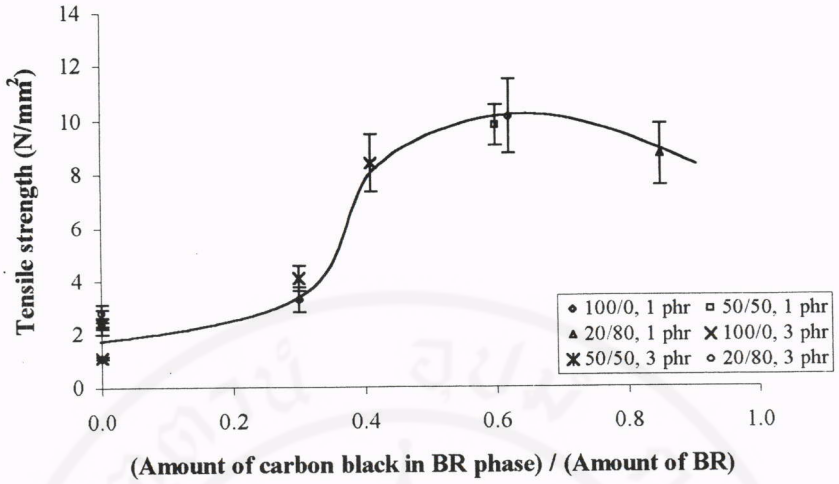

Figure 3.64 Effect of carbon black distribution on tensile strength with different blend ratios and WB16 loadings (marks on y axis are unfilled compound)

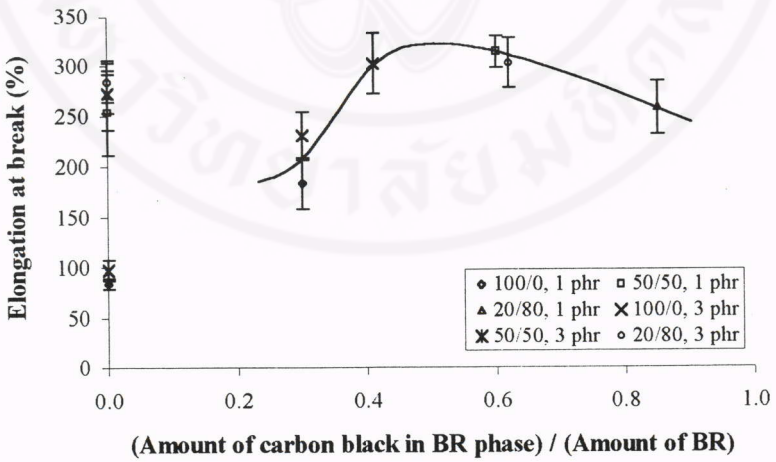

Figure 3.65 Effect of carbon black distribution on % elongation at break with different blend ratios and WB16 loadings (marks on y axis are unfilled compound)

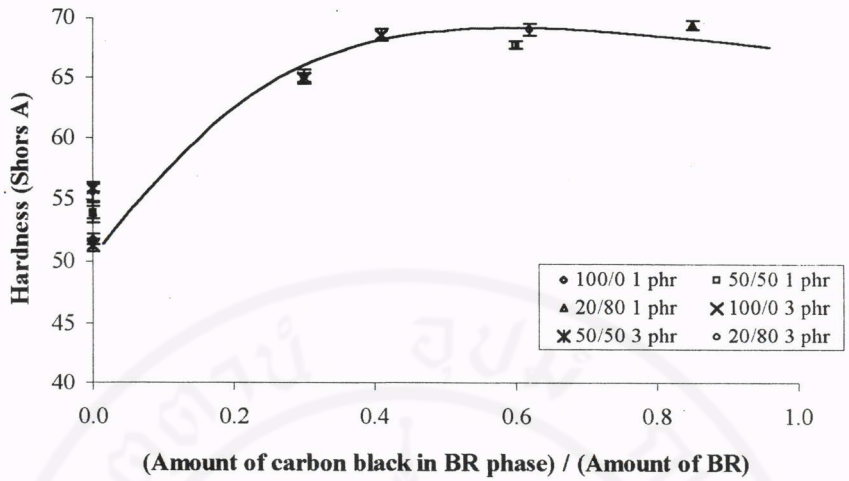

Figure 3.66 Effect of carbon black distribution on hardness with different blend ratios and WB16 loadings (marks on y axis are unfilled compound)

3.3.3 Ethylene Octene Rubber (EOR)

Figure 3.67 reveals the relative Mooney viscosity (the ratio of viscosity compound with to that without EOR) of unfilled BR/NBR with varied blend ratios as a function of EOR content. It can be seen that the addition of EOR decreases the viscosity of both BR and NBR, meaning the EOR is able to function as a plasticizing agent for BR and NBR. The plasticizing efficiency of EOR is more significant in NBR than BR, which can be seen from the greater negative magnitude in slops of the plots.

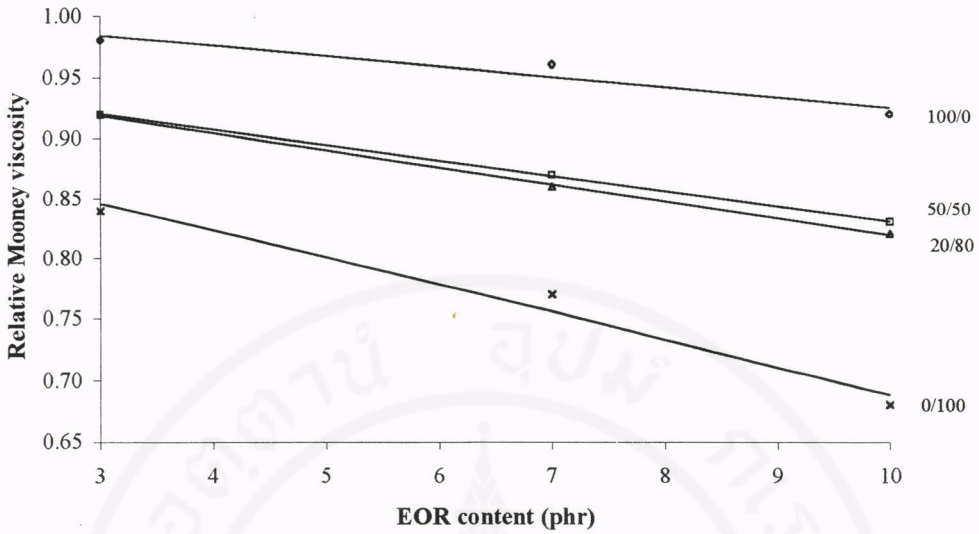

Blend Ratio	Fitted Equation	
100/0	y = -0.0084x + 1.0092	R^2 = 0.9276
50/50	y = -0.0128x + 0.9589	R^2 = 0.9589
20/80	y = -0.0143x + 0.9622	R^2 = 0.9989
0/100	y = -0.0226x + 0.9138	R^2 = 0.9764

Figure 3.67 Relationship between relative Mooney viscosity and blend ratio in compounds with different EOR loadings

From Figure 3.68, the relationship between EOR content and deviation value of the Mooney viscosity from the additive line is illustrated. In the case of 20/80 BR/NBR, the deviation value of Mooney viscosity from the additive line reduces with increasing EOR content, which is probably attributed to the reduction in interfacial tension. In other words, the EOR probably acts as a compatibiliser. However, in the 50/50 blend, the magnitude in slope of the plot is relatively small, probably caused by a migration of EOR to BR phase.

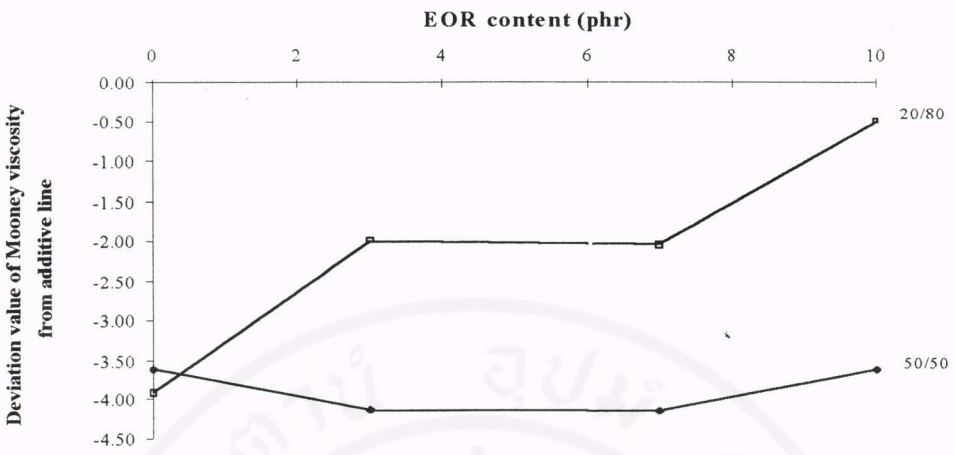

Figure 3.68 Relationship between EOR loading and deviation value of Mooney viscosity from the additive line

Cure properties are illustrated in Figures 3.69 and 3.70. In the case of pure components, cure rate reduces whereas cure time increases with an addition of EOR. By contrast, it can be seen that in the blend systems, the cure rate increases whereas cure time decreases when EOR 3 phr is added. Consequently, in theory, if EOR migrates to BR, NBR or both, the cure properties should be in agreement with those of the pure components. According to the results of blend systems, it is proposed that the EOR should reside at the interface between NBR and BR phase acting as a compatibiliser. Therefore, from results of Mooney viscosity and cure properties, it is evident that the EOR does exist in the interfacial area between two phases. However, at a larger amount of EOR, cure rate decreases, which is probably due to the saturation of EOR at the interfacial area. Thus, the excess of EOR starts to migrate to the BR, which can be seen from the result of carbon black distribution. Accordingly, the viscosity of the blend with BR matrix at high loading of EOR (at blend ratio 50/50) is reduced and carbon black will then migrate increasingly to BR matrix phase

as shown in Table 3.18. On the contrary, in the case of 20/80 where NBR is the matrix, WB16 would migrate to NBR after a saturation in BR, resulting in a decrease in NBR viscosity and thus a decrease in the amount of carbon black in BR phase at high EOR loading.

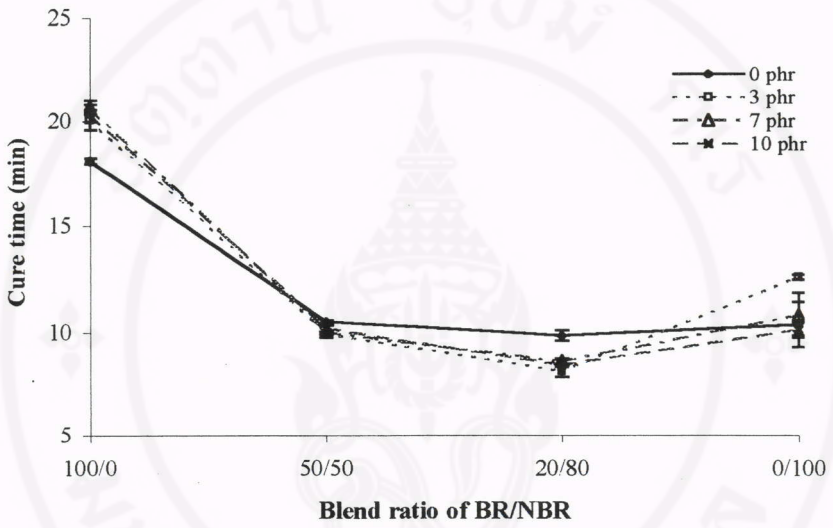

Figure 3.69 Relationship between cure time and blend ratio in compounds with different EOR loadings

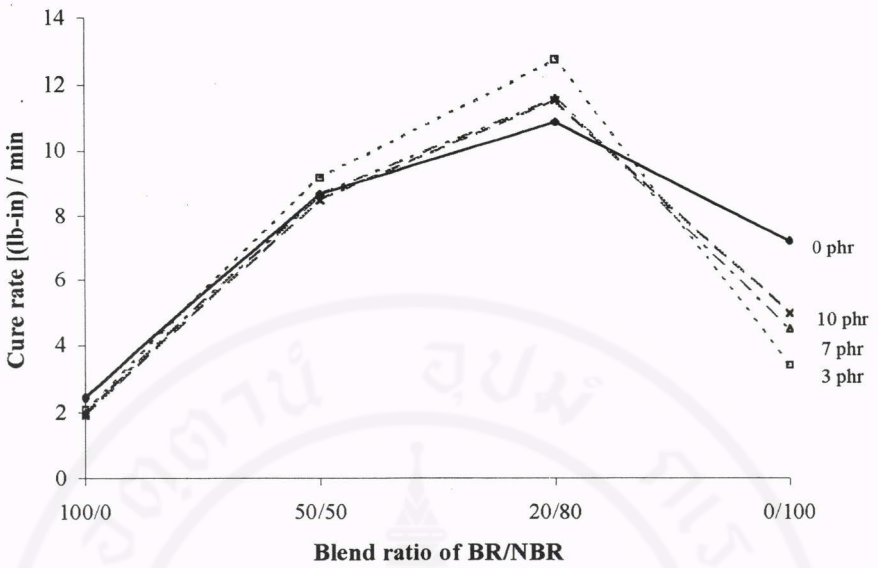

Figure 3.70 Relationship between cure rate and blend ratio in compounds with different EOR loadings

Table 3.18 Distribution of black in blends with different EOR loadings

BR/NBR blends ratio	Amount of carbon black[a] in BR phase (phr)			
	0 phr	3 phr	7 phr	10 phr
50/50	30.0	21.2	24.2	27.1
20/80	15.5	18.1	16.9	15.5

[a] *N330 carbon black loading of 30 phr*

The effects of blend ratio, carbon black distribution and loading of EOR on cure properties are illustrated in Figures 3.71 to 3.73 and those on mechanical properties are illustrated in Figures 3.74 to 3.77. The results show similar trend to those of compounds with 60NS and WB16. Thus, similar discussion as mentioned earlier can be applied to the results.

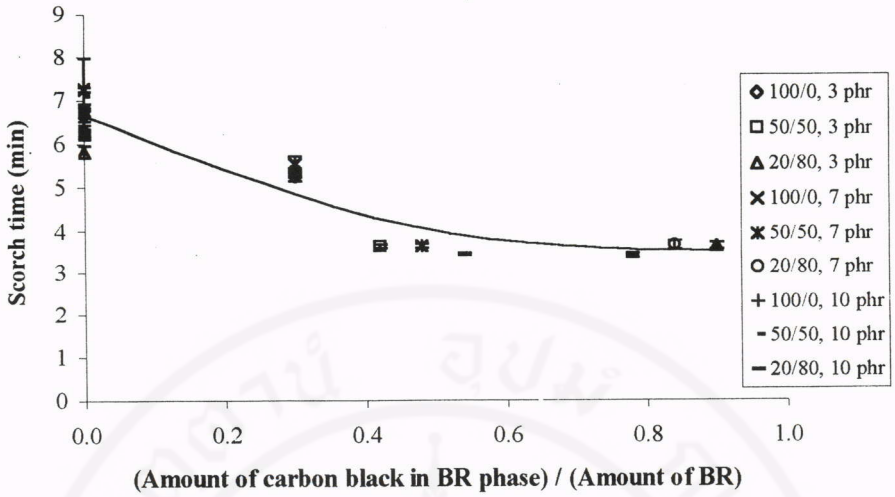

Figure 3.71 Effect of carbon black distribution on scorch time in compounds with different blend ratios and EOR loadings (marks on y axis are unfilled compound)

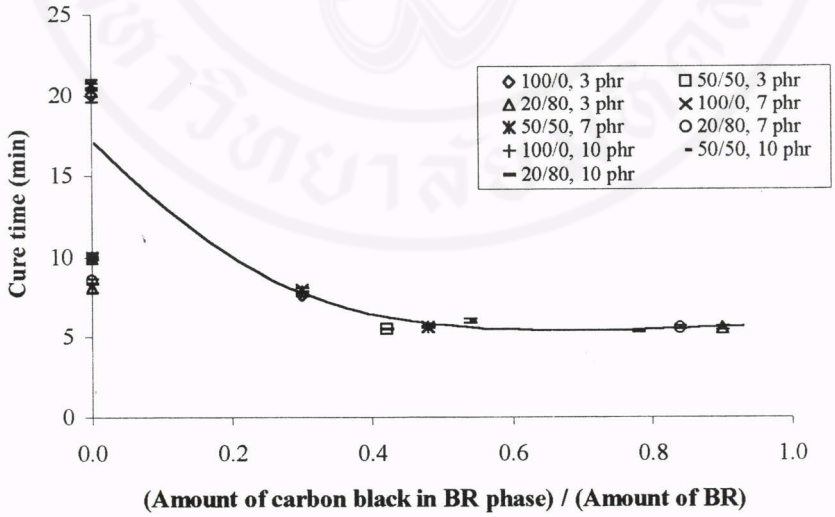

Figure 3.72 Effect of carbon black distribution on cure time in compounds with different blend ratios and EOR loadings (marks on y axis are unfilled compound)

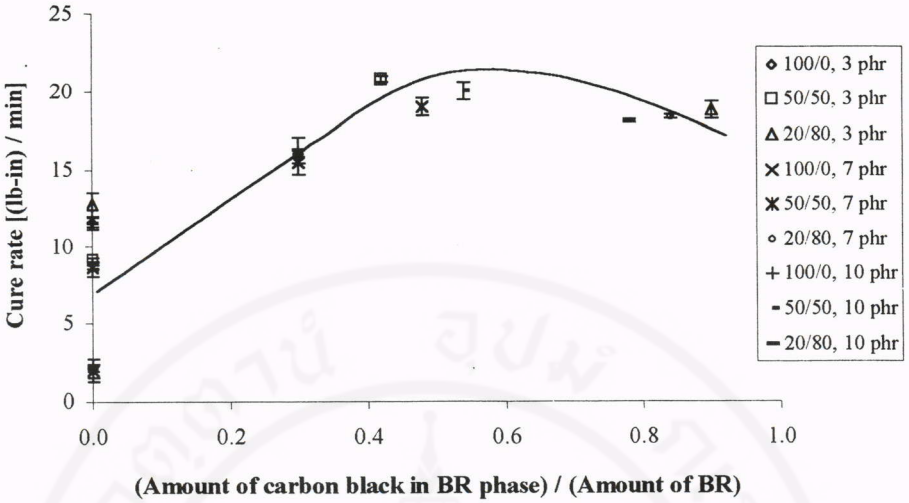

Figure 3.73 Effect of carbon black distribution on cure rate in compounds with different blend ratios and EOR loadings (marks on y axis are unfilled compound)

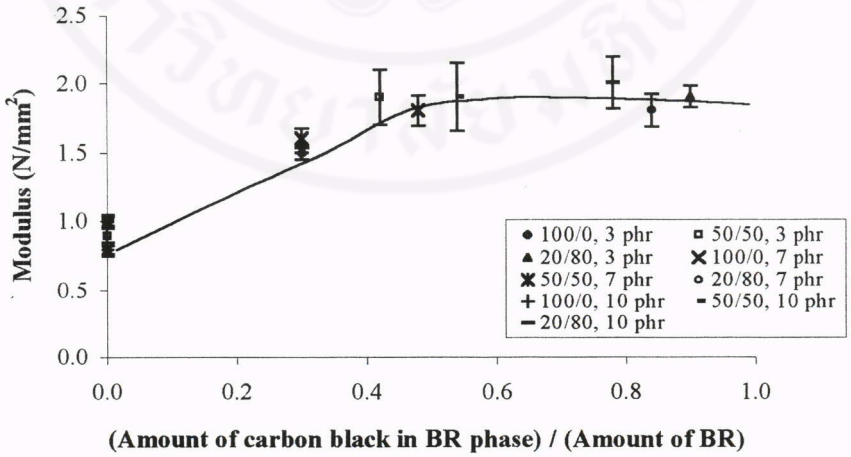

Figure 3.74 Effect of carbon black distribution on modulus at 50% strain with different blend ratios and EOR loadings (marks on y axis are unfilled compound)

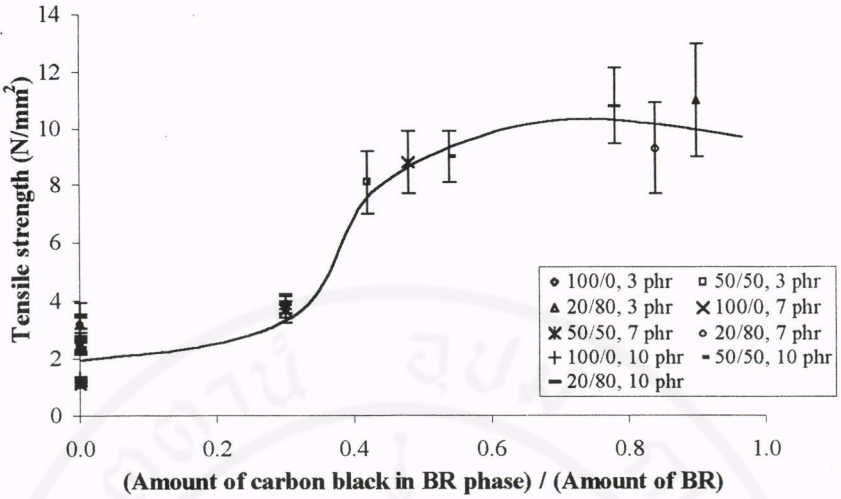

Figure 3.75 Effect of carbon black distribution on tensile strength with different blend ratios and EOR loadings (marks on y axis are unfilled compound)

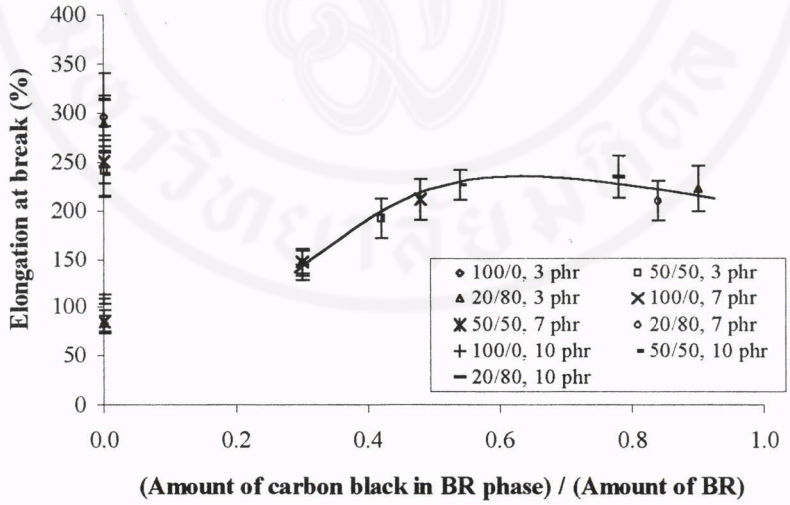

Figure 3.76 Effect of carbon black distribution on % elongation at break with different blend ratios and EOR loadings (marks on y axis are unfilled compound)

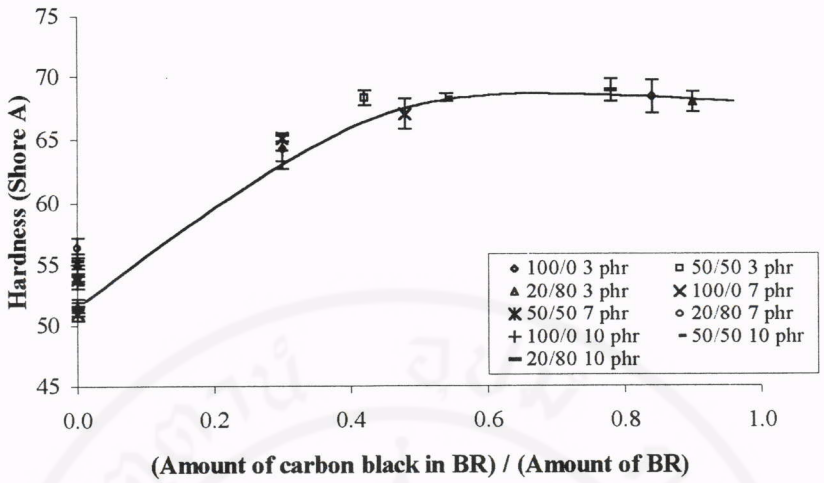

Figure 3.77 Effect of carbon black distribution on hardness with different blend ratios and EOR loadings (marks on y axis are unfilled compound)

CHAPTER IV

CONCLUSIONS

PART I : Effects of blend ratio of BR/NBR, carbon black surface area and black loading

1. Mooney viscosities of blends are lower than the theoretical values and also lower than pure components due to the poor interaction between BR and NBR.

2. Relative viscosity (Mooney viscosity of filled compound to that of unfilled compound) of BR is higher than that of NBR due to the stronger interaction between carbon black and BR.

3. Relative viscosity and % bound rubber content increase with increasing carbon black surface area.

4. Imbalance of curatives (sulphur and CBS) between BR and NBR phases leads to a denser network in matrix than dispersed phase.

5. T_{max} is affected by phase morphology of blends. T_{max} of N220 is higher than those of N330 and N660 respectively, because of the greatest reinforcing effect.

6. Cure properties of unfilled compounds are strongly affected by the blend ratio. In the case of filled compound, the effect of carbon black distribution overrides the effect of blend ratio and black loading on cure properties.

7. Modulus and tensile strength of blends show synergistic effect. Relative tensile strength increases with increasing carbon black surface area due to the increased reinforcing effect.

8. For the mechanical properties of unfilled compound, the effect of blend ratio strongly affects % elongation at break and slightly affects tensile strength, modulus and hardness. However, in the case of filled compound, the effect of carbon black distribution overrides the effect of blend ratio.

9. Oil resistance of blends is affected significantly by phase morphology of the blends.

PART II : Factors affecting carbon black distribution in BR/NBR blend

1. BR is more preferential for carbon black to reside than NBR due to the relatively low viscosity of BR phase and relatively strong interaction between carbon black and BR.

2. The carbon black distribution is strongly affected by the blend ratio and black loading. However, the carbon black distribution is slightly affected by carbon black surface area.

3. The effects of blend ratio and mixing sequence are more dominated in carbon black distribution in blends than effects of viscosity difference between BR and NBR and rubber-filler interaction.

PART III : Effect of some additives on carbon black distribution in BR/NBR blends

1. Struktol 60NS and Struktol WB16 in blends migrate preferentially to BR phase due to the strong interaction between Struktol and BR phase and/or good solubility of Struktol in BR phase. EOR is believed to reside at the interface between BR and NBR phase. After a saturation in the interface, the excess of EOR starts to migrate to BR phase, and to NBR after a saturation in BR phase.

2. Cure properties and mechanical properties of unfilled compounds are strongly affected by blend ratio and additive loading. However, in the case of filled compounds, the influence of carbon black distribution override those blend ratio and additive loading effects.

REFERENCES

1. Frisch HL, Klempner D. A topologically interpenetrating elastomeric network. Rubber Chem Technol. 1970; 43: 883-886.
2. Mark EJ, Erman B, Eirich RF, editor. Science and technology of rubber. Elastomer blends. London: Acadamic; 1994.
3. Bohn L. Incompatibility and phase formation in solid polymer mixtures and graft and block copolymers. . Rubber Chem Technol. 1968; 41: 495-513.
4. Pazonyi T, Dimitrov M. Preparation and properties of polymer mixtures. Rubber Chem Technol. 1967; 40: 1119-1125.
5. Bhowmick AK, De SK. Effect of curing temperature and curing system on structure-property relations of rubber blends. Rubber Chem Technol. 1980; 53: 960-974.
6. Leblanc LJ. Interphase distribution of curatives in natural rubber/polybutadiene blends. Plast Rubber Process Appl. 1982; 2(4): 361-368.
7. Callan JE, Hess WM, Scott CE. Elastomer blends. Compatibility and relative response to fillers. Rubber Chem Technol. 1971; 44: 814-837.
8. Corish PJ. Fundamental studies of rubber blends. Rubber Chem Technol. 1967; 40: 324-340.
9. Inoue T, Shomura F, Ougizawa T, Miyasaka K. Covulcanization of polymer blends. Rubber Chem Technol. 1985; 58: 873-884.

10. Hess WM, Herd CR, Vegvari PC. Characterization of immiscible elastomer blends. Rubber Chem Technol.1993; 66(3) 329-375.

11. Callan JE, Topcik B, Ford FP. Butyl/EPDM blends processing and properties. Rubber Word. 1965; 61: 60-69.

12. Hess WM, Scott CE, Callan JE. Carbon black distribution in elastomer blends. Rubber Chem Technol. 1967; 40(2): 371-384.

13. Maiti S, De SK, Bhowmick KA. Quantitative estimation of filler distribution in immiscible rubber blends by mechnical damping studies. Rubber Chem Technol. 1992; 65: 293-302.

14. Cotton RG, Murphy JL. Mixing of carbon black with rubber. VI. Analysis of NR/SBR blends. Rubber Chem Technol. 1988; 61: 609-618.

15. Gardiner BJ. Curative diffusion between dissimilar elastomers and its influence on adhesion. Rubber Chem Technol. 1968; 41: 1312-1328.

16. Gardiner BJ. Studies in the morphology and vulcanization of gum rubber blends. Rubber Chem Technol. 1970; 43: 370-399.

17. Hess WM, Vegvari PC, Swor RA. Carbon black in NR/BR blends for truck tires. Rubber Chem Technol. 1985; 58: 350-382.

18. Marsh AP, Voet A, Price LD, Mullens TJ. Fundamentals of electron microscopy of heterogeneous elastomer blends. Rubber Chem Technol. 968; 41: 344-355.

19. Kraus G, editor. Reinforcement of elastomers. New York: John Wiley & Sons; 1965.

20. Smith RW, Andries JC. New methods for electron microscopy of polymer blends. Rubber Chem Technol. 1974; 47: 64-78.

21. Bauer RF, Dudley EA. Compatibilization of rubber blends through phase interaction. Rubber Chem Technol. 1977; 50: 35-42.

22. Hess WM, Chirico VE. Elastomer blend properties-Influence of carbon black type and location. Rubber Chem Technol. 1977; 50: 301-326.

23. Sirisinha C, Thunyarittikorn J, Yartpakdee S. Study of carbon black distribution in butadiene rubber-nitrile/butadiene rubber blends based on damping properties. Effect of some grades of carbon black. Plast Rubber Compos Process Appl. 1998; 27(8): 373-375.

24. Sircar AK, Lamond TG, Pinter PE. Effect of heterogeneous carbon black distribution on the properties of polymer blends. Rubber Chem Technol. 1974; 47: 48-56.

25. Sinha D, Bandyopadhyay S, Kole S, Das CK. Effect of the mixing sequence on the rheological behaviour of black filled elastomer blends by extrusion rheometry. Plastics Rubber Proc. 1985; 5: 203-207.

26. Sircar AK, Lamond TG. Strain-dependent dynamic properties of carbon-black reinforced vulcanizates. I. Individual elastomers. Rubber Chem Technol. 1975; 48: 79-96.

27. Sircar AK, Lamond TG. Strain-dependent dynamic properties of carbon-black reinforced vulcanizates. I. Elastomer blends. Rubber Chem Technol. 1975; 48: 79-96.

28. Sircar AK. Softer conductive rubber compounds by elastomer blending. Rubber Chem Technol. 1981; 54: 820-834.

29. Kiselev YV. Influence of the amount of filler at the interface between incompatible rubbers on the strength of the adhesive bond. Inter Polym Sci Technol. 1994; 21(7): 52-55.

30. Schuster RH. Relation between morphology of blends and physical properties of the elastomers. Inter Polym Sci Technol. 1997; 24(2): 5-13.

31. McDonald GC, Hess WM. Carbon black morphology in rubber. Rubber Chem Technol. 1977; 50: 842-862.

32. Tinker JA. Crosslink distribution and interfacial adhesion in vulcanized blends of NR and NBR. Rubber Chem Technol. 1967; 63: 503-515.

33. Mark EJ, Erman B, Eirich RF, editor. Science and technology of rubber. The science of rubber compounding. London: Acadamic; 1994.

34. Dannenberg EM. Bound rubber and carbon black reinforcement. Rubber Chem Technol. 1986; 59: 512-524.

35. Go HJ, Ha SC. Rheology and Properties of EPDM/BR blends with or without a homogenizing agent or a coupling agent. J Appl Polym Sci. 1996; 62: 509-521.

36. Varughese S, Tripathy DK. Rubber to filler interaction studies-a dynamic mechanical thermal analysis approach. Plast Rubber Compos Process Appl. 1992; 17(4): 219-223.

APPENDICES

APPENDIX A : Effects of blend ratio, carbon black surface area and black loading on properties

Table A1 Rheological and cure properties of compounds

Compound	ML (1+4)	Cure properties			
		T_{max} (lb-in)	T_{min} (lb-in)	Scorch time (min)	Cure time (min)
Unfilled cpd.					
100/0	38.5 ± 0.0	35.15 ± 0.06	5.72 ± 0.16	6.04 ± 0.11	18.02 ± 0.08
80/20	35.9 ± 0.4	35.54 ± 0.04	5.02 ± 0.00	6.38 ± 0.13	11.53 ± 0.14
50/50	35.5 ± 0.2	35.19 ± 0.11	4.50 ± 0.06	6.56 ± 0.10	10.29 ± 0.04
20/80	36.3 ± 0.3	32.91 ± 1.01	3.90 ± 0.12	7.10 ± 0.11	9.50 ± 0.14
0/100	41.2 ± 0.4	29.88 ± 1.25	3.77 ± 0.04	6.43 ± 0.11	10.20 ± 0.65
N330 black					
100/0	61.9 ± 0.5	49.10 ± 0.19	9.09 ± 0.09	4.54 ± 0.07	7.11 ± 0.05
80/20	59.8 ± 0.5	50.60 ± 0.57	8.98 ± 0.07	3.49 ± 0.06	5.49 ± 0.05
50/50	57.6 ± 0.4	49.42 ± 0.16	8.46 ± 0.18	3.32 ± 0.04	5.19 ± 0.06
20/80	58.0 ± 0.0	46.13 ± 0.55	7.28 ± 0.16	3.28 ± 0.04	5.43 ± 0.05
0/100	63.0 ± 0.0	47.26 ± 0.61	6.85 ± 0.10	3.26 ± 0.01	6.10 ± 0.07
N660 black					
100/0	55.2 ± 0.1	48.22 ± 0.15	7.95 ± 0.09	4.58 ± 0.02	8.48 ± 0.02
8020	53.0 ± 0.0	48.64 ± 0.80	7.67 ± 0.12	4.05 ± 0.08	6.06 ± 0.04
50/50	49.2 ± 0.3	48.36 ± 0.17	7.04 ± 0.18	3.31 ± 0.05	5.20 ± 0.05
20/80	53.5 ± 0.4	45.89 ± 0.71	5.95 ± 0.12	3.20 ± 0.02	5.20 ± 0.05
0/100	59.6 ± 0.6	44.81 ± 0.38	5.52 ± 0.06	3.19 ± 0.02	6.11 ± 0.04
N220 black					
100/0	65.8 ± 0.9	50.35 ± 0.41	8.82 ± 0.09	4.42 ± 0.04	7.11 ± 0.01
80/20	66.0 ± 0.4	50.62 ± 0.16	8.81 ± 0.40	3.42 ± 0.01	5.46 ± 0.02
50/50	65.3 ± 0.3	50.66 ± 0.46	8.50 ± 0.15	3.27 ± 0.02	5.30 ± 0.04
20/80	66.5 ± 0.9	48.40 ± 0.55	7.41 ± 0.10	3.13 ± 0.02	5.10 ± 0.04
0/100	67.0 ± 0.4	46.28 ± 1.24	6.36 ± 0.09	3.10 ± 0.07	5.19 ± 0.06
Black loading 50 phr					
100/0	92.8 ± 0.3	61.53 ± 0.39	13.53 ± 0.12	3.28 ± 0.09	5.41 ± 0.04
50/50	97.3 ± 0.4	59.38 ± 2.89	14.28 ± 0.04	2.55 ± 0.05	4.57 ± 0.03
20/80	95.5 ± 1.3	60.48 ± 1.18	12.10 ± 0.21	2.37 ± 0.04	4.52 ± 0.05
0/100	104.3 ± 0.5	59.43 ± 0.70	11.09 ± 0.30	2.35 ± 0.04	8.08 ± 0.47

Table A2 Mechanical properties

Specimen	Modulus @ 50% strain (MPa)	Tensile Strength (MPa)	Elongation at break (%)	Hardness (shore A)	tan δ_{max}	
					BR phase	NBR phase
Unfilled cpd.						
100/0	0.87 ± 0.04	1.14 ± 0.09	74.0 ± 10.41	49.3 ± 0.5	1.57	-
80/20	0.87 ± 0.04	1.81 ± 0.12	172.7 ± 17.48	49.4 ± 0.3	1.15	0.25
50/50	0.90 ± 0.04	2.20 ± 0.23	233.8 ± 31.88	50.6 ± 0.9	0.41	0.67
20/80	0.89 ± 0.04	2.83 ± 0.20	284.7 ± 20.84	51.9 ± 0.4	0.10	1.36
0/100	0.88 ± 0.04	2.54 ± 0.23	272.4 ± 21.27	52.6 ± 0.4	-	1.62
N330 black						
100/0	1.7 ± 0.10	4.4 ± 0.42	159.1 ± 14.38	62.9 ± 2.1	1.03	-
80/20	1.8 ± 0.10	6.2 ± 0.55	165.8 ± 17.96	66.9 ± 0.8	0.61	0.25
50/50	2.1 ± 0.11	9.8 ± 0.98	212.2 ± 12.45	65.5 ± 1.0	0.22	0.68
20/80	2.1 ± 0.15	8.8 ± 0.78	182.9 ± 13.62	65.6 ± 0.9	0.07	1.03
0/100	2.0 ± 0.08	9.9 ± 0.90	198.8 ± 10.73	63.0 ± 0.3	-	1.15
N660 black						
100/0	1.4 ± 0.04	3.4 ± 0.29	147.7 ± 10.19	60.3 ± 0.3	1.24	-
8020	1.6 ± 0.08	5.2 ± 0.59	177.0 ± 14.42	62.6 ± 0.6	0.61	0.25
50/50	1.7 ± 0.12	7.4 ± 1.01	201.8 ± 18.10	63.1 ± 0.3	0.23	0.76
20/80	1.8 ± 0.12	8.5 ± 1.23	197.9 ± 23.77	65.1 ± 0.5	0.06	1.15
0/100	1.9 ± 0.05	10.7 ± 1.30	221.89 ± 16.57	64.1 ± 1.1	-	1.35
N220 black						
100/0	1.5 ± 0.14	5.0 ± 0.80	178.7 ± 29.53	62.2 ± 0.8	0.97	-
80/20	1.7 ± 0.05	6.6 ± 0.69	185.6 ± 12.15	64.7 ± 2.1	0.60	0.26
50/50	1.9 ± 0.10	10.6 ± 1.22	234.4 ± 17.25	66.0 ± 0.6	0.21	0.68
20/80	2.1 ± 0.19	12.4 ± 2.26	235.6 ± 32.65	65.4 ± 1.3	0.07	1.11
0/100	1.8 ± 0.15	11.5 ± 2.24	244.5 ± 30.95	65.3 ± 1.1	-	1.13
Black loading 50 phr						
100/0	2.7 ± 0.14	7.4 ± 0.71	131.1 ± 7.92	74.3 ± 0.5	0.71	-
50/50	3.2 ± 0.30	11.0 ± 0.86	140.6 ± 15.58	77.5 ± 1.3	0.15	0.60
20/80	3.3 ± 0.20	11.7 ± 1.50	138.4 ± 13.15	78.0 ± 0.0	0.06	0.90
0/100	2.8 ± 0.18	12.8 ± 1.69	199.2 ± 18.75	78.5 ± 0.7	-	1.06

APPENDIX B : Effect of some factors on carbon black distribution

Table B1 Damping properties

Compound	tan δ_{max}	
	BR phase	**NBR phase**
Preblend @ 30°C		
Unfilled cpd.		
100/0	1.61	-
80/20	1.16	0.26
50/50	0.41	0.67
20/80	0.11	1.34
0/100	-	1.66
Preblend @ 30°C		
Filled cpd.		
100/0	1.03	-
80/20	0.60	0.25
50/50	0.21	0.68
20/80	0.07	1.02
0/100	-	1.17
Preblend @ 140°C		
Unfilled cpd.		
100/0	1.64	-
80/20	1.16	0.19
50/50	0.46	0.60
20/80	0.09	1.34
0/100	-	1.68
Preblend @ 140°C		
Filled cpd.		
100/0	1.14	-
80/20	0.68	0.27
50/50	0.23	0.73
20/80	0.09	1.08
0/100	-	1.31
Silica		
100/0	0.50	-
50/50	0.22	0.69
20/80	0.07	1.06
0/100	-	1.11
High Nitrile		
Unfilled cpd.		
20/80	0.13	1.29
0/100	-	1.96
High Nitrile		
Filled cpd.		
20/80	0.07	1.16
0/100	-	1.17
NBR masterbatch @ 30°C		
Unfilled cpd.		
100/0	1.61	-
50/50	0.41	0.67
20/80	0.11	1.34
0/100	-	1.66

Table B1 Damping properties (continued)

Compound	tan δ_{max}	
	BR phase	**NBR phase**
NBR masterbatch @ 30°C Filled cpd.		
100/0	1.03	-
50/50	0.28	0.61
20/80	0.09	1.08
0/100	-	1.25
NBR masterbatch @ 100°C Unfilled cpd.		
100/0	1.61	-
50/50	0.40	0.69
20/80	0.11	1.36
0/100	-	1.66
NBR masterbatch @ 100°C Filled cpd.		
100/0	1.03	-
50/50	0.26	0.66
20/80	0.07	1.05
0/100	-	1.26

APPENDIX C : Effects of some additive on properties

Table C1 Rheological and cure properties of compounds

Compound	ML (1+4)	Cure properties			
		T_{max} (lb-in)	T_{min} (lb-in)	Scorch time (min)	Cure time (min)
S60NS 5 phr Unfilled cpd.					
100/0	34.0 ± 0.0	32.37 ± 0.22	4.62 ± 0.03	7.02 ± 0.09	19.07 ± 0.02
50/50	32.6 ± 0.3	31.11 ± 0.27	3.69 ± 0.4	7.09 ± 0.07	10.07 ± 0.05
20/80	31.9 ± 0.1	27.31 ± 0.30	3.18 ± 0.04	6.29 ± 0.06	8.27 ± 0.03
0/100	37.1 ± 0.8	22.65 ± 0.97	3.07 ± 0.02	6.06 ± 0.01	9.20 ± 0.40
S60NS 5 phr Filled cpd.					
100/0	54.8 ± 0.3	45.68 ± 0.08	7.84 ± 0.06	4.58 ± 0.01	7.21 ± 0.02
50/50	52.3 ± 0.4	42.14 ± 1.34	7.35 ± 0.06	3.29 ± 0.06	5.15 ± 0.08
20/80	53.9 ± 0.9	37.23 ± 0.33	6.56 ± 0.08	3.19 ± 0.02	5.19 ± 0.11
0/100	56.8 ± 1.6	36.81 ± 1.03	5.98 ± 0.16	3.19 ± 0.01	7.15 ± 0.37
S60NS 15 phr Unfilled cpd.					
100/0	29.4 ± 0.3	26.72 ± 1.09	4.10 ± 0.46	10.06 ± 0.16	19.38 ± 0.13
50/50	26.1 ± 0.6	24.67 ± 0.18	3.40 ± 0.07	7.42 ± 0.07	10.16 ± 0.07
20/80	23.3 ± 0.3	19.36 ± 1.01	3.05 ± 0.26	7.09 ± 0.06	9.38 ± 0.50
0/100	24.9 ± 0.5	15.43 ± 0.57	2.80 ± 0.03	6.50 ± 0.13	9.39 ± 0.31
S60NS 15 phr Filled cpd.					
100/0	44.4 ± 0.5	36.27 ± 0.20	6.36 ± 0.04	5.20 ± 0.08	7.28 ± 0.07
50/50	40.0 ± 0.0	31.09 ± 0.48	6.00 ± 0.05	3.59 ± 0.05	5.39 ± 0.10
20/80	34.8 ± 0.3	28.52 ± 0.42	5.51 ± 0.16	3.38 ± 0.06	6.01 ± 0.13
0/100	36.4 ± 0.3	29.72 ± 1.01	5.10 ± 0.18	3.28 ± 0.08	7.43 ± 0.25

Table C1 Rheological and cure properties of compounds (continued)

Compound	ML (1+4)	Cure properties			
		T_{max} (lb-in)	T_{min} (lb-in)	Scorch time (min)	Cure time (min)
WB16 1 phr Unfilled cpd.					
100/0	33.3 ± 0.4	32.50 ± 0.32	5.25 ± 0.04	8.05 ± 0.26	18.22 ± 0.13
50/50	34.6 ± 0.5	31.04 ± 0.55	4.06 ± 0.07	6.22 ± 0.04	8.05 ± 0.04
20/80	37.4 ± 0.5	30.68 ± 0.64	3.85 ± 0.06	5.35 ± 0.03	9.49 ± 0.12
0/100	42.8 ± 0.5	33.34 ± 0.63	3.85 ± 0.03	5.25 ± 0.10	9.41 ± 0.13
WB16 1 phr Filled cpd.					
100/0	56.1 ± 0.3	48.17 ± 0.25	9.11 ± 0.13	4.19 ± 0.07	6.28 ± 0.04
50/50	56.0 ± 0.0	44.05 ± 0.35	8.07 ± 0.17	3.14 ± 0.04	5.02 ± 0.02
20/80	58.6 ± 0.8	42.39 ± 0.46	7.38 ± 0.12	3.15 ± 0.03	6.35 ± 0.38
0/100	62.0 ± 0.4	44.84 ± 0.67	6.73 ± 0.13	3.18 ± 0.02	7.58 ± 0.65
WB16 3 phr Unfilled cpd.					
100/0	29.6 ± 0.95	21.03 ± 0.85	3.79 ± 0.12	9.34 ± 0.24	16.49 ± 0.14
50/50	33.3 ± 0.29	27.44 ± 1.56	4.14 ± 0.11	6.21 ± 0.09	8.34 ± 0.01
20/80	34.0 ± 0.71	28.97 ± 0.72	4.06 ± 0.09	5.34 ± 0.01	7.42 ± 0.11
0/100	40.1 ± 0.25	30.72 ± 0.23	3.97 ± 0.07	5.16 ± 0.02	9.41 ± 0.08
WB16 3 phr Filled cpd.					
100/0	49.7 ± 0.4	35.77 ± 0.46	7.07 ± 0.04	4.08 ± 0.11	6.14 ± 0.04
50/50	53.3 ± 0.4	37.63 ± 0.56	7.29 ± 0.02	3.25 ± 0.04	5.10 ± 0.10
20/80	54.3 ± 0.7	39.16 ± 0.78	6.73 ± 0.04	3.28 ± 0.03	4.55 ± 0.08
0/100	60.2 ± 0.5	42.22 ± 1.39	6.23 ± 0.06	3.16 ± 0.08	5.14 ± 0.10
EOR 3 phr Unfilled cpd.					
100/0	37.8 ± 0.18	32.93 ± 0.49	4.80 ± 0.06	6.39 ± 0.32	20.02 ± 0.28
50/50	32.5 ± 0.22	33.76 ± 0.11	4.13 ± 0.12	6.42 ± 0.04	9.56 ± 0.04
20/80	33.5 ± 0.16	32.65 ± 0.76	3.46 ± 0.06	5.49 ± 0.08	8.06 ± 0.17
0/100	34.8 ± 0.19	26.98 ± 0.99	3.21 ± 0.35	5.38 ± 0.03	12.35 ± 0.07
EOR 3 phr Filled cpd.					
100/0	N/A	47.32 ± 0.55	8.41 ± 0.06	5.14 ± 0.07	7.40 ± 0.04
50/50	N/A	47.32 ± 0.20	8.03 ± 0.09	3.37 ± 0.02	5.31 ± 0.02
20/80	N/A	44.06 ± 0.53	7.11 ± 0.08	3.37 ± 0.05	5.35 ± 0.07
0/100	N/A	41.15 ± 0.06	5.99 ± 0.08	3.31 ± 0.02	8.11 ± 0.23
EOR 7 phr Unfilled cpd.					
100/0	36.8 ± 0.18	31.09 ± 0.43	4.55 ± 0.03	7.14 ± 0.44	20.40 ± 0.20
50/50	30.8 ± 0.11	31.89 ± 0.14	4.08 ± 0.07	6.47 ± 0.02	9.59 ± 0.02
20/80	31.2 ± 0.10	29.90 ± 0.32	3.36 ± 0.06	6.17 ± 0.08	8.34 ± 0.08
0/100	31.9 ± 0.07	24.60 ± 0.56	2.93 ± 0.06	5.59 ± 0.14	10.48 ± 0.63
EOR 7 phr Filled cpd.					
100/0	N/A	46.97 ± 0.83	8.62 ± 0.22	5.32 ± 0.10	8.00 ± 0.06
50/50	N/A	45.67 ± 0.57	7.91 ± 0.06	3.38 ± 0.03	5.37 ± 0.02
20/80	N/A	42.37 ± 0.10	6.99 ± 0.05	3.38 ± 0.06	5.34 ± 0.05
0/100	N/A	39.99 ± 0.36	5.92 ± 0.10	3.41 ± 0.05	8.12 ± 0.12

Table C1 Rheological and cure properties of compounds (continued)

Compound	ML (1+4)	Cure properties			
		T_{max} (lb-in)	T_{min} (lb-in)	Scorch time (min)	Cure time (min)
EOR 10 phr Unfilled cpd.					
100/0	35.6 ± 0.22	30.67 ± 0.40	4.50 ± 0.10	6.49± 0.29	20.22 ± 0.25
50/50	29.4 ± 0.10	29.92 ± 0.46	3.87 ± 0.03	7.05 ± 0.11	10.10 ± 0.08
20/80	29.9 ± 0.36	28.37 ± 0.43	3.33 ± 0.03	6.13 ± 0.02	8.23 ± 0.01
0/100	28.0 ± 0.54	23.31 ± 0.34	2.97 ± 0.04	6.02 ± 0.02	10.08 ± 0.19
EOR 10 phr Filled cpd.					
100/0	N/A	49.97 ± 0.83	8.62 ± 0.22	5.19 ± 0.06	7.52 ± 0.17
50/50	N/A	45.67 ± 0.57	7.91 ± 0.06	3.26 ± 0.02	10.10 ± 0.08
20/80	N/A	42.37 ± 0.10	6.99 ± 0.05	3.23 ± 0.04	5.20 ± 0.04
0/100	N/A	39.99 ± 0.36	5.92 ± 0.10	3.25 ± 0.03	8.07 ± 0.07

Table C2 Mechanical properties

Specimen	Modulus @ 50% strain (MPa)	Tensile Strength (MPa)	Elongation at break (%)	Hardness (shore A)	tan δ_{max}	
					BR phase	NBR phase
S60NS 5 phr Unfilled cpd.						
100/0	0.8 ± 0.03	1.1 ± 0.07	88.01 ± 0.85	49.3 ± 0.5	1.40	-
50/50	0.9 ± 0.04	2.0 ± 0.11	233.5 ± 17.64	51.2 ± 0.6	0.40	0.65
20/80	0.9 ± 0.06	3.4 ± 0.43	331.7 ± 34.37	52.3 ± 0.5	0.11	1.22
0/100	0.9 ± 0.04	2.9 ± 0.41	299.3 ± 44.15	53.7 ± 0.2	-	1.62
S60NS 5 phr Filled cpd.						
100/0	1.4 ± 0.07	5.0 ± 0.60	200.0 ± 18.86	63.7 ± 0.6	0.99	-
50/50	1.6 ± 0.05	10.4 ± 1.19	264.9 ± 21.70	67.0 ± 0.6	0.20	0.69
20/80	1.6 ± 0.12	10.0 ± 0.72	250.2 ± 35.01	67.9 ± 0.5	0.07	1.06
0/100	1.5 ± 0.05	7.1 ± 1.31	262.7 ± 29.83	67.9 ± 0.3	-	1.22
S60NS 15 phr Unfilled cpd.						
100/0	0.7 ± 0.00	1.1 ± 0.04	106.9 ± 9.29	47.3 ± 0.5	1.22	-
50/50	0.7 ± 0.05	2.1 ± 0.15	286.9 ± 37.83	49.4 ± 0.5	0.47	0.53
20/80	0.8 ± 0.04	3.0 ± 0.22	332.4 ± 19.57	52.6 ± 0.7	0.11	1.16
0/100	1.2 ± 0.05	2.8 ± 0.31	287.8 ± 31.00	58.6 ± 0.3	-	1.50
S60NS 15 phr Filled cpd.						
100/0	1.2 ± 0.05	5.6 ± 1.17	257.7 ± 42.54	61.30.5	0.92	-
50/50	1.4 ± 0.07	8.0 ± 1.03	273.9 ± 19.79	63.90.6	0.20	0.69
20/80	1.6 ± 0.05	9.3 ± 1.19	261.8 ± 24.72	66.60.3	0.07	0.93
0/100	2.1 ± 0.09	9.9 ± 1.70	238.6 ± 33.38	71.80.3	-	1.06

Table C2 Mechanical properties (continued)

Specimen	Modulus @ 50% strain (MPa)	Tensile Strength (MPa)	Elongation at break (%)	Hardness (shore A)	tan δ_{max}	
					BR phase	NBR phase
WB16 1 phr Unfilled cpd.						
100/0	0.7 ± 0.05	1.1 ± 0.05	84.4 ± 5.26	51.8 ± 0.4	1.60	-
50/50	0.9 ± 0.04	2.3 ± 0.31	253.7 ± 41.85	53.9 ± 0.8	0.38	0.68
20/80	0.9 ± 0.03	2.6 ± 0.32	271.6 ± 34.76	53.9 ± 0.5	0.10	1.29
0/100	0.9 ± 0.03	2.2 ± 0.26	236.9 ± 29.55	54.6 ± 0.5	-	1.63
WB16 1 phr Filled cpd.						
100/0	1.2 ± 0.05	3.3 ± 0.47	183.3 ± 25.02	65.1 ± 0.6	0.98	-
50/50	1.5 ± 0.07	9.8 ± 0.76	313.8 ± 15.51	67.8 ± 0.3	0.20	0.69
20/80	1.6 ± 0.04	8.7 ± 1.14	257.4 ± 26.25	69.5 ± 0.4	0.06	1.02
0/100	1.5 ± 0.05	10.3 ± 1.30	288.5 ± 23.24	68.5 ± 0.4	-	1.15
WB16 3 phr Unfilled cpd.						
100/0	0.7 ± 0.03	1.1 ± 0.05	97.8 ± 9.95	51.30.5	1.59	-
50/50	0.9 ± 0.05	2.4 ± 0.20	272.6 ± 19.14	55.90.3	0.31	0.79
20/80	0.9 ± 0.05	2.8 ± 0.32	284.0 ± 19.73	55.60.8	0.09	1.33
0/100	0.9 ± 0.04	2.5 ± 0.21	255.1 ± 16.14	55.10.5	-	1.60
WB16 3 phr Filled cpd.						
100/0	1.2 ± 0.05	4.1 ± 0.48	230.323.5	65.0 ± 0.4	1.03	-
50/50	1.5 ± 0.10	8.4 ± 1.07	302.030.77	68.6 ± 0.8	0.19	0.69
20/80	1.6 ± 0.10	10.1 ± 1.37	302.625.28	69.1 ± 0.5	0.07	1.01
0/100	1.6 ± 0.04	11.7 ± 2.17	305.733.26	69.9 ± 0.6	-	1.14
EOR 3 phr Unfilled cpd.						
100/0	0.8 ± 0.04	1.1 ± 0.05	82.4 ± 7.97	51.5 ± 0.4	1.52	-
50/50	0.9 ± 0.05	2.4 ± 0.25	241.4 ± 25.67	53.9 ± 0.8	0.33	0.77
20/80	1.0 ± 0.05	3.2 ± 0.36	289.4 ± 28.79	55.1 ± 0.8	0.10	1.23
0/100	1.0 ± 0.03	2.8 ± 0.25	270.6 ± 19.95	55.8 ± 1.0	-	1.55
EOR 3 phr Filled cpd.						
100/0	1.5 ± 0.05	3.9 ± 0.32	146.2 ± 13.56	64.3 ± 1.0	1.00	-
50/50	1.9 ± 0.20	8.1 ± 1.11	192.6 ± 20.00	68.3 ± 0.6	0.19	0.67
20/80	1.9 ± 0.08	11.0 ± 1.99	222.9 ± 23.38	68.0 ± 0.8	0.07	0.09
0/100	1.8 ± 0.06	9.3 ± 0.42	203.3 ± 6.77	68.0 ± 0.7	-	1.17
EOR 7 phr Unfilled cpd.						
100/0	0.8 ± 0.03	1.1 ± 0.09	84.7 ± 11.60	51.0 ± 0.6	1.50	-
50/50	1.0 ± 0.04	2.5 ± 0.25	251.0 ± 22.12	53.8 ± 0.3	0.37	0.68
20/80	1.0 ± 0.03	3.2 ± 0.26	295.5 ± 18.04	56.4 ± 0.8	0.10	1.15
0/100	1.0 ± 0.05	2.6 ± 0.25	262.7 ± 21.74	57.0 ± 1.2	-	1.43
EOR 7 phr Filled cpd.						
100/0	1.6 ± 0.07	3.7 ± 0.27	147.8 ± 12.87	65.1 ± 0.3	0.93	-
50/50	1.8 ± 0.11	8.8 ± 1.11	212.0 ± 21.16	67.0 ± 1.2	0.22	0.64
20/80	1.8 ± 0.12	9.3 ± 1.62	210.5 ± 20.10	68.4 ± 1.3	0.07	0.95
0/100	1.8 ± 0.08	10.4 ± 1.56	212.8 ± 18.13	68.4 ± 0.3	-	1.10

Table C2 Mechanical properties (continued)

Specimen	Modulus @ 50% strain (MPa)	Tensile Strength (MPa)	Elongation at break (%)	Hardness (shore A)	tan δ_{max}	
					BR phase	NBR phase
EOR 10 phr Unfilled cpd.						
100/0	0.8 ± 0.05	1.3 ± 0.04	108.0 ± 4.96	51.5 ± 0.7	1.51	-
50/50	1.0 ± 0.04	2.4 ± 0.19	238.4 ± 23.62	53.4 ± 0.3	0.35	0.62
20/80	1.0 ± 0.05	3.5 ± 0.43	313.7 ± 27.35	55.3 ± 0.3	0.10	1.11
0/100	1.0 ± 0.05	3.0 ± 0.35	306.6 ± 23.58	56.5 ± 0.4	-	1.36
EOR 10 phr Filled cpd.						
100/0	1.5 ± 0.05	3.7 ± 0.45	144.9 ± 16.45	64.1 ± 1.4	0.87	-
50/50	1.9 ± 0.25	9.0 ± 0.91	226.6 ± 15.47	68.3 ± 0.3	0.24	0.62
20/80	2.0 ± 0.19	10.8 ± 1.34	234.8 ± 21.78	68.9 ± 0.9	0.07	0.93
0/100	1.8 ± 0.11	10.0 ± 1.60	225.2 ± 20.70	68.9 ± 0.3	-	1.07

APPENDIX D : Specification of oil used for swelling test

GRENA-DX™

Manufacturer : Bangjak Petroleum, Co., Ltd.

Kinematic viscosity	
At 40°C, cSt.	152.70
At 100 °C, cSt.	15.00
Flash point (COC), °C	256
Content	Paraffinic, 67 volume %
	Aromatic, 5 volume %
	Napthenic, 25 volume %
	Additive, 3 volume %

BIOGRAPHY

NAME	Miss Nootjaree Prayoonchatphan
DATE OF BIRTH	17 November 1974
PLACE OF BIRTH	Bangkok, Thailand
INSTITUTION ATTENDED	Prince of Songkla University, 1993-1997: Bachelor of Science (Polymer Science)
	Mahidol University, 1997-2000: Master of Science (Polymer Science)